

Ministry of Science and Higher Education of the Russian Federation
Federal State Budgetary Educational Institution of Higher Education
Nosov Magnitogorsk State Technical University

The 5th International
Youth Scientific and Technical Conference

MAGNITOGORSK

ROLLING PRACTICE

2020

Proceedings of the 5th International Youth Scientific and Technical Conference

Edited by A.G. Korchunov

*The Conference was funded by the Federal State Budgetary Institution Russian
Foundation for Basic Research
(Contract No. 20-08-20004\20 dated 17.02.2020)*

Magnitogorsk
2020

Editorial Board:

Korchunov A.G. (Editor-in-Chief)
Konstantinov D.V. (Deputy Editor-in-Chief)
Ivekeeva P.V. (Publishing Editor)
Medvedeva E.M.

*The proceedings of the conference are indexed
by the Russian Science Citation Index and Google Scholar*

Magnitogorsk Rolling Practice 2020: Proceedings of the 5th International Youth Scientific and Technical Conference. Ed. by A.G. Korchunov. Magnitogorsk: Publishing House of Nosov Magnitogorsk State Technical University, 2020, 145 p.

ISBN 978-5-9967-2113-9

These scientific publications constitute the proceedings of the 5th International Youth Scientific and Technical Conference «Magnitogorsk Rolling Practice 2020» devoted to metal and alloy forming.

Subjects of the reports delivered by young researchers show a considerable interest in research areas related to development of finite element models of metal and alloy forming processes using special software, innovative cold and hot plastic working processes, new materials with a higher level of performance, methods used to determine true resistance of metals and alloys to deformation, and physical simulation of metal and alloy forming processes.

The Conference had a title of the winner of the competition held by the Russian Foundation for Basic Research for the best projects of organizing scientific events in the Russian Federation in 2020.

ISBN 978-5-9967-2113-9

© Nosov Magnitogorsk State
Technical University, 2020

Министерство науки и высшего образования Российской Федерации
Федеральное государственное бюджетное образовательное учреждение
высшего образования
«Магнитогорский государственный технический университет им. Г.И. Носова»

The 5th International
Youth Scientific and Technical Conference

MAGNITOGORSK

ROLLING PRACTICE

2020

Материалы V международной молодежной
научно-технической конференции

Под редакцией А.Г. Корчунова

*Конференция проводится при финансовой поддержке
ФГБУ «Российский фонд фундаментальных исследований»
(Договор № 20-08-20004\20 от 17.02.2020)*

Магнитогорск
2020

Редколлегия:

Корчунов А.Г. (главный редактор)
Константинов Д.В. (зам. главного редактора)
Ивекеева П.В. (отв. редактор)
Медведева Е.М.

*Материалы трудов конференции индексируются
Российским индексом научного цитирования и Google Scholar*

Magnitogorsk Rolling Practice 2020: материалы V международной молодежной научно-технической конференции / под ред. А.Г. Корчунова. Магнитогорск: Изд-во Магнитогорск. гос. техн. ун-та им. Г.И. Носова, 2020. 145 с.

ISBN 978-5-9967-2113-9

Представлены материалы докладов V международной молодежной научно-технической конференции «Magnitogorsk Rolling Practice 2020», посвященной вопросам обработки металлов и сплавов давлением.

Тематика докладов молодых ученых свидетельствует о существенном интересе к научным направлениям, связанных с разработкой конечно-элементных моделей процессов обработки металлов и сплавов давлением в специализированных программных комплексах, инновационных процессов холодной и горячей пластической обработки, новых материалов с повышенным уровнем эксплуатационных характеристик, методик определения истинного сопротивления металлов и сплавов деформации, физического моделирования процессов обработки металлов и сплавов давлением.

Конференция проводилась в статусе победителя конкурса Российского фонда фундаментальных исследований на лучшие проекты организации научных мероприятий на территории Российской Федерации в 2020 г.

ISBN 978-5-9967-2113-9

© Магнитогорский государственный
технический университет
им. Г.И. Носова, 2020

MAGNITOGORSK ROLLING PRACTICE 2020: OUTCOMES AND PROSPECTS

Korchunov A.G.

Nosov Magnitogorsk State Technical University

In November of 2020 NMSTU held the 5th anniversary International Youth Scientific and Technical Conference *Magnitogorsk Rolling Practice 2020* devoted to metal and alloy forming. In 2014 scientists of Nosov Magnitogorsk State Technical University introduced the initiative of holding the international youth forum devoted to basic and applied issues of metal and alloy forming [1]. The idea of organizing the youth scientific and practical conference received an encouraging response from researchers, specialists and students. Relevance of subjects of the conference is proved by a geographic growth of participants and its constant support by the Russian Foundation for Basic Research (RFBR)*. Plenary sessions for different years of the conference included reports given by leading scientists: T.G. Langdon, J.M. Cabrera Marrero, P. Tandon, M. Dabala, Hailiang Yu, I. Calliari, G.I. Raab, A. Zhilyaev, A.M. Glezer, V.N. Trofimov, A.V. Vydrin, E. Korznikova, and A. Pesin. Many young researchers presented their research results at previous conferences prepared and successfully defended their theses and got PhD in engineering. Communications as part of the conference gave an impetus to strengthening collaboration between young researchers of leading research schools, building new research teams capable of achieving the most challenging objectives [2-3].

This year the Conference had a title of the winner of the competition held by the Russian Foundation for Basic Research for the best projects of organizing scientific events in the Russian Federation. In view of the current epidemiological situation, the Organizing Committee of the Conference decided to hold an online conference (Fig.1).



Fig.1. E-conference *Magnitogorsk Rolling Practice 2020*

The conference program included reports delivered by young researchers in sessions “Innovative technology and materials in metal forming”, “Cross-disciplinary solutions in advanced materials engineering (iSmart-MetalForming)” and “Fundamental challenges of metal forming in the scope of current demands of the global industry”, the workshop on “Basics of finite element modeling in Abaqus” and individual consultations on the difficulties of research for young researchers.

Over 100 participants from 32 universities, industrial companies and research institutions took part in the virtual conference sessions. Total online time of the conference exceeded 20 hours.

The information partners of the Conference included journals, such as *FERROUS METALLURGY. Bulletin of Scientific, Technical and Economical Information, Ferrous Metals, CIS Iron and Steel Review, Vestnik of Nosov Magnitogorsk State Technical University, Theory and Technology of Metallurgical Production, and Mechanical Equipment of Metallurgical Plants.*

The conference participants were welcomed by the members of the Program Committee: Puneet Tandon, Indian Institute of Information Technology, Design and Manufacturing (Jabalpur, India), Irene Calliari, the University of Padua (Padua, Italy), and Megumi Kawasaki, Oregon State University (the USA).

They emphasized in their speeches the importance of holding the conference in such a complicated epidemiological situation, a good opportunity for young researchers from various research schools to share their experience and knowledge, promoting the development of prospective research areas. They put a particular emphasis on giving reports in English to take an active part in international conferences of the highest level.

In spite of rather an unconventional online format and a young age of speakers, their reports had a high scientific level, and speakers wanted to present their research results as clearly and attractively as possible and showed themselves to be quite mature researchers capable of solving complicated issues in metal and alloy forming.

Subjects of the reports made by young researchers show that there is a current interest in research areas related to developing:

- finite element models of metal and alloy forming processes using special software: DEFORM 3D, Abaqus and others,
- innovative cold and hot metal forming processes,
- new materials with a higher level of performance properties,
- new methods used to determine true resistance of metals and alloys to deformation, and
- physical simulation of metal and alloy forming processes.

Thus, we may state a great commitment of young researchers, specialists, students and postgraduate students to development and introduction of innovative research products, having a basic and applied value for developing potential of the metal and alloy forming industry, its expansion and diversification, contributing to a successful settlement of production issues in an efficient relationship between science and the industry.

Following the results of the sessions, the committee determined nominees, diploma and prize winners of the conference.

The nomination “The best start to science” was awarded to three young researchers: Nikita Bunits (Moscow Institute of Steel and Alloys, Moscow), Alexandra

Tymchenko (Karaganda State Industrial University, Temirtau, Kazakhstan), and Ilya Tsyrganovich (the Sukhoi State Technical University of Gomel, Gomel, Belarus). The nomination “The best progress in research” was awarded to Ekaterina Ustinova (Ural Federal University, Yekaterinburg, Russia). The nomination “The best practical implementation” was awarded to Denis Voroshilov (Siberian Federal University, Krasnoyarsk). The nomination “The best numerical simulation” was awarded to Denis Salikhyanov (Ural Federal University, Yekaterinburg).

The 3rd degree diplomas were awarded to Nikita Zavartsev (OJSC ROSNITI, Chelyabinsk, Russia) for his report on “Research of the heating temperature influence on technological plasticity of steel grade 15KH13N2 (AISI 414) applicable to the screw rolling process” and Olesya Biryukova (Nosov Magnitogorsk State Technical University, Magnitogorsk, Russia) for her report on “Development of the asymmetric rolling technology for aluminum alloys”. The 2nd degree diploma was awarded to Luca Pezzato (the University of Padua, Padua, Italy) for his report on “Potential biomedical applications of AZ61 magnesium alloy after large strain extrusion machining”.

The winner of the conference getting the 1st degree diploma was Mikhail Erpalov (Ural Federal University, Yekaterinburg, Russia) presenting his report on “Theoretical and experimental analysis of a neck profile of cylindrical specimens”.

The best reports were named and their authors were invited to publishing in journals, information partners of the conference, indexed in Scopus and included into the List of leading Russian peer-reviewed scientific publications.

The participants thanked the organizers for a very high professional level of the conference, for its well-thought agenda, smooth running of the event in an online format and expressed their confidence that the youth scientific forum would have a long-term and successful future.

The organizers, for their part, presented a draft program of the next conference, combining advantages of offline events with best practices of online technologies.

We intend to hold a plenary session with invited leading scientists, globally known in the area of metal and alloy forming, expand a program of industrial tours, present a unique complex of asymmetric rolling and incremental forming of the international laboratory “Mechanics of Gradient Nanomaterials”, and visit ski resorts located near Magnitogorsk.

The Conference came to an end, and its participants agreed to meet at the 6th International Youth Scientific Conference *Magnitogorsk Rolling Practice*.

References

1. Chukin M.V., Korchunov A.G., Tulupov O.N. International projects of Nosov Magnitogorsk State Technical University. Blanking Production in Mechanical Engineering. 2019. No. 6. pp. 243-245.
2. Korchunov A.G. International Youth Scientific and Practical Conference *Magnitogorsk Rolling Practice 2018* held at Nosov Magnitogorsk State Technical University. Ferrous Metals. 2018. No. 9. pp. 6-8.
3. Korchunov A. Magnitogorsk Rolling Practice 2019: the benchmark for young scientists from around the world. CIS Iron and Steel Review. 2019. No. 17. pp. 70–72.

The conference was funded by the Russian Foundation for Basic Research (Contracts No. 20-08-20004\20, 18-38-10016\18)

SESSION 1 – Innovative Technology and Materials in Metal Forming

POTENTIAL BIOMEDICAL APPLICATIONS OF AZ61 MAGNESIUM ALLOY AFTER LARGE STRAIN EXTRUSION MACHINING (LSEM)

Luca Pezzato, Rachele Bertolini, Stefania Bruschi,
Andrea Ghiotti, Manuele Dabalà
University of Padova, Padova, Italy
luca.pezzato@unipd.it

Magnesium alloys are very promising candidates for producing degradable and absorbable temporary implants, since they have the ability to dissolve in human environment and remain non-toxic thanks to their high biocompatibility [1]. Intense grain refinement followed by Severe Plastic Deformation (SPD) is one of the main strategies used by researchers to increase corrosion resistance of magnesium alloys [2].

A previous study [3] proves that Large Strain Extrusion Machining (LSEM) represents an efficient cutting strategy to achieve an intense SPD layer near the machined surface.

LSEM is a single-step plane strain deformation process that combines large shear strains induced by machining with proper dimensional control of the extruded chips. The obtained chips are in form of sheet produced directly from the bulk material in a single stage of deformation. (Fig. 1) shows a scheme of the process. A constraining tool is placed above the cutting tool, which travels at cutting speed V_0 , with the aim of extruding the chip from t_0 to t .

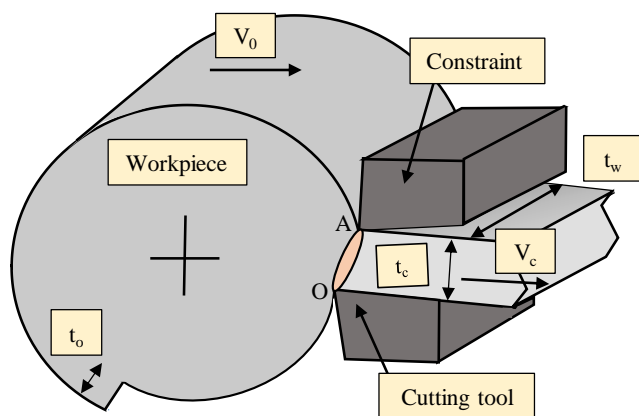


Fig. 1. Scheme of the LSEM process

The material objective of the study was a commercially available AZ61 magnesium alloy in annealed condition (Fig.2a). The LSEM tests were carried out on a Mori Seiki™ lathe equipped with a specially designed apparatus that included the constraint tool placed above the cutting tool to fulfill large strain extrusion cutting conditions, and

the liquid nitrogen supply system. The microstructure of the obtained bars and chips was evaluated with optical microscope analysis, the mechanical properties – with Vickers micro-hardness measurements and the corrosion properties – with potentiodynamic polarization tests in simulated body fluid at 37°C.

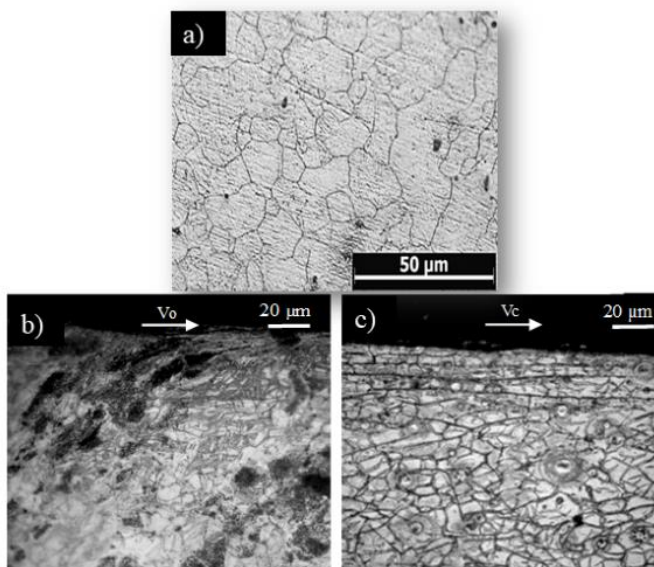


Fig. 2. Microstructure of the annealed AZ61 alloy (a), of the bar after LSEM under cryogenic cooling (b) and of the chip coming from LSEM

An SPD region near the machined surface formed by heavily deformed grains, which are strained and elongated along the cutting speed direction, can be found in the bar after LSEM (Fig.2b) whereas an equiaxed structure can be found in the chip (Fig.2c). The application of liquid nitrogen as cooling medium led to the formation of a thicker SPD layer characterized by finer grain compared with the corresponding dry case. As a result, the corrosion performance is improved. With regard to the chips, harder chips characterized by a cold-worked microstructure are obtained when machining with liquid nitrogen compared with the dry case. This cause leads to slight decrease in the corrosion resistance compared with the latter.

References

1. Peron M, Torgersen J, Berto F. Mg and Its Alloys for Biomedical Applications. Mechanical Failure. 2017. Vol. 7. pp. 252.
2. Zheng YF, Gu XN, Witte F. Biodegradable metals. Materials Science & Engineering R. 2014. Vol. 77. pp. 1–34.
3. Bertolini R, Bruschi S, Ghiotti A, Pezzato L, Dabalà M, Large strain extrusion machining of magnesium alloys for biomedical applications. Procedia CIRP. 2018. Vol. 71. pp. 105-110.

HARDNED TAPE SUBSTRATES MADE ON (CU-NI-ME) - ALLOYS FOR 2^D GENERATION HIGH-TEMPERATURE SUPERCONDUCTOR WIRE

Suaridze T., Khlebnikova Yu., Egorova L.

*M.N. Mikheev Institute of Metal Physics of the Ural Branch of the Russian Academy of Sciences, Yekaterinburg, Russia
Teona_S@imp.uran.ru*

In this work, the process of texture formation in thin metal tapes made of ternary alloys (Cu–40% Ni–1.3% Mn, Cu–40% Ni–0.8% Mo and Cu–40% Ni–0.5% Nb) was studied in order to obtain tape substrates used in film multilayer compositions, including those used to make high-temperature superconductor wire of the second generation (2G HTS wire). The cubic texture perfection degree is analyzed by the electron backscattered diffraction techniques. Tensile tests of textured tape substrates from Cu–40% Ni–Me alloys have been carried out.

Copper alloys with a cubic recrystallization texture are interesting as substrates for 2G HTS wire due to the fact that a perfect biaxial cubic texture close to the single crystal {100} <001> can be obtained on them, and also because of their non-magnetization properties and low cost. The value of the stacking fault energy (SFE) of copper has a value close to the lower limit, at which a classical deformation texture of the "copper" type is formed, and during annealing, a sharp cubic texture can be formed. The low SFE of copper naturally limits the amount of the alloying element when creating FCC-alloys based on copper with a biaxial cubic texture, since alloying always reduces the SFE [3, p. 210].

In the course of the research work, the ternary alloys Cu – 40% Ni – Me were melted on the basis of oxygen-free 99.95% pure copper and 99.99% pure nickel. The purity of other alloying elements was not lower than 99.94%. All alloys were melted in alundum crucibles in an argon atmosphere in a vacuum-induction furnace. After forging and grinding, blanks for cold rolling were obtained. Cold deformation of blanks was carried out in 2 stages: stage 1 - on a rolling mill with a diameter of 180 mm, the degree of deformation is ~ 90%, stage 2 - on a duo rolling mill with polished rolls to a thickness of 100-80 μm. The total degree of cold deformation was 98.6-99.1%. Then, a series of recrystallization annealing of the tape samples was carried out at the temperatures of 1000, 1050 and 1100 °C, in order to form a sharp biaxial texture in the alloys. The annealing time was 1 hour.

As a result of the EBSD analysis of ternary alloys after the corresponding technological procedures, it was found that a sharp biaxial cubic texture is realized on the surface of the alloys after all conditions of recrystallization annealing. The proportion of cubic grains after annealing ranged from 72 to 97%. The optimal conditions of recrystallization annealing, which makes it possible to obtain the most perfect texture on the surface of all samples, is annealing at 1050°C for 1 h. As a result of such annealing, 94, 96, and 97% grains with {001}<100> orientation were formed in Cu–40% Ni–1.3% Mn, Cu–40% Ni–0.5% Nb, and Cu–40% Ni–0.8% Mo alloys, respectively.

The structure investigation of textured tapes made of Cu–40% Ni–Me alloys (where Me = Mn, Nb, Mo) showed that a uniform structure without any inclusions is formed in these alloys.

The evaluation of the mechanical characteristics showed that the value of the yield strength for Cu–40% Ni–1.3% Mn, Cu –40% Ni–0.5% Nb and Cu–40% Ni–0.8% Mo

alloys is 85, 102, and 108 MPa, respectively. Copper alloying contributed to the strengthening of tapes made of Cu-40% Ni-Me alloys by 3.4-4.3 times compared with tapes made of pure copper. The yield strength of the latter is only 25 MPa.

As a result, it was found that the tape substrates made of ternary alloys Cu-40% Ni-Me (Me=Mn, Nb, or Mo), which combine a perfect cubic texture, non-magnetic characteristics and high strength, can be used for epitaxial deposition of buffer and superconducting layers in the production of 2G HTS wires.

The reported study was funded by RFBR and the Sverdlovsk Region, project number 20-43-660034.

References

1. Gallistl B., Kirchschrager R., Hassel A.W. Biaxially textured copper-iron alloys for coated conductors. *Physica Status Solidi A*. 2012. V. 209. No. 5. pp. 875-879.
2. Varanasi C.V., Barnes P.N., Yust N.A. Biaxially textured copper and copper-iron alloy substrates for use in $YBa_2Cu_3O_{7-x}$ coated conductors. *Superconductor Science and Technology*. 2006. V. 19. pp. 85-95.
3. Shtremel M.A. Strength of alloys. P. I. Lattice defects. Moscow: MISIS, 1999. 384 p.

FEM SIMULATION OF TEMPERATURE CHANGES DURING ASYMMETRIC CRYOROLLING OF ALUMINUM

Pustovoitov D., Pesin A., Biryukova O.

*Nosov Magnitogorsk State Technical University, Magnitogorsk, Russia
pustovoitov_den@mail.ru*

Conventional strengthening mechanisms applicable to aluminum alloys like solid solution strengthening, work hardening and precipitation hardening have their own limitations [1]. A possible way to further increase strength of aluminum alloys is to form an ultrafine grain (UFG) structure using severe plastic deformation (SPD) methods [2]. Cryorolling and asymmetric rolling are techniques that have potential application for large-scale industrial production of UFG aluminum alloys [3]. Cryorolling is a simple rolling process in which the cryogenic temperature is maintained by liquid nitrogen [4]. Deformation at cryogenic temperature is one of the main mechanisms leading to improvement in both strength and ductility of UFG aluminum alloys as well as narrow grain size distribution, bimodal structure, gradient structure [5]. The great advantages of cryorolling are the high accumulation of dislocations and the suppression of dynamic recovery in the processed material [6]. Asymmetric rolling is a process in which the speeds of the top and bottom rolls are different [7-10]. It is well known that shear strain plays a critical role in the grain refinement [10]. The great advantage of asymmetric rolling is a creation of additional high shear strain in the processed material. Asymmetric cryorolling is a technique that combines the advantages of cryorolling and asymmetric rolling, and can result in greater grain refinement compared to the other techniques [11]. The asymmetric cryorolling technique has been used successfully to produce UFG aluminum alloys. Yu et al. [11] carried out experiments on the asymmetric cryorolling process for Al 1050 and Al 6061 alloys in a multifunction rolling mill with of 50 mm diameter work roll under dry friction condition. For Al 1050, when the rolls speed ratio was 1.4, the grain size was about 211 nm [11]. The grain size of the

processed material continuously decreases with increasing the applied shear strain. High shear strain through sheet thickness can be obtained by asymmetric cryorolling with the high thickness reduction per pass and high friction coefficient. However it leads to the problem with the heat generated in the roll gap. The temperature rise during the asymmetric cryorolling can be as large as to increase the sheet temperature above the cryogenic temperature. So the prediction of sheet temperature during asymmetric cryorolling is very important. There are only some experimental investigations on the microstructural evolution and the corresponding mechanical properties of aluminum alloys processed by asymmetric cryorolling. However, no research on finite element simulation of asymmetric cryorolling has been found. The goal of this paper is the finite element simulation and analysis of the temperature rise during asymmetric cryorolling of Al 1100, Al 5083 and Al 6061-T6 alloys. The results of investigation can be useful for the development of the optimal treatment process of aluminum alloys by cryogenic SPD to obtain the UFG structure and high strength properties. Asymmetric cryorolling with high thickness reduction per pass, high rolls speed ratio and high friction coefficient leads to serious increase of the effective strain up to mode of SPD when $e > 1.0$. However it leads to temperature rise of the strip above the cryogenic temperature. Effective strain can be extremely high ($e = 4.1$) during asymmetric cryorolling with thickness reduction $e = 60\%$ and the rolls speed ratio of 55%. However the temperature rise exceeds 300 K in this case and the cryogenic conditions are not provided. Cryogenic conditions when the strip temperature is maintained in the range from 77 K to 173 K during asymmetric cryorolling of aluminum alloys with a large strain ($e > 1.0$) can be obtained with decreasing of roll temperature from 300 K to 77 K and with decreasing of rolling velocity from 1.0 - 10.0 m/s to 0.05 - 0.1 m/s or lower. However the main disadvantage of the low rolling velocity is the low productivity of the asymmetric cryorolling process. Low strength aluminum alloys (e.g. Al 1100) can be processed with high thickness reductions per pass (up to 40%). Medium and high strength aluminum alloys (e.g. Al 5083 and Al 6061-T6) should be processed with the decreased thickness reductions per pass (e.g. no more than 20%). The results of investigation can be useful for the development of the optimal treatment process of aluminum alloys by cryogenic SPD to obtain the ultrafine grain structure and high strength properties.

The reported study was funded by RFBR according to the research project № 18-58-45013 IND_a.

References

1. Elagin V.I. Paths of development of high-strength and heat-resistant structural aluminum alloys in the 21st century. Metal Science and Heat Treatment. 2007. no. 9, pp. 3-11.
2. Sabirov I., Murashkin M.Yu., Valiev R.Z. Nanostructured aluminium alloys produced by severe plastic deformation: New horizons in development. Materials Science & Engineering: A. 2013. vol. 560, pp. 1-24.
3. YU H., Tieu K., Lu C. Advanced rolling technologies for producing ultrafine-grain/nanostructured alloys. Procedia Engineering. 2014. vol. 81, pp. 96-101.
4. Panigrahi S.K., Jayaganthan R. Development of ultrafine grained high strength age hardenable Al 7075 alloy by cryorolling. Materials & Design. 2011. vol. 32, pp. 3150-3160.
5. Sabirov I. Enhanced ductility of ultra-fine grained metallic materials. Letters on

materials. 2015. vol. 5, pp. 347-353.

6. Shanmugasundaram T., Murty B.S., Subramanya S.V. Development of ultrafine grained high strength Al-Cu alloy by cryorolling. *Scripta Materialia*. 2006. vol. 54, pp. 2013-2017.

7. Ji Y.H., Park J.J. Development of severe plastic deformation by various asymmetric rolling processes. *Materials Science and Engineering: A*. 2009. vol. 499, pp. 14-17.

8. Park J.J. Finite-element analysis of severe plastic deformation in differential-speed rolling. *Computational Materials Science*. 2015. vol. 100, pp. 61-66.

9. Pesin A., Pustovoytov D. Finite element simulation of extremely high shear strain during a single-pass asymmetric warm rolling of Al-6.2Mg-0.7Mn alloy sheets. *Procedia Engineering*. 2017. vol. 207, pp. 1463-1468.

10. Zuo F., Jiang J., Shan A. Shear deformation and grain refinement in pure Al by asymmetric rolling. *Transactions of Nonferrous Metals Society of China*. 2008. vol. 18, pp. 774-777.

11. YU H., Lu C. Tieu K. Liu X., Sun Y., Yu Q., Kong C. Asymmetric cryorolling for fabrication of nanostructural aluminum sheets. *Scientific Reports*. 2012. vol. 2, pp. 1-5.

RESTORATION OF THE STEEL BILLET CONTINUOUS CASTING MACHINE ROLLER FACE BY DIRECT LASER FUSION

Pashkeev K., Bykov V., Radionova L., Samodurova M.

*South Ural State University (National Research Institute), Chelyabinsk, Russia
vitaliy.bykov.97@mail.ru*

A robotic complex set of the Laboratory for Mechanics, Laser Processes and Digital Production Technologies was used in this work. [1]

To carry out this research, we took two steel billet continuous casting machine rollers provided by SMS Group (Fig. 1). The steel grade of the rollers is 21CrMoV5-7. It should be noted that the two rollers had different wear on their faces. The main requirement was that the diameters of the rollers remained the same after completion of the work.



Fig. 1. Worn steel billet continuous casting machine rollers

During the work, it was necessary to select such surfacing modes that would ensure minimum porosity, the absence of cracks and that would make it possible to obtain a surface with a hardness of 30-55 HRC according to the customer's requirements. [2-3]

Having analyzed the powder alloy market, we decided to use Castoline Eutalloy

number 16004, with a particle size from 61 to 151 μm and a very fine martensitic structure, to rebuild the steel billet continuous casting machine roller faces. The chemical composition of the alloy is according to the certificate.

Preliminary testing of surfacing modes was carried out on thick-walled pipes made of steel grade C25. The appearance of the obtained samples is shown in Figure 2.

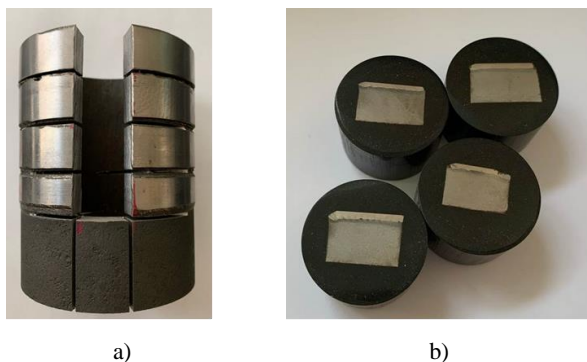


Fig. 2. Appearance: a) beads after direct laser fusion; b) metallographic specimens

Studies of the microstructure at x100 (Fig. 3, a) and x500 (Fig. 3, b) magnification of the sample showed that the surface quality corresponds to the required characteristics, namely, it allows to obtain a minimum porosity of at least 1% in the coating and prevent the formation of cracks and microcracks.

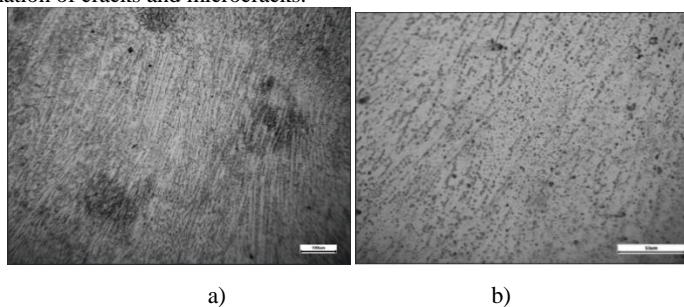


Fig. 2. Microstructure of the deposited layer:
a) at x100 magnification; b) at x500 magnification

Microhardness measurements were carried out on a stationary universal hardness tester model HV-1000. The hardness values were 43 HRC.

References

1. Bykov Vitaly, Radionova Ludmila, Samodurova Marina. Restoration of the Roll Necks Worn Surface by Direct Laser Fusion. MAGNITOGORSK ROLLING PRACTICE 2019 Materials IV International Youth Scientific and Practical Conference. Magnitogorsk, 2019. Vol. 1. pp. 120–122.

2. Grigoryants Alexander. Equipment and Technology for Laser Processing of Materials. Moscow: Vysshaya Shkola, 1990. 159 p.

3. Misyurov Alexander, Fedorov Boris. Laser cladding technology. Moscow: Bauman Moscow State Technical University, 2004. 40 p.

TECHNOLOGICAL HEREDITY AND THE QUALITY OF PARTS MADE BY SHEET STAMPING OF TITANIUM ALLOYS

Adyev E., Burdukovsky V.

*Ural Federal University named after the first President of Russia B.N.Yeltsin,
Yekaterinburg, Russia
eadiev@yandex.ru*

Due to their physical and mechanical properties, as well as constantly decreasing production costs, titanium alloys are widely used today in various fields of technology, especially in the production of parts for aerospace industry. The requirements for the quality of manufactured parts due to the specifics of their work in these areas are very high. As is well-known, the properties of products are formed during the entire set of technological processes involved in their manufacture. Changes in the properties of products during their manufacture and operation are explained by the phenomenon of technological heredity. Technological heredity refers to the phenomenon of transferring the properties of objects from previous technological operations to subsequent ones. The development of the technological process of sheet stamping requires both obtaining special properties of the metal, without which it is impossible to provide the required strength, performance properties of the part and its service life, and providing the necessary geometry of the part.

Sheet stamping of titanium alloy parts is the final technological process of manufacturing the necessary product. The general process of manufacturing a part takes place with alternating deformation of the metal when obtaining a titanium sheet by rolling and when stamping a sheet billet under the influence of various temperature and force factors. It can be argued that the quality of the part after stamping is determined by the features of all previous operations, starting with the receipt of the sheet blank. A special feature of titanium alloys is their low thermal conductivity, high chemical activity, and limited deformability in a cold state. In this regard, most of the titanium alloy deformation processes involve heating of the metal.

One of the important properties of a rolled sheet that is to be stamped is its ability to deform without destruction. The integral indicator of this property is stampability. Stampability depends primarily on the characteristics of plasticity, strength and the ability of the metal to resist the localization of deformation during the deformation process.

The overall structure of the process can be represented as a sequence of changes in the main parameters of the shape, metal structure, strength and ductility characteristics, surface quality and other parameters from the workpiece to the finished part (Fig.1).

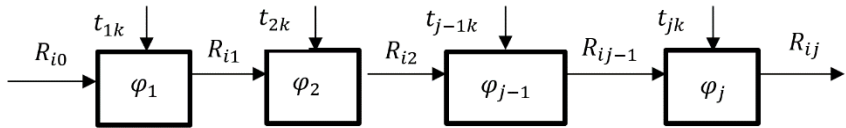


Fig.1. The structure of the technological process: φ_i - technological operations; R_{ij} - initial parameters of the workpiece; t_{ik} - technological parameters of the processing mode

The technological heredity of properties in the part manufacturing process can be described by a graph that reflects the transmission coefficients and the influence of physical, mechanical and geometric parameters. The initial vertex of the graph when describing the technological process is a blank, the final vertex is a finished part. The edges of the graph show the transfer of the workpiece properties during processing. The edge transfer is described by a heredity coefficient K that reflects quantitative changes in properties and is equal to the ratio of the previous S_j and subsequent S_{j+1} values of the property:

$$K = \frac{S_j}{S_{j+1}}.$$

Heredity coefficients describe the influence of technological factors on the considered property for the operation and can be represented in this way:

$$K_l = k_l t_{l_1}^{k_{l_1}} t_{l_2}^{k_{l_2}} \dots t_{l_n}^{k_{l_n}}.$$

To determine the effect of technological heredity on the performance properties of parts obtained by sheet stamping, we recommend a sequence of parameters: characteristics of strength, plasticity, grain size, structural uniformity, surface roughness, and the value and sign of residual stresses.

Methods of technological control and control of technological heredity of parts properties include: measurement of physical, mechanical and geometric parameters of the workpiece and the part during processing; determination of technological heredity mechanisms based on transfer coefficients and the mutual influence of technological and operational properties, development of manufacturing quality control measures.

The reported study was funded by RFBR 19-38-90222 Improvement of the principles of alloying and parameters of external influence to increase the thermal stability and the level of physical and mechanical properties of aviation materials based on titanium and nickel.

References

1. Mazharova G. E. Processing of titanium alloys by pressure. Moscow: Metallurgiya, 1989.
2. Davydov Yu. P. Sheet stamping of titanium alloys. Moscow: Metallurgiya, 1998.
3. Tlustenko S. F, Pervushin A. N. Formation of structure and properties of titanium alloys by mechanical properties in the processes of metal processing by pressure. Bulletin of Samara State Aerospace University 2011. No. 1 (25). pp. 110-118.

4. Zamyatin V. M., Baum B. A. On the question of metallurgical heredity and formation of properties of metal products. Samara: Samara State Technical University, 2010.
5. Kheifets M. L., Vasiliev A. S. Controlled heredity of quality parameters in machine parts. Proceedings of the National Academy of Sciences of Belarus, Series: Physical and Technical Sciences. 2015, No. 1. pp. 10-23.
6. Vasiliev A. S. Formation of operational properties of parts in processing environments. Bulletin of YuUrGU, Series: Mechanical Engineering. 2017. V. 17, No. 1. pp. 33-44.

APPLICATION OF SSRVE CONCEPTION FOR MODELING OF FERRITIC-PEARLITIC STEEL WIRE DRAWING

Konstantinov D., Emaleeva D., Kuznetsova A.

*Nosov Magnitogorsk State Technical University, Magnitogorsk, Russia
const_dimon@mail.ru*

The single pass drawing of rods (a range of diameters from 5 mm to 40 mm) with small reduction (1-3 mm) is one of the most important processes for mechanical engineering, military and car industries. In this case, the final products are different axes, shafts and rod constructions, which are usually used under the static and cyclic loads during all life period of products. For this reason, the inhomogeneity of mechanical properties due to non-uniform deformation is crucial in prediction of the potential reliability of the finished product [1-6]. This problem plays particularly important role in the case of rod drawing process of ferritic-pearlitic steels [7], because inhomogeneity of deformation can lead to large differences in mechanical properties in the workpiece layers. Numerical modelling of the process of rod drawing can be a support for the design of best technologies for these steels. Thus, development of the model, which describes phenomena occurring in the microstructure of the ferritic-pearlitic steels during drawing, was the main objective of the work. Macro level models do not take into account the complicated behavior of the ferritic-pearlitic microstructure in the micro scale [8-9]. Therefore, development of modeling methods, which allow predicting the properties distribution in the metal volume with the behavioral features of the microstructure under the influence of the deformation, was needed [10]. It is an important theoretical problem, which involves specific numerical solutions. Due to necessity of application very fine mesh with large number of elements, these solutions are computationally very costly. Thus, numerical representation of ferritic-pearlitic steels microstructure does not allow using it directly in numerical simulations. Therefore, statistical methods were used to generate Statistically Similar Representative Volume Element (SSRVE) (Figure 1), which simplifies original microstructure.

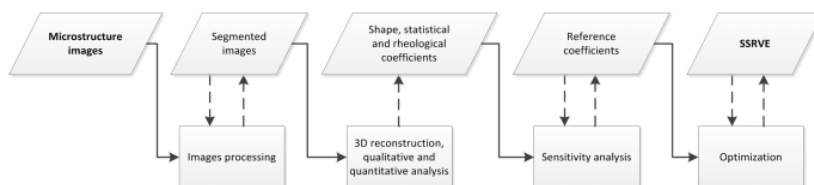


Fig. 1. SSRVE creation scheme

The results showed that multiscale modeling has revealed new technological modes of rod drawing from position of favorable stress-strain state. However, the classical techniques of the multiscale simulations of phenomena occurring in the microstructure are not always optimal from the perspective of the required computational resources. Therefore, the SSRVE concept was applied in the present paper and the following goals were reached: 1) simplifying and automating the process of creating a microstructure model; 2) reduction of the computing time; 3) reduction of the required computational resources. All these goals were reached while the accuracy of the prediction was kept on the reasonably stable level. Further prospective development of the SSRVE conception is application to steels with a more complex microstructure (like as TRIP-steel) and accounting for different deformation mechanisms.

The reported study was funded by RFBR according to the research project №16-38-00619 mol_a.

References

1. S.-B. Son, H. Roh, S.-H. Kang, Relationship between microstructure homogeneity and bonding stability of ultrafine gold wire, *Journal of Materials Science*, 45 (2010) 236-244.
2. L. Sadok, Ł. Luksza, J. Majta, Inhomogeneity of mechanical properties in stainless steel rods after drawing, *Journal of Materials Processing Technology*, 44 (1994) 129-141.
3. M.A. Polyakova, A.E. Gulin, E.M. Golubchik, Alternate drawing as the way for improving mechanical properties of medium carbon steel wire, *IOP Conf. Series: Materials Science and Engineering*, 411 (2018) №012058
4. M.V. Chukin, M.A. Polyakova, K.G. Pivovarova, Y.Y. Efimova, A.E. Gulin, Structure and Properties of Carbon Steel Wire in Drawing, *Steel in Translation*, 48 (2018) 441-445
5. G.H. Hasani, R. Mahmud, A. Karimi-Taheri, On the strain inhomogeneity in drawn copper wires, *International Journal of Material Forming*, 3 (2009) 59-64.
6. A. Pesin, A. Korchunov, D. Pustovoytov, K. Wang, D. Tang, Z. Mi, Finite element simulation of shear strain in various asymmetric cold rolling processes, *Vestnik of Nosov Magnitogorsk State Technical University*, 4 (2014) 32-40.
7. I. Watanabe, D. Setoyama, N. Nagasako, N. Iwata, K. Nakanishi, Multiscale prediction of mechanical behavior of ferrite–pearlite steel with numerical material testing, *International Journal for Numerical Methods in Engineering*, 89 (2012) 829-845.
8. G.B. Sarma, B. Radhakrishnan, T. Zacharia, Finite Element Simulations of Cold Deformation at the Mesoscale, *Computational Materials Science*, 12 (1998) 105-123.
9. D. Konstantinov, A. Korchunov, Multi-Scale Computer Simulation Of Metal Forming Processes, *Vestnik of Nosov Magnitogorsk State Technical University*, 1 (2015) 36-43.
10. S. Wiewiorowska, Determination of content of retained austenite in steels with TRIP effect deformed at different strain rates, *Steel Research International*, 81 (2010) 262-265.

THE STRUCTURE AND PROPERTIES OF CuNiCrSi ALLOY AFTER RADIAL-SHEAR ROLLING

Bunits N., Gamin Y., Kadach M.

*National University of Science and Technology MISiS, Moscow, Russia
lthewall1@gmail.com*

Copper-based alloys (e.g., the CuNiCrSi system) are widely used as conductors, contactors and welding electrodes as a replacement for the popular CuCr and CuCrZr alloys [1]. The above alloy combines high hardness and electrical conductivity. The radial-shear rolling method (RSR) [2] proposed in this article as a technique for producing semi-finished products from copper alloys is currently used to produce bars from titanium alloys [3, 4], steels [5] and other alloys. A lot of research has been carried out to better understand the RSR of aluminum alloys [6, 7], magnesium alloys [8] and copper [9]. However, the main methods for producing semi-finished products in the form of bars from copper and aluminum alloys include pressing or drawing [1].

The aim of this work is to study the changing structure and properties of the CuNiCrSi alloy after hot RSR. CuNiCrSi alloy ingots with a diameter of 110 mm were rolled on a three-roll mill MISiS-130T into bars with a diameter of 60 mm through the following stages: 110 mm→90 mm→75 mm→65 mm→60 mm, with a total drawing coefficient $\mu=3.36$. The temperature of the workpiece before rolling was $T=900\text{ }^{\circ}\text{C}$.

After rolling, the bars were subjected to the following regime of heat treatment (HT): soaking for 1 h at $960\text{ }^{\circ}\text{C}$, then quenching in water; then aging for 4 hours at $495\text{ }^{\circ}\text{C}$ and cooling in air. After RSR and HT, the microhardness and electrical conductivity of the bars were measured and the microstructure was analyzed in three zones: 1 - the center of the bar; 2 - $\frac{1}{2}$ radius; 3 - surface.

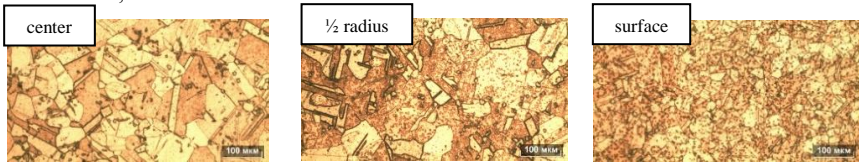


Fig. 1. The microstructure of the alloy CuNiCrSi (x100 magnification)

After RSR (Fig. 1), a characteristic gradient microstructure with a fine grain ($<50\text{ }\mu\text{m}$) in the surface layer is formed, which is attributed to the localization of shear deformations in the zone of contact with the tool [9]. Fig. 2 shows graphs showing how the microhardness changes across the cross section of the bars.

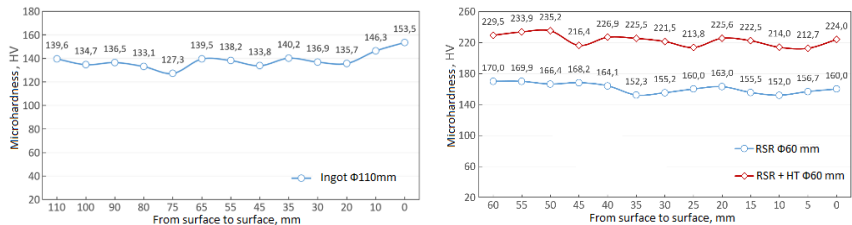


Fig. 2. Distribution of microhardness across the cross section of the CuNiCrSi alloy: as-received ingot (a) and after RSR and RSR + HT (b)

The hardness of the original ingot averages 130...150 HV. After deformation, the cross-sectional hardness increased to 155...170 HV. After HT, the hardness increased to 215...230 HV. The electrical conductivity of the bars after RSR was 30.17 %IACS (Table 1), and, following HT, it increased to 45.17 %IACS.

Table 1 – Electrical conductivity of CuNiCrSi samples

As-received ingot		After RSR		After RSR + HT	
MSm/m	% IACS	MSm/m	% IACS	MSm/m	% IACS
19.80	34.10	17.50	30.17	26.20	45.17

In the Specification (Russian Standard) for hot-pressed semi-finished products made of the CuNiCrSi alloy, the hardness should be at least 180 HB (190 HV), the electrical conductivity – 24 MSm/m (41.4 %IACS). Thus, the properties of the bars obtained by RSR method exceed the regulatory requirements even with a total $\mu=3.36$.

References

1. Osintsev O.E., Fedorov V.N. Copper and copper alloys. Domestic and foreign brands: a directory. 2nd revised ed. Moscow: Innovative Engineering, 2016. 360 p.
2. Galkin S.P., Goncharuk A.V., Daeva E.K., Mikhailov V.K., Romantsev B.A. Multipass screw-rolling system. Steel in Translation. 2003. 33(9). pp. 45-47.
3. Karpov B.V., Patrin P.V., Galkin S.P., Kharitonov E.A., Karpov I.B. Radial-Shear Rolling of Titanium Alloy VT-8 Bars with Controlled Structure for Small Diameter Ingots (≤ 200 mm). Metallurgist. 2018. 61(9-10). pp. 884-890.
4. Romantsev B.A., Goncharuk A.V., Aleshchenko A.S., Gamin Y.V. Production of hollow thick-walled profiles and pipes made of titanium alloys by screw rolling. Russian Journal of Non-Ferrous Metals. 2015. 56(5). pp. 522-526.
5. Romantsev B.A., Gamin Y.V., Goncharuk A.V., Aleshchenko A.S. Innovative Equipment for Producing Cost-Effective Hollow Billets for Mechanical-Engineering Parts of Small Diameter. Metallurgist. 2017. 61(3-4). pp. 217-222.
6. Akopyan T.K., Belov N.A., Aleshchenko A.S. et al. Formation of the gradient microstructure of a new Al alloy based on the Al-Zn-Mg-Fe-Ni system processed by radial-shear rolling. Materials Science and Engineering A. 2019. 746. pp. 134-144.
7. Akopyan T.K., Aleshchenko A.S., Belov N.A., Galkin S.P. Effect of Radial-Shear Rolling on the Formation of Structure and Mechanical Properties of Al-Ni and Al-Ca Aluminum-Matrix Composite Alloys of Eutectic Type. Physics of Metals and Metallography. 2018. 119(3). pp. 241-250.
8. Dobatkin S., Galkin S., Estrin Y. et al. Grain refinement, texture, and mechanical properties of a magnesium alloy after radial-shear rolling. Journal of Alloys and Compounds. 2019. 774. pp. 969-979.
9. Russian Journal of Non-Ferrous Metals. 2020. No. 2.

TREATMENT OF MULTICOMPONENT AL-SI-FE ALLOYS

Ivasik V., Andreyashchenko V.

*Satpaev Ekibastuz Technical and Engineering Institute, Ekibastuz, Kazakhstan
Vi-ta.z@mail.ru*

Modern forming methods are applied to deform a wide range of materials. This is especially true for methods implementing severe plastic deformations. A distinctive

feature of SPD methods is the ability to form an increased level of mechanical, physical and operational properties of processed materials [1]. In addition, as a result of processing by SPD methods, it is possible to deform materials that experience difficulties with plastic deformation under normal conditions. Dominant compressive stresses and formed shear deformations provide a significant refinement of the microstructure and structural components down to the ultrafine-grained and nanoscale structures. When working with these methods, the group of alloys of the Al-Si-Fe system is of a particular interest. This group of alloys is being intensively studied; however, scientists most often focus on aluminum or iron of the triple phase diagram of the Al-Si-Fe alloy. At the same time, there is already enough information that an increase in the proportion of iron and silicon causes properties that are fundamentally different from properties of alloys with an element concentration of less than 5-8%. An analysis of the crystallization features of the Al-Si-Fe alloy [2], as well as earlier studies [3, 4] of the formed phase composition revealed the formation of a highly symmetric phase component. When the temperature reaches 755° C, the Al_3Fe_2Si phase is formed. The Al_3Fe_2Si phase or the τ_5 phase has a hexagonal lattice with the parameters of $a = 1.2404$ and $c = 2.6234$. The τ_5 phase is observed up to a temperature of 551° C. With a further decrease in temperature, the τ_5 phase is completely transformed into the τ_6 phase, which has a monoclinic lattice. The presence of highly symmetric phase components will provide plastic deformation of the alloy under study. To process the alloy, we used the method of equal channel angular pressing with back pressure (ECAPBP). Back pressure was ensured by a step in the tool outlet channel. After the deformation, the processed workpieces were examined using a transmission electron microscope.

Three cycles of ECAPBP promotes the appearance of equilibrium boundaries (indicated by arrows in Fig. 1). In this case, the prevailing grain size is 0.2-0.25 μm . The inclusions of aluminum and silicon carbides are located both along the grain boundaries and within the grain. The grain boundaries are fixed by inclusions with a size of 0.01-0.1 μm , which causes their turn and facilitates grain refinement. As a result of the processing, a compact alloy with an ultrafine-grained structure and nanostructure was produced.

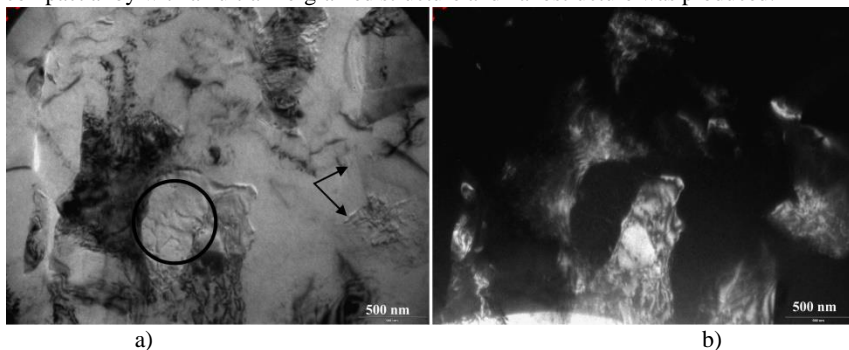


Fig. 1. An Al-Si-Fe alloy after 3 cycles of ECAPBP (TEM), x48000:
a) bright field; b) dark field

References

1. Andreyashchenko V.A. Evolution of Al-Si-Mn-Fe aluminum alloy microstructure in the equal-channel angular pressing with back pressure. *Materials Letters*. 2019.

No. 254. pp. 433–435.

2. Qi M., Kang Y., Li J., Shang B. Improvement in mechanical, thermal conductivity and corrosion performances of a new high-thermally conductive Al-Si-Fe alloy through a novel R-HPDC process. *Journal of Materials Processing Technology*. 2020. Vol. 279. Article 116586.

3. Andreyashchenko V.A., Naizabekov A.B., Bassov V.V. Analyze of Microstructure of Composition Material Al-Si-Fe System. *Journal of Nano- and electronic physics*. 2014. Vol. 6. No. 3. pp. 03007-1-03007-3.

4. Naizabekov A. B., Andreyashchenko V. A. Analysis and study of the possibility of producing an Al-Si-Fe alloy by an equal channel angular pressing method. *Mining and Metallurgy in Kazakhstan. State and prospects: Proceedings of the International Scientific and Practical Conference*. Almaty, 2012. pp. 313-317.

APPLICATION OF RADIAL-SHEAR STRAIN IN THE PRODUCTION OF LONG COMPONENTS WITH ULTRAFINE-GRAINED STRUCTURE

Kharitonov V.¹, Usanov M.², Polyakova M.¹

¹*Nosov Magnitogorsk State Technical University, Magnitogorsk, Russia*

²*Nosov Magnitogorsk State Technical University, Beloretsk Branch, Beloretsk, Russia*
barracuda_m@mail.ru

Currently, one of the most progressive and highly effective approaches to improving the combination of physical and mechanical properties in metals and alloys is based on deliberate formation of ultrafine-grained (UFG) and ultrafine structures in the material by means of various metal forming techniques. These techniques are based on the principles of severe plastic deformation (SPD), in which the structure refinement depends on the following factors: the strain rate; hydrostatic pressure; scale factor and non-monotonic nature of the strain. The main principle of SPD is to ensure a high accumulated degree of strain in the metal when forming a billet without bringing it to fracture [1].

The main (basic) SPD methods are based on the application of either torsion strain – torsion under pressure (TP), or a straining process with a change in the trajectory of the strain path – equal channel angular pressing (ECAP). The issue of achieving the UFG structure in long components (which primarily include wire) is of particular interest since almost all of the known SPD methods are discrete and allow to produce bars of small length.

Of all the currently proposed continuous methods of wire nanostructuring, the methods of equal channel angular drawing and torsion under pressure are the closest to practical application.

Based on the data of applying the principles of these methods, various methods have been proposed for processing long products, such as ECAP drawing, continuous shear drawing – CSD, accumulative angular drawing – AAD, and shear drawing.

Since 2001, the Department of Mechanical Engineering and Metallurgical Technologies (currently the Department of Materials Processing Technologies) at Nosov Magnitogorsk State Technical University (NMSTU), under the guidance of Professor V. A. Kharitonov, has been researching the use of radial shear strain for wire production. This method is called radial-shear drawing (RSD) and implies a simultaneous application of linear strain and torsion shear strain during drawing.

Radial-shear drawing is a method of producing wire by radial-shear strain, which is carried out by applying a front pulling force to the wire (wire rod) without torsion, while simultaneously rotating the roller drawing around the wire. The roller drawing has three non-drive rollers located at an angle of 120° to each other, with feed angles $\beta > 16^\circ$. Each roller has a working cone and a calibration belt [2].

The prototype of radial-shear drawing is radial-shear rolling, which has become widespread for the production of round bars using both hot and cold strain. The principal difference between radial-shear rolling and drawing is the supply of energy to the strain center: when rolling, it is carried out through the drive rolls, and when pulling – through the front end of the workpiece.

A. Yu. Manyakin from NMSTU was first to conduct an experimental study of the RSD installation kinematics. He showed that the drawing force is about 30% lower than when drawing through a monolithic draw die. An experimental laboratory study conducted on U12A steel wire showed that radial-shear drawing helps achieve a deeper penetration of compression strain across the wire cross-section enhancing the wire formability and reducing the number of cycles involved in the wire manufacturing process.

M.Yu. Usanov was first to simulate the process of cold radial-shear drawing in Deform-3D and study the stress-strain state of and the drawing force for workpieces made of steel St3 and steel grade 80 at the following tapered roller angles: $\alpha=4^\circ$, 6° and 8° . He established the following dependencies [3, 4]:

- due to the rotation of the rollers around the workpiece, the stresses act cyclically, which creates a "helical" metal flow and an inhomogeneous stress state with tensile stresses in the center and compressive stresses on the wire surface.

- with a decrease in the tapered roller angle, the torsion angle decreases, which leads to an increase in the accumulated degree of strain.

- the drawing force is significantly lower compared with solid die drawing and tends to increase as the strength of the workpiece decreases due to a wider contact area.

Studies have shown that the use of RSD dies allows to shorten the drawing route by 1-2 passes compared with solid die drawing. The use of the classic roller drawing technique in the drawing operation involving RSD dies will lead to an additional increase in the accumulated degree of strain across the wire cross-section.

Based on the authors' research results, two methods of wire production are proposed:

- a method for producing high-carbon steel with a crushed structure by forming the torsion angle γ (RF patent No. 2498870);

- a method for manufacturing high-tensile wire reinforcement, in which, before being profiled, the workpiece is deformed in RSD dies with equal extensions and torsion in opposite directions (RF patent No. 2502573).

The reported study was funded by RFBR according to the research project №18-58-45008 IND_a.

References

1. R.Z. Valiev, R.K. Islamgaliev, I.V. Alexandrov. Bulk nanostructured materials from severe plastic deformation. Progress in Materials Science. 2000. Vol. 45. pp. 103–189.
2. Kharitonov, V. A., Usanov M.Y. Study of radial-shear wire broaching based

on modelling. Metallurgist. 2014. Vol. 57, Issue 11-12. pp. 1015–1021.

3. Kharitonov V. A., Usanov M.Y. Evaluating the effectiveness of drawing methods with torsion in the manufacture of carbon wire with UFG structure. Letters On Materials. 2016. Vol. 6, Issue 2. pp. 116–121.

4. Usanov M.Yu., Kharitonov V.A. The effectiveness of deformation torsion for the manufacture of UFG structured carbon wire. Vestnik of Nosov Magnitogorsk State Technical University. 2016. Vol. 14, No. 4. pp. 66–71. doi:10.18503/1995-2732-2016-14-4-66-71

COLD HYDROSTATIC EXTRUSION METHOD FOR MAKING MAGNESIUM RODS AND FINE WIRES

Komkova D., Antonova O., Glukhov A., Kalonov A., Volkov A.

*M.N. Mikheev Institute of Metal Physics of the Ural Branch of the Russian Academy of Sciences, Yekaterinburg, Russia
komkova_d@imp.uran.ru*

Magnesium alloys are of interest to the aerospace, automotive and electronic industries due to their low density and high specific strength. Moreover, in recent years, magnesium alloys are of great interest to medicine as materials of good biocompatibility and biodegradability. However, at low temperatures, magnesium demonstrates poor formability. It is caused by the structural features of the hcp-lattice and a limited number of active slip systems. The formation of the fine-structure by severe plastic deformation methods (SPD) such as high-pressure torsion (HPT) or equal-channel angular pressing (ECAP) improves the ductility of materials [1]. But most of the SPD-methods are mainly of academic interest. At the same time, the method of hydroextrusion allows to obtain long rods and sections from magnesium alloys. Nevertheless, for successful deformation of magnesium by hydroextrusion, deformation temperatures above 100°C are required. Application of the lower deformation temperatures leads to the destruction of the sample [2].

In this study, the possibility of magnesium deformation by hydroextrusion at room temperature is shown. A cylindrical magnesium billet with the diameter of Ø10 mm and the length of 70 mm was placed in a thick-walled shell made of copper alloy. The shell is used to prevent magnesium from cracking during hydroextrusion. The assembly (Mg-billet inside Cu-shell) was subjected to one pass of extrusion at room temperature. During deformation, the copper shell was destroyed, and a long magnesium Ø5 mm rod was formed. Mg-rods obtained by such method show high ductility and could be subjected to extrusion at room temperature without the shell or they can be drawn down to smaller diameter rods.

The yield strength of magnesium rods reaches 111 MPa. Moreover, it is found that low-temperature annealing leads to an increase in the yield strength up to 145 MPa. We attribute this temperature-related phenomenon to the processes of self-blocking of dislocations during low-temperature annealing of pre-deformed magnesium [3, 4].

Particular attention is given to the development of technologies for producing fine and extra-fine wires. For example, the paper [5] describes the results of a study that looked at the extra-fine wires with a diameter of up to 0.03 mm made of a wrought magnesium alloy Mg₉₇Zn₁Y₂. However, the method for producing such an alloy and the subsequent process of deformation treatment are complicated. As for pure Mg, there is

lacking information on the use of SPD-methods to produce wires with diameters less than 1.5 mm.

Based on the combination of hydroextrusion in the shell and the following cold drawing, we have developed a process for producing extra-fine Mg-wires. A Mg-rod is inserted into a Cu or Al shell and deformed by hydroextrusion at room temperature. In this case, the shell does not crack during the extrusion process. Then, the several Cu (Al) /Mg-rods obtained are inserted into a Cu (Al) shell with holes located at equal distance from each other, and the assembly is subjected to hydroextrusion. A certain scheme is used to produce Cu/Mg or Al/Mg-composites with different number of Mg-filaments (Fig. 1a) [6]. The diameter of such composites could reach 0.25 mm after drawing. The diameter of the Mg-wires inside the matrix depends on the overall diameter of the composite. Chemical etching in HF and H₂SO₄ acids is used to remove Mg-wires from the Cu- or Al-matrix. As a result, the shell dissolves leaving fine wires of Mg. For example, 0.25 and 0.10 mm Mg-wires have been obtained by extraction from composites (Fig. 1b).

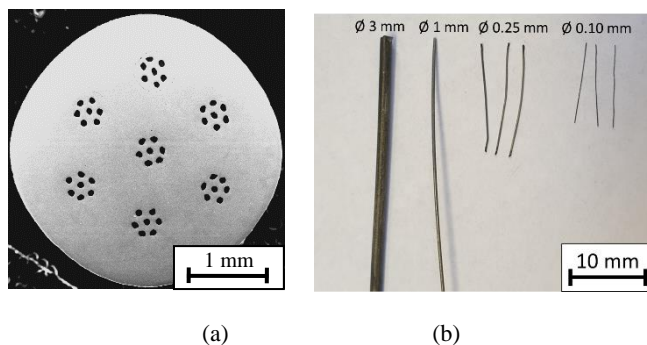


Fig. 1. Cu/49Mg-composite obtained by HE (a); magnesium rods and wires of different diameters obtained by HE in the shell and cold drawing (b)

Such thin Mg-wires could be quite useful in medicine for production of biodegradable and biocompatible ligatures and surgical staples, stents and implants [7]. Therefore, the presented results could support a wider application of magnesium alloys in both the industry and science.

This study was funded by the Russian Foundation for Basic Research (RFBR project No. 18-33-00474) as a part of the following state assignment: "Pressure", No. AAAA-A18-118020190104-3.

References

1. R.N. Harsha et al. *Materials Today: Proceedings*. 2018. Vol. 5. pp. 22340–22349.
2. J. Swiostek et al. *Materials Science and Engineering: A*. 2006. Vol. 424. pp. 223–229.
3. A.Yu. Volkov, I.V. Kliukin. *Materials Science and Engineering: A*. 2015. Vol. 627. pp. 56-60.
4. B.A. Greenberg et al. *Crystallography Reports*. 2012. Vol. 57. pp. 541–549.
5. Y. Kawamura et al. 2018. LPSO2018 Abstracts. p. 52.

6. A.Yu. Volkov et al. Physics of Metals and Metallography. 2018. Vol. 119. pp. 946-955.

7. Y. Zheng. Materials Science and Engineering Reports. 2014. Vol. 77. pp. 1-34.

FEM SIMULATION OF STRAIN GRADIENT IN LOW-CARBON STEEL SHEETS AFTER ASYMMETRIC COLD ROLLING

Pustovoytov D.¹, Pesin A.¹, Zhilyaev A.², Tandon P.³

¹*Nosov Magnitogorsk State Technical University, Magnitogorsk, Russia*

²*Institute for Metals Superplasticity Problems, Russian Academy of Sciences, Ufa, Russia*

³*Indian Institute of Information Technology, Design and Manufacturing, Jabalpur, India
pustovoitov_den@mail.ru*

High strength of metallic materials can be achieved by well-known strategy such as grain refinement by severe plastic deformation (SPD) [1]. However, SPD usually leads to dramatic loss of ductility of materials [2]. Ductility is measured under tensile loading either as total elongation to failure or as uniform elongation. The decrease in ductility with increasing strength is often observed because high strength metallic materials often have low strain hardening rate, as in the case of cold worked metals and nanostructured metals.

Nature is a rich source of inspiration for the design and fabrication of high-performance materials for different engineering application [3]. Gradient structures exist overall in the nature in many biological systems, because they have superior properties over homogeneous structures. Recently gradient microstructures were introduced into metallic materials, including steel, aluminum, copper and other alloys. Creating of gradient microstructure through the thickness of processed materials represents a new strategy for producing a superior combination of high strength and good ductility. In gradient metallic materials the grain size increases gradually from nanoscale at the surface to coarse-grained in the core. For gradient materials high ductility is attributed to an extra strain hardening due to the presence of strain gradient and the change of stress states, which generates geometrically necessary dislocations and promotes the generation and interaction of forest dislocations. Gradient metallic materials have great potential in engineering applications. Generally, the gradient microstructure can be produced by surface SPD technique, such as sliding friction treatment, surface mechanical attrition treatment, surface mechanical grinding treatment, high pressure surface rolling, fast multiple rotation rolling, skinpass cold rolling. The common feature of all these processes is the imparting large plastic strain on the surface of materials. These processes, however, suffer from either low processing efficiencies or limited processed layer thicknesses. Strain gradient can be considered as a mechanism of creating of gradient microstructures. Providing of predetermined strain gradient in metallic materials can be achieved by asymmetric rolling (AR), when circumferential speeds of the top and bottom work rolls are different. AR as a method of SPD can be used for grain refinement both in the surface layer and in the core of the processed material. Since the AR is a continuous process, it has great potential for industrial production of large-scaled sheets. Strain distribution through sheet thickness strongly depends on rolls speed ratio, rolls diameters, thickness reduction per pass, contact friction coefficient.

Many works studied the strain distribution through sheet thickness during AR by using finite element method (FEM). Most of them were focused on process parameters (friction coefficient, the rolls speed ratio and the thickness reduction per pass) which can provide uniform strain distribution through sheet thickness. FEM analysis of the deformation characteristics was presented in, It was found that to obtain a high uniform plastic strain through the sheet thickness the rolls speed ratio (in %) should be equal to thickness reduction per pass (in %). The non-linear effect of the rolls speed ratio on the accumulated strain during AR was found in. It was shown that a very high nonuniform strain distribution through the sheet thickness can be reached when the rolls speed ratio is slightly less than thickness reduction per pass. However, investigations over a wide range of process parameters, which can provide predetermined strain gradient during asymmetric rolling arc yet unknown. The goal of this investigation is searching the optimal process parameters over a wide range of thickness reductions (5...60%), work rolls speed ratios (1...60%), diameters of the rolls (150...450 mm), Coulomb friction coefficients (0.1...0.4) and initial sheet thicknesses (1...8 mm), which can provide predetermined strain gradients during a single-pass asymmetric cold rolling. This paper presents the distributions of the plastic strain through sheet thickness of low-carbon steel AISI 1015 processed by a single-pass AR. The results of investigation can be used for design of technology of producing large-scaled metallic sheets with gradient microstructure.

The predetermined strain gradient through sheet thickness can be achieved by the two different strategies: 1) symmetric rolling with high contact friction; 2) asymmetric rolling with high rolls speed ratio and high contact friction. The main disadvantage of the first strategy is a low strain gradient and a significant increase of the rolling load because of high contact friction. The main disadvantage of the second strategy is a multiple increase of the rolling torques.

Friction coefficient, the rolls speed ratio and the thickness reduction per pass are the main factors which provide synergistic effect on the amount of the effective strain during asymmetric rolling. FEM simulations over a wide range of process parameters have shown, that extremely high strain gradient $\epsilon \sim 4..8$ through sheet thickness can be reached by a single-pass asymmetric rolling, when initial sheet thickness $h_0 = 1.0$ mm, diameter of the rolls $D = 450$ mm, thickness reduction per pass $a = 60\%$, friction coefficient $f = 0.4$ and the rolls speed ratio $AV = 50\%$.

The results of investigation can be used for design of technology of producing large-scaled metallic sheets with gradient microstructure. Further experimental investigation of the asymmetric rolling process is required.

The reported study was funded by RFBR according to the research project № 18-58-45013 IND_a.

References

1. Valiev R.Z., Islamgaliev R.K., Alexandrov I.V. Bulk nanostructured materials from severe plastic deformation (2000) *Progress in Materials Science*, 45 (2), pp. 103-189.
2. Liu Z., Meyers M.A., Zhang Z., Ritchie R.O. Functional gradients and heterogeneities in biological materials: Design principles, functions, and bioinspired applications (2017) *Progress in Materials Science*, 88, pp. 467-498

3. Huang, Y., Wan, L., Lv, S., Liu, H., Feng, J. Gradient micro-structured surface layer on aluminum alloy fabricated by in situ rolling friction stir welding (2013) *Materials and Design*, 52, pp. 821-827.

STEEL WIRE DRAWING IN DOUBLE DIES: PROCESS FEATURES

Martyanov Yu., Bobarikin Yu., Tsyrganovich I.

Sukhoi State Technical University of Gomel, Gomel, Republic of Belarus

You_rock@tut.by

To increase productivity of metal working processes, a double die wire drawing process is proposed. This process provides high productivity by improving the uniformity of stress distribution across the wire cross section [1]. In this case breakage during wire drawing and equipment downtime can be reduced.

With the help of three-dimensional scanning, the geometrical parameters of the drawing channel were obtained. Based on the obtained geometrical parameters, a numerical model of double- and single-die drawing was built [2]. Based on the simulation results, it was confirmed that the stress state corresponds to the hardness distribution obtained by processing the experimental results.

To determine the equivalent stress distribution in the wire cross-section during the drawing process from the ratio of the extracts of the first die to the second die, additional calculations were made in intermediate versions of the relations of the extracts of the die. The results of the uniformity of equivalent stresses distribution are shown in Figure 1.

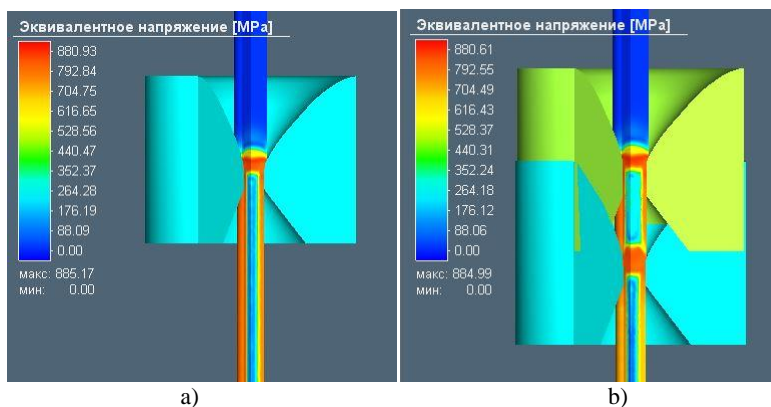


Fig. 1. The results of the uniformity of equivalent stresses distribution: a) single die; b) double die

Figure 1 shows that the stress values in the deformation zone of the first and the second drawing die are almost equal. The stress distribution is uniform in the wire cross section in the deformation zone. After drawing, the stress distribution in the wire is such that the stresses are rising from the center to the surface with no abnormal transition zones. A uniform stress distribution in the wire means a more complete defor-

mation of the wire cross section, which is confirmed by the obtained data on the distribution of microhardness across the cross section. The uniformity of microhardness distribution across the wire cross section after double die drawing is approximately twice higher compared with that in a single die drawn wire. The uniformity evaluation criterion is the standard deviation of the hardness values.

Based on the results of the experiment, it was determined that the most uniform distribution of microhardness across the steel wire cross section is observed in the double die drawn specimens (the standard deviation is 26 units for a double die versus 54 units for a single die). The double die drawn wire has a higher overall hardness compared with the single die drawn wire.

The dependence of the stresses in the wire on the Kd ratio in the investigated section is described by the formula (1):

$$\sigma_{\text{avg}} = 8381.4Kd^3 - 23130Kd^2 + 21391Kd - 5862.8 \quad (1)$$

where σ_{avg} – the average drawing stress in deformation zones during drawing, MPa;
Kd – a ratio between drawing in the first die and drawing in the second die.

Based on the research results, it was determined that the highest drawing stress occurs when drawing in a single die. The double-die wire has a higher hardness compared with the single-die wire. This means more intense wire hardening when drawing in a double die. An increase in Kd leads to an increase in the drawing stress. According to the results of numerical simulation, the most uniform stress distribution is observed at Kd = 0.927. The distribution of drawing stresses in the numerical model corresponds to the distribution of microhardness across the cross section of a thin wire after the experiment, which confirms the adequacy of the constructed model.

References

- 1 V.A. Evdonich. Study of the effect of the application of the double finish drawing die on the plastic properties of steel high carbon wire. *Casting and Metallurgy*. 2019. No. 3. pp.112-117.
- 2 Y.L. Bobarikin, Y.V. Martyanov. Research of the influence of high-carbon steel wire drawing speed on stresses and deformations on wire cross section. *Casting and Metallurgy*. 2019. No. 1. pp. 50-55.

NEW TECHNIQUE OF METAL SURFACE RESTORATION AND REINFORCEMENT

Belevskii L., Belevskaya I., Efimova Yu.

*Nosov Magnitogorsk State Technical University, Magnitogorsk, Russia
l.belevskiy@mail.ru*

At some heavy-manufacturing plants, up to 30% of the output consists of large composite components, in which the working surfaces—for example, for rollers in rolling mills, drive gears, and universal spindles—may be restored so as to extend the working life [1, 2]. This approach is particularly useful for large products such as rollers, each of which may be of mass 230 t in thicksheet mills. The wear of the working surface of the roller barrel is no more than 5–7% of the initial diameter when the roller

is discarded as scrap. For gears, the wear of the working surfaces at the end of the expected life is no more than 0.5% of the total mass. Repeated use of the gear hub is possible if a new gear crown is employed. If a composite design is employed, long spindles may also be restored: the shaft may be reused, while the damaged heads are replaced. In ensuring the reliability and durability of new and restored composite components of this type, a critical problem is to increase the carrying capacity of prestressed joints. Other conditions being equal, their carrying capacity depends on the frictional coefficient f at the contacting surfaces, which may vary widely as the state of the surface changes. In the design of composite rollers and gears, we usually assume that $f = 0.12\text{--}0.14$ [2, 3]. We know that, in machining the contacting plane samples of frictional bolt joints for rotating wire brushes, $f = 0.35$; in sand or shot blasting, $f = 0.58$; and the frictional coefficient is practically the same in laser finishing [4]. The carrying capacity of a prestressed joint may also be increased by electrospark alloying [1] and laser quenching [5].

Study of the microstructure by means of an optical microscope shows that, in all cases, a deformed layer is formed on the surface. A layer of increased etchability (thickness $\approx 50\ \mu\text{m}$) is seen on the surface of the sample treated by the sectional brush (Fig. 1a). The microhardness of the surface layer is 6000 MPa; that of the base is 2000 MPa. The results show that a hard nanostructured surface layer (fragment size up to $0.13\ \mu\text{m}$) may be obtained by means of the rotating wire brush (Fig. 1b). The fatigue strength of prestressed joints is reduced by 60% or more at the contact points on account of local stress concentration and fretting damage. Cold working of frame structures by a hammer face was proposed at the Central Research Institute of Manufacturing Technology. In this method, corrugation in the form of sharp grooves of considerable depth is formed at the machined surface. Cold working neutralizes the harmful influence of the contact pressure and stress concentration on the fatigue strength of the parts and increases the shear strength by a factor of 10–40 in comparison with milled surfaces. The fatigue limit of model plates with corrugated surfaces is at least 1.3 times that of uncorrugated plates.

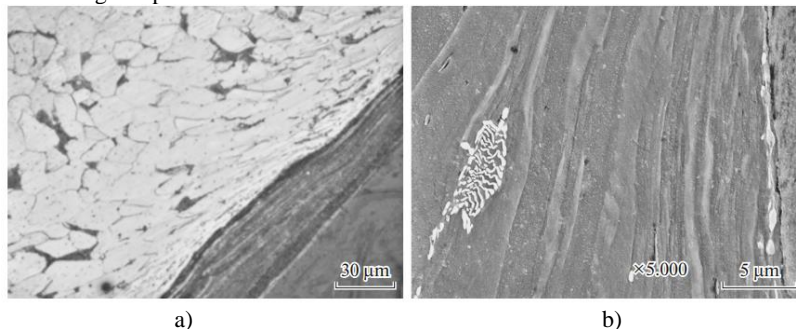


Fig. 2. Microstructure of the surface layer of steel 20 according to an optical microscope (a) and a scanning electron microscope (b).

The proposed approaches may be used in the manufacture of metal components and elsewhere.

The reported study was funded by RFBR according to the research project №17-38-50226 mol_nr.

References

1. Lebed', V.T., Tarel'nik, N.V., and Lashkarev, O.N., Quality improvement of the connection of large-sized composite products, *Visn. Nats. Transp. Univ.*, 2015, no. 4 (1113), pp. 181–184.
2. Belevskii, L.S., Firkovich, A.Yu., Sudorogin, I.V., et al., *Sostavnye prokatnye valki: monografiya (Composite Mill Rolls: Monograph)*, Magnitogorsk: Magnitogorsk. Gos. Tekh. Univ., 2004.
3. Vorovich, I.I., Safronov, Yu.V., and Ustinov, Yu.A., *Prochnost' koles slozhnoi konstruksii (Strength of Complex Wheels)*, Moscow: Mashinostroenie, 1967.
4. Veiko, V.P., Smirnov, V.N., and Chirkov, A.M., *Lazernaya ochildka v mashinostroenii i priborostroenii (LaserBased Purification in Machine and Device Engineering)*, St. Petersburg: S.-Peterb. Nats. Issled. Univ. Inf. Tekhnol., Mekh., Opt., 2013.
5. Alekhin, A.G., Increase of the load-bearing capacity of the pressure couplings based on laser hardening, *Extended Abstract of Cand. Sci. (Tech.) Dissertation*, Volgograd: Volgograd State Univ., 2004.

THE METAL-SAVING TECHNOLOGY OF PIPE ROLLING IN A REDUCING MILL

Orlov A., Loginov Yu.

*Ural Federal University named after the first President of Russia B.N.Yeltsin,
Yekaterinburg, Russia
Alor110@mail.ru*

As is known, when reducing pipes with tension, thickened ends are formed, and they need to be cut.

End thickening is caused by an uneven tension between the mill stands, which leads to increased metal consumption [1].

This paper considers one of the known methods for improving the uniformity of pipe ends, which consists in preliminary thinning of the pipe end cross section in the rolling mill in order to compensate for the subsequent wall thickening in the reduction mill [1,2].

Before a thinning procedure could be developed, production data on the geometry and difference of the end sections were processed [3]. Statistical analysis of thickened ends geometry data showed that a change in wall thickness along the pipe end length can be expressed as a linear relationship.

The obtained linear regression equations are used to calculate the length of the thickened ends depending on the wall thickness tolerances.

The calculated data were further used to develop a methodology for calculating the end thinning regimes of the rough pipe sections in order to compensate for their thickening during subsequent reduction.

The methodology provides the following sequence of calculations.

The length of the front or rear thinned ends was calculated using the condition of thickened end volume constancy according to the experimental data and the volume of the thinned end.

The overall dimensions of the thickened ends after the reduction mill were determined based on actual data. The methodology involves reduction of the ends with a

calculated length in stands 5 and 6 of an 8-stand continuous mill. Only a slight reduction of the pipe walls is achieved in stands 7 and 8, and a gap is formed for the subsequent extraction of the mandrel.

In fact, reduction is carried out by decreasing or increasing the distance between the tool in stands 5 and 6, because the screwdown is usually located on the upper roll. The maximum displacement of the rolls during reduction of the front and rear ends is determined by the maximum reduction on the wall compensating for the thickening.

In this case, the displacement time (closer or further) of the upper roll 5 or 6 of the stand is determined by the length of the thinned end and the average speed of its rolling in the corresponding stand.

The average rolling speed is determined by the maximum speed with maximum wall thinning and the rolling speed in normal mode. The maximum rolling speed is calculated based on the second volumes constancy condition during rolling in stands 5 and 6 (the kinematic tension coefficient is assumed to be 1). In this case, the elongation ratio distribution during rolling of the ends in stands 5 and 6 is $2/3$, which is pursuant to the recommendations given in [4].

Due to the increase in the thinned end rolling speed, the rotation frequency was calculated for the rolls in stands 5 and 6 using the second volumes constancy condition.

When rolling the front end of the pipe in stand 5, the roll rotation frequency sees a linear reduction to the normal mode. Similarly, the roll speed gets adjusted in stand 6 where the pipe front end is rolled.

It should be noted that when the rear end is thinned, it is not necessary to adjust the roll speed because this section of the pipe is rolled during thinning at first only in stand 5, and then only in stand 6, i.e. not in a continuous rolling mode [4].

The average linear displacement velocity of the upper roll of the corresponding stand during rolling of the front or rear end was determined by the value and time of roll displacement.

In conclusion, the developed processing regimes and technical requirements will be used in the future for the preparation of technical specifications, which will enable the development of an automatic pipe end thinning system for the continuous mill TPA-80.

References

1. Danchenko V. N., Chus A. V. Longitudinal rolling of pipes. Moscow: Metallurgiya, 1984. 136 p.
2. Orlov G.A., Orlov A.G. A method of manufacturing pipes. Patent RF, No. 2 677 404. Published: 01.16.2019. No. 2.
3. Orlov G.A., Orlov A.G., Ashkanov S.E. Analysis of the end spacing of pipes after a reduction mill. *Izvestiya Vuzov. Ferrous Metallurgy*, 2017. No. 3. pp. 250-251.
4. Panyushkin E. N., Danchenko V. N., Kondratiev S. V. Development of a methodology for calculating technological parameters and operating modes of the preliminary thinning system of the end sections of "rough" pipes in a continuous mill TPA 30-102. *Modern problems of Metallurgy. Dnepropetrovsk*, Vol. 11, 2008. pp. 155-162.

DEVELOPMENT AND TESTING OF NEW STEEL GRADES BY MODELING THE COMPLEX DYNAMIC PROCESSES INVOLVED IN THEIR PRODUCTION AND OPERATION

Pozhidaeva E., Chikishev D.

*Nosov Magnitogorsk State Technical University, Magnitogorsk, Russia
pozhidaeva.e@icloud.com*

One of the important functions performed by oil pipelines is to ensure reliable and safe operations by minimizing failure risks.

The importance of this research is related to frequent pipeline failures that can lead to catastrophic consequences. Besides the conventional defects of the welded connections, scratch and compression marks, some metal defects manifest themselves as stratification.

The full-scale tests have shown that, having slight deviations in the specified criteria, some pipes have been successfully tested and some have failed due to cracks and their positions.

We looked at the principles behind the development of high-strength steels and studied the technique that helps evaluate upgraded materials for crack resistance.

In the search for new promising steel grades, we developed an algorithm that allows to make an informed choice when it comes to structural materials.

By applying the new algorithm, one can search for new technologies and process solutions that would conform with the constantly changing requirements to low-alloy steels.

The most significant factors were identified that cause segregation in steel plates. The effect of the chemical composition (*C, Mn, V, Nb*) and process factors (roll speed, reduction rate) on defects growth was analyzed. Qualitative and quantitative analyses were carried out to understand the effect of the plate thickness, the temperature regimes and the chemical composition.

Mathematical modelling was performed to simulate the process of rolling workpieces with internal defects. Threshold stress levels were analyzed for the first time that can help eliminate the segregation defect.

A number of various techniques was applied to determine the crack resistance (fracture toughness) under static load.

As a result of comprehensive research, new types of tests have been developed for innovative materials that can help improve the classification of existing steels and other materials.

The conducted research helped develop techniques to predict the growth of segregation based on mathematical modelling; rank the defect nucleation factors; estimate the threshold stress level in the workpiece that can help eliminate segregation.

The algorithm was applied to search for new steel grades with separate properties that would satisfy the demand for low labour and material costs.

References

1. Chikishev, D. & Pozhidaeva, E. *International Journal of Advanced Manufacturing Technology*. (2017) 92: 3725. <https://doi.org/10.1007/s00170-017-0435-6>
2. Salganik, V. Chikishev, D. & Pozhidaeva, E. *Materials Science Forum*, Vol. 870, pp. 584-592, 2016.

THE EFFECT OF HIGH STRAIN-RATE DEFORMATION AND ANNEALING ON THE EVOLUTION OF THE STRUCTURE AND PROPERTIES OF CU–CR–ZR ALLOYS

Abdullina D.¹, Khomskaya I.¹, Zeldovich V.¹,
Frolova N.¹, Kheifets A.¹, Shorokhov E.²

¹ *M.N. Mikheev Institute of Metal Physics of the Ural Branch of the Russian Academy of Sciences, Yekaterinburg, Russia*

² *Russian Federal Nuclear Center-Zababakhin All-Russian Research Institute of Technical Physics, Snezhinsk, Russia*
abdullina@imp.uran.ru

This paper examines the effect of high strain rate deformation (10^5 s^{-1}) attained by dynamic channel-angular pressing (DCAP) and annealing on the microstructure and mechanical and functional properties of low-alloyed dispersion-hardened Cu–Cr–Zr alloys. DCAP [1-3] represents a high strain rate (10^5 s^{-1}) version of ECAP [4]. It was established earlier [1-3] that the deformation induced by simple shear, which forms the structure in the case of ECAP [4], in the case of DCAP is a high strain rate process; furthermore, the specimen is subjected to a shock wave deformation of compression, which creates an additional source of deformation-induced strengthening, and is impacted by temperature. It was shown that specific nonequilibrium SMC and NC structures delivering enhanced properties [3] are formed during the DCAP of copper, which is the result of high strain rate cyclic processes of fragmentation and dynamic recrystallization.

It has been determined that the alloying of copper with chromium (0.09–0.14wt.%) and zirconium (0.04–0.08wt.%) microadditions changes the mechanisms of submicrocrystalline (SMC) structure formation and elastic energy relaxation during DCAP: a cyclic nature of structure formation due to alternative high-rate processes of fragmentation and dynamic recrystallization changes under the influence of fragmentation and partial strain ageing with the precipitation of second-phase nanosized particles.

Annealing (ageing) temperature and time regimes have been established for the Cu–Cr–Zr SMC alloys processed by DCAP aimed at enhancing their mechanical properties and electrical conductivity. Thus, it has been shown that the optimal combination of microhardness (HV=1880 MPa), electrical conductivity (80% IACS), strength ($\sigma_{0.2}$ =464 MPa, σ_u =542 MPa) and ductility (δ = 11 %) in the Cu–0.14Cr–0.04Zr SMC alloy can be obtained through DCAP and ageing at 400°C for 1 h. The enhanced mechanical properties of the alloys versus those of copper are associated with additional strengthening due to precipitation of Cu_3Zr and Cr nanoparticles (5–10 nm) during DCAP and ageing.

It has been shown that the low-alloyed Cu–Cr–Zr alloys have a high ability to strengthen by means of DCAP and SPD by sliding friction [5]. Using the Cu–0.09Cr–0.08Zr alloy as an example, the authors demonstrate that the wear rate of specimens with a SMC structure obtained by DCAP decreases by a factor of 1.4 as compared with coarse-grained state. It was established that a combination of DCAP + ageing at 400°C + SPD by friction results in a friction-induced nanocrystalline structure with the grain size of 15–60 nm in the surface layer, which provides high microhardness (3350 MPa) and a minimum friction coefficient (0.35).

The dynamic properties of alloys with a SMC structure obtained by DCAP have been studied. The tests were carried out under conditions of shock compression at a pressure of 5.6–6.8 GPa and a strain rate of $(0.9\text{--}2.0) \times 10^5 \text{ s}^{-1}$ [6]. By analyzing the evolution of the structure and mechanical properties – and namely, the dynamic elastic

limit, dynamic yield stress, and the spall strength of the alloys – before and after different regimes of DCAP, the authors were able to evaluate the influence of the dispersity and imperfection of the crystal structure on its resistance to high strain rate deformation and fracture. It has been shown that the grain refinement from 200–300 to 0.2–0.3 μm increased the dynamic properties of alloys by 1.5–2.4 times as compared with their initial coarse-grained state.

This research work was carried out as part of the following governmental assignment: “Structure”, No. AAAA-A18-118020190116-6; it was partially funded by RFBR – Grant No. 20-43-660034.

References

1. Shorokhov E.V., Zhgilev I.N., Valiev R.Z. RF Method for dynamic processing of materials. Patent No. 2283717. Byull. Izobret., 2006. No. 26. p. 64.
2. Zeldovich V.I., Shorokhov E.V., Frolova N.Yu., Zhgilev I.N., Kheifets A.E., Khomshaya I.V., Gundyrev V.M. High-Strain-Rate Deformation of Titanium Using Dynamic Equal-Channel Angular Pressing. *Physics of Metals and Metallography*. 2008. Vol. 105, No. 4. pp. 402–408.
3. Khomshaya I.V., Shorokhov E.V., Zeldovich V.I., Kheifets A.E., Frolova N.Yu., Nasonov P.A., Ushakov A.A., Zhgilev I.N. Study of the structure and mechanical properties of submicrocrystalline and nanocrystalline copper produced by high-rate pressing. *Physics of Metals and Metallography*. 2011. Vol. 111, No. 6. pp. 612–622.
4. Valiev R.Z., Aleksandrov I.V. *Bulk Nanostructured Metallic Materials: Obtaining, Structure, Properties*. Moscow: IKTs Akademkniga, 2007. 398 p.
5. Khomshaya I.V., Kheifets A.E., Zeldovich V.I., Korshunov L.G., Frolova N.Yu., Abdullina D.N. The formation of friction-induced nanocrystalline structure in submicrocrystalline Cu–Cr–Zr alloy processed by DCAP. *Letters on Materials*. 2018. Vol. 8, No. 4. pp. 410–414.
6. Khomskaya I.V., Razorenov S.V., Garkushin G.V., Shorokhov E.V., Abdullina D.N. Dynamic strength of submicrocrystalline and nanocrystalline copper obtained by high-strain-rate deformation. *Physics of Metals and Metallography*. 2020. Vol. 4, No. 121. pp. 391–397.

STRUCTURE AND PROPERTIES OF ROLLED SHEETS MADE OF ALUMINUM-MAGNESIUM ALLOYS WITH DIFFERENT SCANDIUM CONTENT: A COMPARATIVE ANALYSIS

Belokonova I., Sidelnikov S., Voroshilov D., Yakiviyuk O.
Siberian Federal University, Krasnoyarsk, Russia
iribelokonova@gmail.com

The relevance of this work is due to the fact that the shipbuilding and automotive industries have a demand for sheet metal with enhanced strength and performance (for example, corrosion resistance) [1]. Aluminum-magnesium alloys possess such characteristics. However, the resource of their mechanical properties has long been exhausted. Recent studies have shown that doping with scandium can potentially improve the mechanical and performance properties of these alloys [2]. At the same time, the relatively high cost of scandium dictates the need to reduce its concentration in the alloy by adding zirconium and other alloying elements.

In this regard, an alloy of aluminum with magnesium (5.2 %) is proposed, in which the content of scandium is 0.12 %, and that of zirconium is 0.13 %. This alloy is referred to as alloy 01580.

The purpose of this research was to develop rational sheet rolling modes for alloy 01580 and to compare the properties of deformed semi-finished products made of it with those of similar semi-finished products made of alloy 01570.

The studies were carried out using a hot rolling mill DUO 330. While developing the rolling regimes, we used proprietary methods, software, and data on the rheological properties of the studied alloys [3]. An analysis of the structure of cast and deformed semi-finished products showed the following (Fig. 1 *a*).

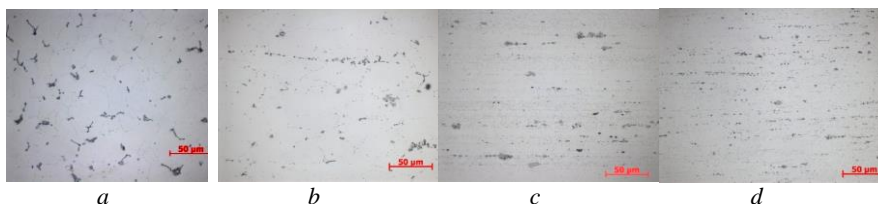


Fig 1. Microstructures of semi-finished products made of alloy 1580 in various conditions ($\times 500$): *a* – ingot after homogenization, $h = 28$ mm; *b* – strip after hot rolling, $h = 10$ mm; *c* – strip after cold rolling, $h = 3$ mm; *d* – strip after rolling and annealing, $h = 3$ mm

A 28 mm thick billet was used that was hot-rolled into 5 and 10 mm strips. The microstructure of the homogenized metal of ingots before rolling consists of crystals of an α -solid solution and inclusions of intermetallic phases located at the boundaries of dendritic cells and grains. These phases typically look like skeletons, veins and irregularly shaped particles. A subgrain structure is formed inside the grains of the solid solution, which is typical for alloys of the Al–Mg system.

It was also found that the use of higher annealing temperatures for the investigated specimens increased the metal's ductility. At the same time, the metal's strength characteristics may turn out to be lower than required (Table 1).

Table 1 – Mechanical properties of metal specimens made of the alloys in view in cast, deformed and annealed states

Type of semi-finished product	h , mm	R_m , MPa	R_p , MPa	A , %
Alloy 1580				
Ingot after homogenization	28	312	183	9.8
Strip after hot rolling	10	369	266	16.0
Strip after cold rolling and annealing	3	390	277	14.0
Alloy 1570				
Ingot after homogenization	28	301	181	7.6
Strip after hot rolling	10	326	204	7.1
Strip after cold rolling and annealing	3	380	252	6.0

Thus, the alloys 1580 and 1570 are comparable in terms of their strength characteristics, while the alloy 1580 has higher plasticity. Therefore, the latter can be recommended for industrial use.

The work is performed as a part of the state assignment for the science of Siberian Federal University, project number FSRZ-2020-0013.

Use of equipment of Krasnoyarsk Regional Center of Research Equipment of Federal Research Center «Krasnoyarsk Science Center SB RAS» is acknowledged.

The reported study was funded by RFBR, the Government of Krasnoyarsk Territory, Krasnoyarsk Regional Fund and Limited Liability Company «Research and production center of magnetic hydrodynamics», project number 20-48-242903.

References

1. Gorbunov Yu.A. The use of aluminum alloy products in the manufacture and repair of land and water transport in RF. *Tekhnologiya legkikh splavov*. 2015. No. 1. pp. 87–92.
2. Baranov V., Sidelnikov S., Zenkin E., Yakivyyuk O. Physical modeling of production regimes to obtain deformed semi-finished products from experimental aluminium alloys doped with scandium. *Materials Science Forum*. 2018. Vol. 918. pp. 54–62.
3. Sidelnikov S.B., Yakivyyuk O.V., Baranov V.N., Konstantinov I.L., Dovzhenko I.N., Lopatina E.S., Voroshilov D.S., Samchuk A.P., Frolov V.A. Computer simulation, analysis of force and temperature-speed parameters of the process of combined machining of Al–Mg–Sc alloys. *IOP Conference Series: Materials Science and Engineering*. 2019. Vol. 544, No. 012018. pp. 1–5.

SIMULATED PRODUCTION OF SEMI-FINISHED ROLLED STOCK FOR COILED TUBING

Alekseev D., Poletskov P., Kuznetsova A., Adishchev P., Emaleeva D.
Nosov Magnitogorsk State Technical University, Magnitogorsk, Russia
d.u.alekseev@mail.ru

The technology of coiled tubing is one of the most promising trends in well drilling and maintenance. This technology is used for both the construction of wells and various maintenance operations. The leading countries in this field are the USA, Canada and China. They produce tubes of a wide range of sizes in 5 strength groups. These countries are also the key suppliers of coiled tubing to Russian mining companies.

The source raw materials in coiled tubing production include hot-rolled coils of low-alloyed steel A606 type 4 [1]. The standard and technical documentation specifies that such steel should combine high strength (for the strength group CT80, the yield strength $\sigma_r \geq 551$ MPa and the ultimate stress $\sigma_b \geq 607$ MPa) and ductility ($\delta_{50} \geq 21$ %) and the following maximum hardness limitations ($HRC \leq 22$) [2]. It is rather difficult to satisfy such conflicting requirements. However, it is possible to fulfill them by using a controlled chemical composition and obtaining a relevant steel structure by means of controlled rolling and accelerated cooling. In order to do it, one needs to understand how the mechanical properties of hot-rolled coils tend to change depending on the main parameters of thermal and mechanical treatment.

The conducted research was based on the physical simulation performed at the facili-

ties of the *Termoderform-MGTU* Research Center [3, 4]. The authors determined how the mechanical properties and the microstructure of steel for coiled tubing tend to change under various regimes of controlled rolling and accelerated cooling. The established regularities served as the basis for the recommended temperature and deformation regimes for the field implementation at PJSC MMK. Hot strip mill 2000 was used for pilot rolling of coils with the size of 3.91x1180 mm and the total weight of 633 t. The mechanical properties of the rolled products satisfied all the requirements of the applicable specification.

The reported study was funded by RFBR according to the research project №16-38-00619 mol_a.

References

1. Poletskov P.P., Alekseev D.Yu., Kuznetsova A.S., Nikitenko O.A. Analysis of technical requirements for semi-finished rolled stock for coiled tubing. *Vestnik of Nosov Magnitogorsk State Technical University*. 2020. Vol. 18, No. 1. pp. 49–54.
2. ASTM A606/A606M – 15. Standard Specification for Steel, Sheet and Strip, High-Strength, Low-Alloy, Hot-Rolled and Cold-Rolled, with Improved Atmospheric Corrosion Resistance.
3. Salganik V.M., Poletskov P.P., Artamonova M.O. et al. Termoderform research and production complex to develop new technologies. *Steel*. 2014. No. 4. pp. 104–107.
4. Salganik V.M., Denisov S.V., Poletskov P.P. et al. Production process physical simulation for hot rolled plates showing a unique set of properties. *Vestnik of Nosov Magnitogorsk State Technical University*. 2014. No. 3. pp. 37–39.

ASSESSMENT OF THE STRUCTURE AND MODIFICATION ABILITY OF THE EXPERIMENTAL AL-3TI-1B BAR LIGATURE OBTAINED BY THE METHOD OF INGOTLESS ROLLING-EXTRUDING

Voroshilov D.¹, Sidelnikov S.¹, Startsev A.², Medvedev M.¹

¹*Siberian Federal University, Krasnoyarsk, Russia*

²*LLC “RUSAL ETC”, Krasnoyarsk, Russia
sibdrug@mail.ru*

To modify aluminum alloys, ligatures of the Al–Ti–B system are currently widely used [1]. However, the practice of using imported inoculants is still popular in Russia, with preference given to the bar ligature composition of Al-5Ti-1B (5% titanium, 1% boron, the rest is aluminum) of “KBM Affilips” foil quality.

The method of ingotless rolling-extruding (IRE) was used to obtain a bar from the experimental Al-3Ti-1B ligature (3% titanium, 1% boron, the rest is aluminum) [2, 3]. The essence of the method is a comprehensive uneven extrusion and shear deformation of the sample, which significantly changes the structure and properties of extruded products. Ingotless rolling-extruding of the experimental ligature was carried out in the laboratory combined processing unit of CRE-200 [2], which is shown in Fig. 1.

A known method was used to obtain the bar [2, 3]. The mechanical properties of the metal of the obtained ligature bars were analyzed with the help of the tensile method on a universal testing machine LFM400. Thus, the tensile strength was 120±3 MPa, the yield strength was 74±3 MPa, and the elongation was 30±1 %. This level of strength and plastic properties ensures the coiling of the resulting bar, which has a diameter of 9 mm. This is a necessary quality that makes an automatic feed of the inoculant possible at industrial foundries.

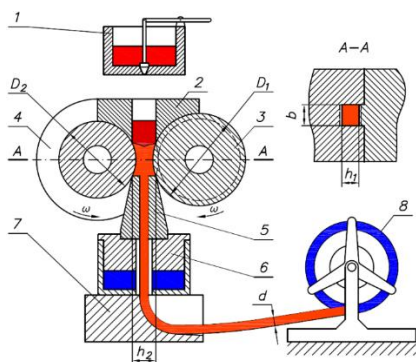


Fig. 1. Combined processing unit CRE-200: 1 – mixer furnace; 2 – proportioner; 3 – roll with a protruded part; 4 – grooved roll; 5 – extruding die; 6 – ring hydraulic cylinder; 7 – tracking unit; 8 – coiler

Figure 2 shows photos of the microstructure of the Al-3Ti-1B ligature in the molten state (Fig. 2 *a*) and in the form of a hot-extruded bar (Fig. 2 *b*) obtained by high-speed crystallization-deformation using the IRE method.

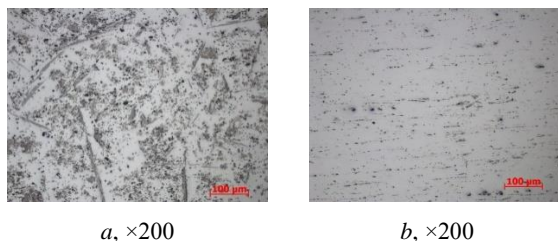


Fig. 2. The microstructure of the ingot (*a*) and bar (*b*) made of the experimental Al-3Ti-1B ligature obtained by the IRE method

The microstructure of the ligature bar is an oriented arrangement of TiB_2 and Al_3Ti particles in the deformation direction. The particle distribution in the bar is not uniform, which is due to the presence of regions with a low density of TiB_2 and Al_3Ti . Al_3Ti particles can reach 50 microns in length. Small amounts of 1.5-0.5 μm TiB_2 particles are present in large quantities in the structure. A qualitative assessment of the microstructure showed that the amount of large Al_3Ti compounds is significantly smaller in the ligature bar than in the ligature ingot. Thus, ingotless rolling-extruding resulted in drastic microstructural changes in the ligature. The agglomerates and accumulations of TiB_2 crystals completely disappeared. As a result of high-speed crystallization-deformation of the metal, they were transformed into filamentous lines of separate particles with the sizes up to 5 microns. As a result of IRE, large Al_3Ti crystals, the sizes of which in the cast structure would reach 200 microns or more, were divided into small 10-50 micron particles.

The work is performed as a part of the state assignment for the science of Siberian Federal University, project number FSRZ-2020-0013.

Use of equipment of Krasnoyarsk Regional Center of Research Equipment of Federal Research Center «Krasnoyarsk Science Center SB RAS» is acknowledged.

References

1. Napalkov V.I., Bondarev B.I., Tararyshkin V.Ch., Chukhrov M.V. Ligatures for the production of aluminum and magnesium alloys. Moscow: Metallurgiya, 1983.
2. Sidelnikov S.B., Lopatina E.S., Dovzhenko N.N., Drozdova T.N. et al. Peculiarities of structure formation and metal properties during high-speed crystallization-deformation and modification of aluminum alloys: a collective monograph. Krasnoyarsk: SibFU, 2015.
3. Sidelnikov S.B., Dovzhenko N.N., Zagirov N.N. Joint and combined methods of processing of non-ferrous metals and alloys: monograph. Moscow: MAKS Press, 2005. 344 p.

UNDERSTANDING THE RELATIONSHIP BETWEEN TENSION AND ENERGY COSTS IN A QUARTO REVERSING MILL ROLLING OPERATION

Strashkova N., Inatovich J.

*Ural Federal University named after the first President of Russia B.N.Yeltsin,
Yekaterinburg, Russia
ankudinova.natasha@mail.ru*

To implement a cold sheet rolling process at operating mills (in particular, at reversing mills) that would be rational from the point of view of energy costs and tension modes, one should understand the effect of tension stresses on the energy efficiency of the process [1, 2, etc.]. Therefore, research aimed at the development of energy-saving modes for cold sheet rolling operations based on the optimal tension ratio is of relevance.

To search for optimal tension stresses, a mathematical apparatus was used [3, etc.]. The process model was presented as the following ratio:

$$W = \min [W(q, u)] , \quad u \in U ,$$

where: W - objective function of the specific power consumption linked to the rolling operation; q - a set of variables characterizing the process status parameters, i.e. a mathematical (formalized) model of the process; u - system control parameters: rear and front tension voltages.

The status and control parameters include certain restrictions applied to them. The mathematical model of the cold sheet rolling process realized on a reversing mill equipped with a working quarto stand and front and rear winders (unwinders) was built on the basis of the papers [4 and 5].

The total energy consumption for the reverse rolling process in each pass was determined by the algebraic sum of the powers N_{Σ} of the electric motors of the working stand N_B , tension winder N_1 and unwinder N_0 (rear winder). At the same time, it was necessary to take into account that the unwinder electric motor works in the generator mode. The specific energy costs will be as follows:

$$W_{\Sigma} = \frac{N_{\Sigma}}{\Pi} , \text{ kWh / t}$$

where: Π - the mill productivity.

The process power parameters, including the tension and the power N_B , were calculated using A.I. Tselikov's method [4], and the required capacities N_1 and N_0 were calculated based on A.A. Korolev's method. The search for the extreme value of the objective functions was based on targeted enumeration of control parameters.

The below figure shows the results of modeling the changing specific energy consumption depending on the magnitude of the front σ_1 and rear σ_0 tension stresses (σ_{s0} and σ_{s1} are the deformation resistance before and after the passage, respectively) when a 1,045 mm wide electrical steel strip was reduced from the thickness of 0.7 mm to the thickness of 0.29 mm on a reversible single-stand mill 1200 in one pass. Currently, the rolling is carried out at $\frac{\sigma_0}{1,15\sigma_{s0}} = 0.001$ (minimum back tension) and $\frac{\sigma_1}{1,15\sigma_{s1}} = 0.192$. The energy costs in this case amounted to 112 kWh / t (Fig. 1).

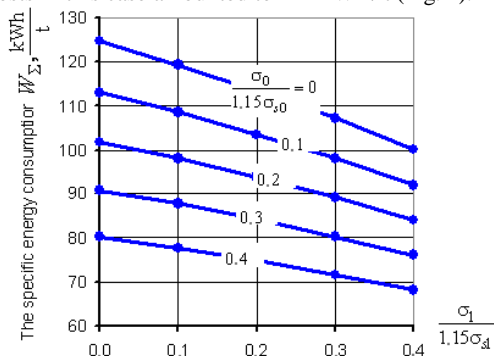


Fig. 1. Relationship between the front σ_1 and rear σ_0 tension and the specific energy consumption during rolling

It can be seen that an increase in the relative back tension to a value of 0.2 will reduce the energy costs to ~ 95 kWh / t, i.e. by 15%.

In the above considered case, the minimum energy consumption of 70 kWh / t can be attained when the front and rear tensions are close to the maximum allowable values.

Firstly, this can be attributed to the fact that as the front tension rises, the lead and, consequently, the length of the lead zone, in which the excess rolling power is removed, increase too. And, secondly, a rising rear tension is associated with a rising power generated by the electric motor of the rear winder (unwinder).

References

1. Garber E.A. Production of rolled products: Reference publication. Volume 1. Book 1. Production of cold rolled strips and sheets (assortment, theory, technology, equipment). Moscow: Teplotekhnika, 2007. pp. 185-187.
2. Chernov P.I., Mukhin Yu.A., Bakhaev K.V. The influence of the interstand tension modes on the specific energy consumption for sheet cold rolling. Proceedings of the Sixth Congress of Rolling Mill Operators. Moscow: Association of distributors. 2006. pp. 186-190.
3. Ventzel E.S. Operations research: tasks, principles, methodology. Moscow: Nauka, 1980. 208 p.
4. Tselikov A.I., Grishkov A.I. et al. Theory of rolling. Moscow: Metallurgy, 1970. 358 p.
5. Korolev A.A. Designs and calculation of machines and mechanisms of rolling mills: Textbook for university students. Moscow: Metallurgiya, 1985. 376 p.

EFFECT OF VARIOUS PROCESS PARAMETERS ON THE BAKE HARDENING EFFECT IN CONTINUOUS HOT-DIP GALVANIZING LINE

Fomin M., Pesin A., Potaptsev D.

Nosov Magnitogorsk State Technical University, Magnitogorsk, Russia

mihail_fomin_95@mail.ru

As before, converter steel sheets continue to play a leading role as a structural material for car manufacturing. Every year, over 60 million cars come off assembly lines and go to the world markets.

The new century has set a new challenge for automotive designers, i.e. to reduce the fuel consumption to 2.5 liters or less per 100 km for a C class car weighing about 1,000 kg. This task could be accomplished by reducing the weight of the vehicle by 20-25 % using thinner steel sheets for the car body. The latter usually accounts for one third of a car's total weight. However, it can only be possible if the strength of steel is increased up to the level that ensures high passenger safety.

Bake hardening (BH) is a phenomenon occurring in steel materials and corresponding to an increase in the yield strength after pre-straining followed by heat treatment baking within a specific temperature range. Classical BH magnitudes are from 30 up to 60 MPa applied after some pre-straining and heating at around 170 °C (443 K) for 20 min [1].

Steels in the BH range are designed for visible (door, hood, tailgate, front wing, roof) and structural (underbody, reinforcement, cross member) parts of a vehicle (Fig. 1) [2].

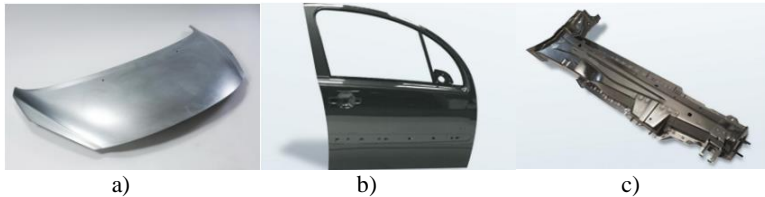


Fig. 1. Visible and structural parts of cars: a) bonnet in CR180BH; b) door in CR240BH; c) front longitudinal beam in CR270BH [2]

The BH value primarily depends on the chemical composition (C, Ti, Nb, N). To maintain the stability of the BH value, manufacturers tend to narrow the chemical composition range. In the course of this study, the impact of annealing temperature on the BH value on a Continuous Hot-Dip Galvanizing Line was observed. It is shown that the magnitude of the BH effect in the steel grades HX180BD and HX220BD depends on the strip temperature at the rapid cooling zone exit (Fig. 2).

For both HX180BD (1) and HX220BD (2), the following regression equations have been approximated:

$$y = 108,36\ln(x) - 642,91; R^2 = 0,1081 \quad (1)$$

$$y = 104,46\ln(x) - 617,62; R^2 = 0,1093 \quad (2)$$

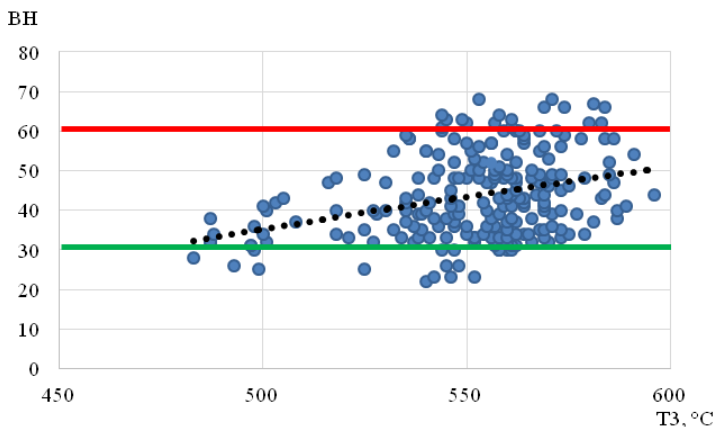


Fig. 2. The effect of the annealing temperature (T_3) on the BH value for HX220BD

To continue this work, it is planned to build a neural network to take into consideration the combined effect of the chemical composition and the temperature T_3 . This will allow us to influence the BH value more effectively. Meanwhile, the given regression equations can be utilized for practical purposes.

The reported study was funded by RFBR according to the research project № 18-58-45013 IND_a.

References

1. Kvackaj T., Mamuzic I. Development of bake hardening effect by plastic deformation and annealing conditions. *Metallurgiya*, 2006. Vol. 45. pp. 51–55.
2. Kuang C.F., Li J., Zhang S.G., Wang J., Liu H.F., Volinsky A.A. Effects of quenching and tempering on the microstructure and bake hardening behavior of ferrite and dual phase steels. *Materials Science and Engineering: A*. 2014. Vol. 613. pp. 178–183.

INVESTIGATION OF ASYMMETRIC ROLLING IN RELIEF ROLLS

**Naizabekov A.¹, Lezhnev S.¹, Tymchenko A.²,
Panin E.², Fedchenko O.², Charaeva Z.²**

¹Rudny Industrial Institute, Rudny, Kazakhstan

²Karaganda State Industrial University, Temirtau, Kazakhstan
sandrachka_97@mail.ru

Analyzing literature sources [1-3] related to asymmetric rolling of thick sheets with the implementation of shear deformations in the longitudinal and transverse directions, methods of asymmetric rolling were considered, where asymmetry is created by both kinematic and geometric parameters. As a result, it was found that asymmetric rolling effectively implements shear deformation in the longitudinal and transverse directions. Therefore, combining these methods will enable to achieve the best results.

This paper describes a method for rolling thick sheets, which includes rolling a blank in relief rolls of the first stand having a significant mismatch of the circumferential speeds followed by alignment of the blank in smooth barrel rolls (Fig.1a).

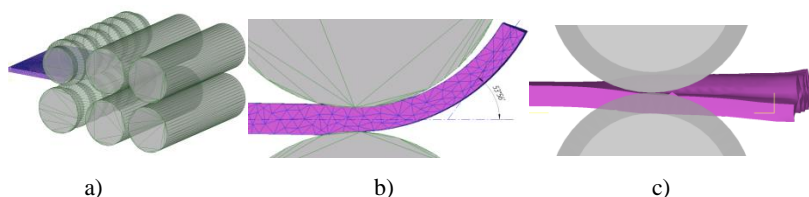


Fig. 1. New technology of thick sheet rolling

a – general view; b – deformation in smooth barrel rolls; c - deformation in relief rolls

To analyze the effectiveness of the proposed method, mathematical modeling was performed in the Deform program. The simulation included a comparison of the proposed rolling method with symmetrical rolling in relief rolls (which is a similar technique) and asymmetric rolling in smooth rolls (which is a well-known method). The following parameters were selected for comparative analysis: equivalent deformation (which characterizes the overall level of metal processing) and the degree of strip bending (which is the angle between the front end of the strip and the horizontal plane).

For asymmetric rolling in both smooth and relief rolls, the following values of the circumferential speeds of the rolls were set:

- 80 rpm / 60 rpm (asymmetry coefficient $k_A = 1.3$);
- 90 rpm / 60 rpm (asymmetry coefficient $k_A = 1.5$).

The original blank had the following dimensions: $h \times b \times l = 10 \times 200 \times 150$ mm. B63 brass was selected as the material, which was heated to 600 °C. An elastic-plastic type of material was used for the blank, and the rolls were made of a rigid material. The diameter of the rolls in all models was equal to 100 mm.

When analyzing the bend of the strip, it was found that asymmetric rolling in smooth rolls causes a significant level of bending of the front end of strip. For example, in the model with the asymmetry coefficient of 1.3, the bending angle exceeds 45 degrees, and in the model with the asymmetry coefficient of 1.5, the bending angle is more than 53 degrees (Fig.1b). At the same time, in all models with relief rolls, the bending angle does not exceed 4 degrees (Fig.1c). This positive effect is achieved due to the fact that the protrusions and depressions formed in the workpiece act as stiffeners preventing the strip from bending in the vertical plane. Consequently, as the billet exits the relief rolls almost horizontally in these models, the billet can be rolled continuously and be captured by the downstream rolls without a problem.

In addition to the strain state, the energy parameters of rolling in relief rolls were also examined as part of the study. Using the work balance method, a formula was derived for determining the specific pressure for rolling in relief rolls. Also, to determine the rolling force, dependencies were established for determining the length of the deformation zone and the width of the total contact surface area. Analysis of the calculated data on the obtained formulas and simulation results showed a high degree of convergence, the error was 6-7 %.

In general, the nature of the strain distribution in this method is similar to that typical of symmetrical rolling in relief rolls. However, 2 facts should be noted here:

1) the overall level of strain is much higher, reaching a difference of more than 40% in the areas of maximum processing;

2) more uniform processing of the metal along the width of the workpiece, which is the result of additional deformation of the longitudinal shift due to the asymmetry factor.

References

1. Perogiv A.A., Smirnov Ye.N., Mityev A.P. Understanding the effect of asymmetric rolling on transverse deformation of thick strips. Young People's Perspective on 21st Century Metallurgy. Proceedings of Ukrainian National Science Conference among DonNTU's Students of Physics and Metallurgy. Donetsk: DonNTU, 2011. pp. 79-80.

2. Belskiy S.M. Steel strip and sheet forming process optimized through the development of symmetric and asymmetric hot rolling techniques. Doctoral dissertation. Lipetsk, 2009. 376 p.

3. Pesin A. M., Salganik V. M., Dyja H., Chikishev D. N., Pustovoitov D. O., Kawalek A. Asymmetric rolling. Theory and Technology. 2012. No. 5. pp. 358-362.

MICROMECHANICS SIMULATION OF COLD ROD DRAWING

Konstantinov D., Korchunov A.

*Nosov Magnitogorsk State Technical University, Magnitogorsk, Russia
const_dimon@mail.ru*

Computer simulation of metal forming processes is one of the key tools of engineering design, which allows one to reduce the labour intensity of the new technology development process. The finite element method (FEM) and the cellular automata (CA) method are traditional calculation methods in this case, each of which allows to achieve the required degree of calculation accuracy of stress-strain state of a metal depending on the goals and objectives of the simulation. The traditional approach to metal forming process simulation is when one assumes that processed metallic materials are isotropic. This approach allows to reduce labour model preparation process, its calculating time, required input data and calculating resources. The development of new advanced materials and methods of metal forming resulted in substantial increase in the requirements for the computer model prediction accuracy [1, 2]. Improving the accuracy of simulation is one of current interest for cold plastic deformation processes, where the stress-strain state parameters are a key determinant of both the final product property formation and process stability. The objective need for accounting the processing material microstructure resulted from the necessity to obtain more complete and accurate information about stress-strain state of a metal in the deformation zone during cold plastic deformation processes. This in turn led to the concept of a multilevel process of plastic deformation according to which the plastic deformation in metals and alloys occurs at different hierarchical scale structural levels [3]. This conceptual approach permitted to systematize the conceptual elements of the implementation and localization of plastic deformation at different scale levels. During the development of a multilevel approach the fact has been proven that the study of micro-level of stress-strain state cannot be carried out without macrolevel estimation and vice versa. At present the results of studies show a lack of predictive ability of the models, assuming that a deformable material is only isotropic [4-7]. Moreover, to describe a range of modern steels (such as steel of grades TWIP, DP, TRIP) from the isotropic material point of view is not possible, as in this case, when simulating cold plastic deformation the

main engineering distinctive features of the microstructural behaviour of these materials will not be considered [1, 2, 8].

A two-level concept of plastic deformation description formed the basis for the creation of multiscale models, designing of which is based on pair-wise interaction of the macro model (the traditional model where isotropic materials are used) and a representative volume model (a microstructure segment model). The first model allows to obtain general information on the macro loading and macro deformations experienced by the deformable metal, and the second model reflects the behaviour of metal individual micro volume at a specific point of macro model under these stresses. Thus, the development of methods for multiscale modeling is an actual theoretical problem of metal forming, and this article is devoted to one of the possible solutions of this problem. A method for simulation of axisymmetric cold plastic deformation processes with allowance for the microstructure of steel was proposed. The use of this method relating to the drawing process of low carbon steel rods permitted to obtain both more accurate and quite different stress-strain state parameters and their distribution: 1. the micro model allowed high tensile longitudinal stresses on the rod axis to be detected, but the macro model showed no areas of negative stress-strain state; 2. multiple localizations of radial compressive strains (from -0.08 to -0.33) were revealed at the micro level of a metal; 3. a micro model allowed to study the straining interaction of the microstructure elements, thus explaining the presence of higher radial strains in the ferrite phase close to a large concentration of perlite grains. The further development of the method proposed aims at the simulation of modern materials of more complex structure such as TRIP, DP, TWIP steels.

The reported study was funded by RFBR according to the research project №16-38-00619 mol_a.

References

1. Wiewiorowska S., Determination of content of retained austenite in steels with TRIP effect deformed at different strain rates, *Steel Research International*. 81 (2010) 262-265.
2. Wiewiorowska S., The influence of strain rate and strain intensity on retained austenite content in structure of steel with TRIP Effect. *Solid State Phenomena*, 165 (2010) 216-222.
3. V.E.Panin, Y.V.Grinyaev, V.I.Danilov et al., *Structural Levels of Plastic Deformation and of Fracture*, Nauka, Novosibirsk, 1990.
4. Hasani G., Mahmudi R., Karimi-Taheri A.. On the strain inhomogeneity in drawn copper wires, *International Journal for Materials Forming*. 80 (2009) 388-391
5. Park H., Lee D., The evolution of annealing textures in 90 pct drawn copper wire, *Metallurgical and Materials Transactions A*. 34A (2003) 531-541.
6. Schroeder J., Balzani D., Brands S.. Approximation of random microstructures by periodic statistically similar representative volume elements based on lineal-path functions, *Archives of Applied Mechanics*. 81 (2011) 975-997.
7. Son S.-B., Roh H., Kang S.-H., Relationship between microstructure homogeneity and bonding stability of ultrafine gold wire, *Journal of Materials Science*. 45 (2010) 236-244.
8. Watanabe I., Setoyama D., Nagasako N., Iwata N., Nakanishi K.. Multiscale prediction of mechanical behavior of ferrite-pearlite steel with numerical material testing, *International Journal for Numerical Methods in Engineering*. 89 (2012) 829-845.

EFFECT OF THERMOMECHANICAL TREATMENT ON THE STRUCTURE AND PHYSICAL AND MECHANICAL PROPERTIES OF AL-7%REM AND AL-0.6%ZR CONDUCTOR ALLOYS PRODUCED BY ELECTROMAGNETIC CASTING

Belov N.^{1,2}, Korotkova N.¹, Timofeev V.³, Akopyan T.^{1,2}

¹ National University of Science and Technology MISiS, Moscow, Russia

² Nosov Magnitogorsk State Technical University, Magnitogorsk, Russia

³ Siberian Federal University, Krasnoyarsk, Russia

nikolay-belov@yandex.ru

In the studies conducted by the All-Russian Institute of Light Alloys (VILS) in the 1970s-1990s led by V.I. Dobatkin [1], the researchers suggested that granular aluminum alloys with added cerium and other REMs (namely, 01417 alloy) could be used to produce heat-resistant alloys. As the granulation technology is rather complicated, the Research and Production Center for Magnetic Hydrodynamics developed another technology consisting in the production of long small-section rods by electromagnetic casting (EMC) [2]. The EMC process takes place at a rather high temperature (up to 900 °C) and ensures an ultra-high rate of solidification (10^3 – 10^4 °C/s). Thus, the same structure can be obtained as in alloys (in particular, a higher percentage of Zr) produced by the granulation technology.

The paper [3] describes a comparative analysis of Al-REM and Al-Zr alloys used to produce heat-resistant wires. By comparing performance properties (electric resistance, strength and heat resistance), manufacturability and cost-effectiveness of Al-0.3%Zr and Al-7%REM alloys, we established a significant advantage of the former. This paper describes a comparative analysis of the alloys of such systems as applicable to the EMC technology. In view of the above [4], we chose to use the alloy with a higher concentration of zirconium (0.6%).

Al-0.6%Zr-0.4%Fe-0.4%Si alloy was used to demonstrate potential applicability of the EMC method to produce wires that can offer a better combination of strength, electrical conductivity and thermal stability attributed, primarily, to a high cooling rate during the solidification process. Experimental and computational methods showed that casting temperatures over 820°C are required to ensure a complete immersion of zirconium in the aluminum solid solution (Al). It was found that, in a cast rod, iron was fully immersed into the phase Al_3Fe_2Si located in the form of thin veins along the boundaries of dendritic cells (Fig. 1a). The as-cast EMC rod has high ductility when high degrees of deformation (over 98%) are applied during cold drawing. Wire annealing at 400 °C results in a considerable increase in electrical conductivity and ensures a high level of strength properties. This is attributed to the formation of nanoparticles of the Al_3Zr phase (Fig. 1b) and, consequently, a lower concentration of Zr in (Al).

The application of the EMC method for the Al-Zr(Fe,Si) alloys has several advantages. Firstly, such advantages include a higher content of Zr in (Al) as compared with the conventional technology, which results in higher strength and maximum operation temperature. Secondly, hot rolling excluded from the wire manufacturing process will make the process easier (to the extent of continuous casting and drawing). Thirdly, such microstructure (submicron eutectic particles, see Fig.1a) contributes to a higher acceptable content of iron and silicon providing economic advantages.

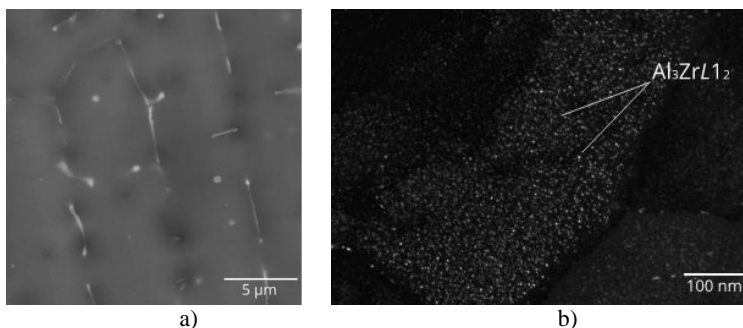


Fig. 1. Structure of the Al-0.6%Zr-0.4%Fe-0.4%Si alloy: a) an original cast rod (8 mm), SEM, b) a wire (0.5 mm) after annealing at 400 °C

References

1. Dobatkin V.I., Elagin V.I., Fedorov V.M. Rapidly solidified aluminum alloys. Moscow: VILS, 1995. 341 p.
2. Avdulov A.A., Usynina G.P., Sergeev N.V., Gudkov I.S. Distinctive features of the structure and properties of long, small-section rods from aluminum alloys cast in an electromagnetic mold. *Non-Ferrous Metals*. 2017. No. 7. pp.73-76.
3. Belov N.A., Alabin A.N., Toleuova A. Comparative analysis of alloying additives as applied to the production of heat-resistant wires. *Metal Science and Heat Treatment*. 2011. Vol. 53, No. 9. pp. 455-459.
4. Belov N.A., Alabin A.N., Eskin D.G., Matveeva I.A. Effect of zirconium additions and annealing temperature on electrical conductivity and hardness of hot rolled aluminum sheets. *Transactions of Nonferrous Metals Society of China*. 2015. Vol. 25. pp. 2817–2826.

UNDERSTANDING THE INFLUENCE OF SPEED CORRECTION MODES ON THE PIPE SURFACE QUALITY DURING CONTINUOUS ROLLING

Toporov V.¹, Panasenko O.¹, Khalezov A.², Nukhov D.²

¹*Seversky Pipe Plant Industrial Joint Stock Company, Polevskoy, Russia*

²*Ural Federal University named after the first President of Russia B.N.Yeltsin, Yekaterinburg, Russia
toporova@stw.ru*

The most common hot-formed seamless pipe production technique includes rolling in a continuous pipe plant [1]. At the stage of pipe rolling in a continuous mill with a long mandrel, the main mechanical properties of the product are acquired and the wall thickness and the profile of the finished pipe are formed with a given dimensional accuracy [2-3]. One of the ways to improve the quality of pipes is to reduce the number of surface defects [4].

During continuous rolling, the pipe is deformed between the moving mandrel and the rolling rolls. Therefore, the optimal choice of the mandrel speed modes and the stability of its movement in the deformation zone have a great influence on the surface quality [5-8]. In this paper, the problems of numerical simulation of the continuous pipe rolling at the FQM mill are set and resolved. By solving the above problems, one was

able to analyze how the deviation of the rolling mill axis and the extractor mill axis due to poor retention of the mandrel between the rolling stands influenced the quality of the rough pipe. It was found that a longer holding time of the mandrel in the extreme position of the FQM mill before it is removed (Fig.1) reduces the metal sliding on the tool surface and thus helps make the mandrel extraction process more stable preventing defects on the inner surface of the rough pipe. The results of solving numerical simulation problems made it possible to formulate technical recommendations aimed at reducing the probability of surface defects in the production of pipes at the FQM mill.

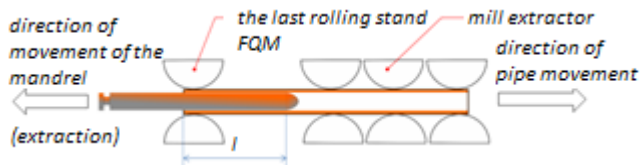


Fig. 1. The stage of the mandrel removal from the deformation zone

References

1. Danchenko V. N., Kolikov A. P., Romantsev B. A., Samusev C. B. Technology of pipe production. Moscow: Internet Engineering, 2002. 638 p.
2. Osadchy V. Ya., Golikov A. P. Production and quality of steel pipes: a textbook for university students. Ed. by V. Ya. Osadchy. Moscow: MGUPI publishing House, 2012. 370 p.
3. Kolikov A. P., Romantsev B. A. Theory of metal processing by pressure. Moscow: Publishing House of MISiS, 2015. 451 p.
4. Radkin Ya. I., Bobarikin Yu. L. Understanding the influence of the rolling mill gauge geometry on the accuracy of the pipe profile. Material Technology. 2018. No. 4. pp. 65-68.
5. Panasenko O. A., Shkuratov E. A., Belov O. I., Pyankov A. G., Pyankov K. P., Struin D. O. Improvement of the Axial Adjustment of the Equipment of Fine Quality Mill on the Basis of Contactless Measuring 3D Systems. Metallurgist. 2019. (63), pp. 690–694.
6. Gulyaev Yu. G., Shifrin E. I., Maksimova-Gulyaeva N. A., Kvitka N. Yu. Method of calculating the parameters for mandrel-free rolling of tubes with allowance for their elastic deformation. Metallurgist. 2008. (52). pp.156–159.
7. Orlov G.A., Loginov Yu.N., Orlov A.G. Complex estimation of hot-rolled steel pipes quality. Chernye Metally. 2018. (4). pp. 41–45. (In Russ.)
8. Orlov G.A., Orlov A.G. Qualimetry Rating of Hot-Rolled Pipes. Solid State Phenomena. 2018. Vol. 284. pp. 1349–1354.

SIMULATION OF WHITE LAYER THICKNESS IN COMBINED WIRE DRAWING

Polyakova M.¹, Gulin A.¹, Stolyarov A.²

¹Nosov Magnitogorsk State Technical University, Magnitogorsk, Russia

²OJSC “MMK-METIZ”, Magnitogorsk, Russia
m.polyakova-64@mail.ru

White layer which is formed on the contact surface between a wire and a die depends on deformation conditions [1-4]. The aim herein is to obtain the model for the

assessment of white layer thickness which is formed in the combined deformational processing by drawing with torsion (Figure 1) in high-carbon 0.7%C steel wire. Finite-element modelling is used to predict the thickness of the white layer. A series of experiments in the combined deformational processing of high-carbon steel wire is conducted at different deformational conditions. Using the quantitative coefficient of anisotropy that characterizes the shape of grains, the thickness of white layer is measured. It is found that the theoretical prediction of white layer thickness matches with experimental data. In addition, the mechanical properties of the processed carbon steel wire are studied by the tensile test.

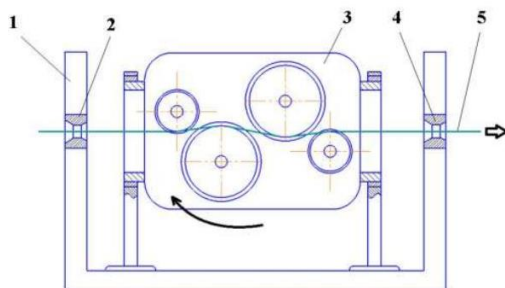


Fig. 1. Principle scheme of the laboratory setup for combined deformational processing in drawing with torsion of carbon steel wire

Analytical estimation of deformation penetration into surface layers of high carbon steel wire 0.7%C in combined deformational processing by drawing with torsion at the contact area with a die was studied. Modeling of wire surface behavior under combined deformational processing made it possible to analyze the peculiar distribution of deformation along the main axis X, Y, and Z. It was stated that maximum value of deformation was observed on the (at a) distance about 10 μm from the contact surface of wire with a die. Relations between the thickness of the layer of intensity plastic deformation dependent on deformation conditions in combined deformational processing by drawing with torsion of high carbon steel wire were achieved. The thickness of this layer was estimated by the coefficient of anisotropy change from the contact surface of the wire with a die to its central area. The experimental results show good precision with modeling data. 3. Peculiarities of carbon steel wire mechanical properties after combined deformational processing by drawing with torsion were studied. The level of high carbon steel wire mechanical properties in combined deformational processing by drawing with torsion is the result of obtaining complicated stress-strain state of the processed metal. The results show that mechanical properties of the processed high carbon steel wire in drawing combined with torsion change in wide range depending on applied deformation. As compared with drawing, the wire tensile strength is higher after combined deformational processing only at lower total reduction in dies. With increasing total reduction in dies the wire tensile strength also increases but its level may be lower or the same as after drawing. Combined deformational processing by drawing with torsion leads to increasing wire yield strength as compared with drawing when total reduction in dies are lower or higher.

The reported study was funded by RFBR according to the research project №18-58-45008 IND_a.

References

1. Sanabria, V., Mueller, S., Gall, S., Reimers, W. Investigation of friction boundary conditions during extrusion of aluminium and magnesium alloys (2014) *Key Engineering Materials*, 611-612, pp. 997-1004.
2. Barbacki, A., Kawalec, M., Hamrol, A. Turning and grinding as a source of microstructural changes in the surface layer of hardened steel (2003) *Journal of Materials Processing Technology*, 133 (1-2), pp. 21-25.
3. Ambrogio, G., Di Renzo, S., Gagliardi, F., Umbrello, D. White and dark layer analysis using response surface methodology (2012) *Key Engineering Materials*, 504-506, pp. 1335-1340.
4. Stolyarov, A.Y. Relations between the micro and macro levels of plastic deformation in the drawing of high-carbon pearlitic steel (2012) *Steel in Translation*, 42 (1), pp. 70-72.

MATHEMATICAL MODELING OF METAL TEMPERATURE DURING HOT SHEET ROLLING

Grigorenko A., Sosedkova M., Radionova L.

*South Ural State University (National Research Institute), Chelyabinsk, Russia
gras1996@mail.ru*

Mathematical modeling is the most innovative area in the process of creating new and optimizing the existing rolling production technologies. Simulation of the temperature processes occurring in the rolled metal in the technological chain and the required structures and properties of the finished rolled products is most important for ensuring high quality [1 - 5]. The analysis of existing models showed the presence of models that were built based on cybernetic approach (i.e. statistical processing of the experimental results) or on the epistemological approach (i.e. on theoretical dependences related to heat transfer processes). The known models are typically too complex to be used in engineering calculations or in automatic control systems.

In this regard, it became necessary to create a mathematical model for the temperature regimes of strip rolling in relation to the 2300/1700 hot rolling mill, as well as to prove its adequacy on the basis of experimental studies carried out at the mill of the Chelyabinsk Metallurgical Plant.

The calculation was done based on the formula [6] for changing the metal temperature at the i -th point of the technological process considering the factors affecting the temperature of the metal during rolling and transportation as part of the mill

$$t_i = t_{i-1} - \Delta t_{rad} - \Delta t_{conv} - \Delta t_{cont} + \Delta t_{def} + \Delta t_h, \quad (1)$$

where t_{i-1} – strip temperature in $(i - 1)$ process point;

Δt_{rad} – temperature loss due to thermal radiation;

Δt_{conv} – temperature loss due to convective heat transfer;

Δt_{cont} – temperature loss due to contact heat transfer;

Δt_{def} – strip heating in the deformation zone due to the energy of plastic strain;

Δt_h – temperature rise in the coiler in the furnaces.

The calculations were carried out for 5x1,540 mm steel sheets of grade AISI 321 rolled from 170x1,540x3,700 mm slabs.

The change in the metal temperature in Mill 2300 and Mill 1700 is shown in Fig.1 and Fig.2. Experimental temperature measurements were carried out in a rolling mill 2300/1700 using a TERA-50 radiation pyrometer. The measurements were carried out in an extension stand and a universal stand. The table shows the calculated and experimental temperatures of the end of rolling in the mill 2300/1700.

Analysis of the adequacy of the model showed that the developed mathematical model can be used to design new and improve existing rolling modes.

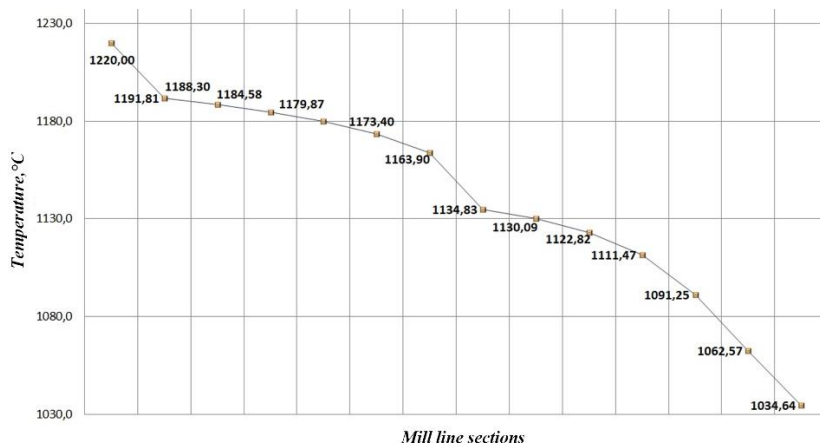


Fig. 1. Metal temperature in Mill 2300

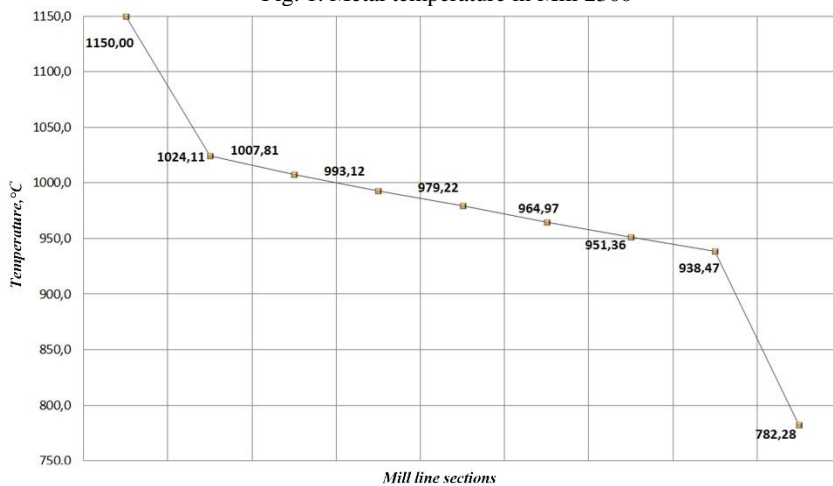


Fig. 2. Metal temperature in Mill 1700

Table. Comparison of calculated and experimental rolling temperatures

Temperature, °C	Widening mill stand, Mill 2300	Universal mill stand, Mill 2300	Rolling stand No. 8, Mill 1700	Coiler Mill 1700
Calculated	1163,9	1062,6	938,5	782,3
Experimental	1130...1100	1100...1050	920...900	800...760

The developed mathematical model was used to study the influence of the following rolling process parameters on the metal temperature along the mill and in the coiler: the heating temperature of the billet, the rolling speed, reduction during each pass, the type of finished product.

This research work was funded by the Ministry of Science and Higher Education of the Russian Federation as part of a governmental assignment related to fundamental scientific research, Contract No. FENU-2020-0020 (2020071GZ).

References

1. S.L. Kotsar, A.D. Belianskii, Iu.A. Mukhin. Sheet rolling production technology. Metallurgiya, Moscow, 1997.
2. A.P. Grudev, L.F. Mashkin, M.I. Khanin. Rolling technology: textbook for university students. Metallurgiya, Moscow, 1994.
3. V.M. Salganik, Y.A. Tverskoy, A.V. Kushnarev, A.G. Soloviev, S.V. Denisov, A.A. Mastruev, Y.V. Kudriakov, A.A. Radionov. Possibilities and options for upgrading MMK's 2500 broadband mill for controlled hot-rolling. *Ferrous Metallurgy*. 1 (2002). pp. 37-38.
4. Y.V. Konovalov, A.S. Khokhlov. Ways to solve the rolling temperature problem. *Pressure Treatment: A collection of research papers*, DSEA, Kramatogorsk, 2012. pp. 185-188.
5. B.A. Dubrovskiy, B.A. Nikiforov, V.A. Kharitonov, L.V. Radionova. Mathematical modeling of the temperature field of round bars on the thermal hardening line of the rolling mill. *Vestnik of Nosov Magnitogorsk State Technical University*, 3 (2005). pp. 53-58.
6. Sosedkova M.A., Grigorenko A.S., Radionova L.V., Lisovskaia T.A., Lezin V.D. Mathematical model of temperature conditions of sheet mills with furnace coilers. *Materials Science Forum*. 2020. Vol. 989 MSF. pp. 711-718.

NUMERICAL MODELING OF COMBINED ASYMMETRIC ROLLING AND BENDING PROCESS

**Abhay Kumar Dubey¹, Harshal Y. Shahare¹,
Pesin A.², Pustovoytov D. ², Hailiang Yu³, Puneet Tandon¹**

¹ *deLOGIC Lab, PDPM Indian Institute of Information Technology, Design and Manufacturing, Jabalpur, Madhya Pradesh, India*

² *Nosov Magnitogorsk State Technical University, Magnitogorsk, Russia*

³ *Hunan Institute of Mechanical and Electrical Engineering, Central South University, Chagsha, Hunan, China
adubey@iitdmj.ac.in*

Asymmetric rolling is a process of producing sheets with enhanced material properties (such as ductility and strength) with a front end curvature (FEC). Aerospace

and automobile industries demand bend sheets with different radii of curvature. In some cases, even sheets of continuously varying curvature are required. We propose a combined asymmetric rolling and bending process – a process that combines asymmetric rolling with incremental bending to obtain bend sheets with improved mechanical properties. Thin metal sheets are asymmetrically cold-rolled and then bent by a punch placed after the rolling mill in the direction of the sheet flow. The front end curvature produced by asymmetric rolling is further increased in the course of incremental bending through repeated hammering to obtain the desired curvature.

With the help of finite element analysis, this paper describes the results of numerical simulation of the combined process. By means of analysis, the authors attempt to establish a relation between the hammering amplitude and frequency on the curvature radius. The effect of different rolling parameters on the bend sheet forming is also investigated. The authors point out some major challenges related to the process. The paper examines the effect of initial thickness on the shape of the rolled sheet and that of the velocity ratio between the two working rolls, and the reduction ratio on the curvature of the bent sheet. The simulation results show that the velocity ratio and amplitude of the hammer are the two most important factors in the proposed combined process, and these parameters greatly influence the bend radius. Finite element analysis is also used to understand the typical bending behaviour of the sheet, as well as the effect of hammering frequency.

The reported study was funded by RFBR according to the research project № 18-58-45013 IND_a.

SIMULATION OF A NEW METHOD OF ACCUMULATED DEFORMATION

Khamatov D., Loginov Yu.

*Ural Federal University named after the first President of Russia B.N.Yeltsin,
Yekaterinburg, Russia
khamatovdd@yandex.ru*

A great deal of attention has been recently paid to the processes of accumulation of large plastic deformations. Such processes help obtain a refined metal structure and increase the durability of metal due to the effect of grain-boundary hardening [1].

The goal is to expand the set of metal forming processes which allow to accumulate deformation without significant shape changing.

It is proposed to apply accumulated plastic deformation to form a spiral wire out of a plastic metal billet (pure silver, grade Ag99.99) and then straighten it [2]. In the case described, the diameter of the wire was 1.2 mm and the diameter of the mandrel was 3.2 mm ($\delta/(2R) = 0.375$).

As it was shown in [2], a deformation degree of $\varepsilon = 0.48$ can be achieved in one winding and unwinding cycle, and such degree refers to the external stretched profile fiber. The same level of deformation, but with the opposite sign, refers to the inner profile fiber adjacent to the surface of the rod. Since a neutral cross section is localized in the center of the wire, near which the strain level is lower, the strains will on average be lower than it was determined for the surface of the wire. However, the deformation accumulation principle will be observed, and thus, the average hardening will increase with further processing stages.

The process of spiraling and further straightening of a workpiece by applying accumulated plastic deformation was simulated with the help of QForm VX 8.2.3. To set the problem in the modeling package, we used the dependence of the deformation resistance of pure silver (99.99%) specified in the paper [3]. The friction factor is set for the contact surface between the workpiece and the tool (which is equal to 0.2 according to A. Levanov), and a tension of 1 MPa is applied to the rear end of the workpiece.

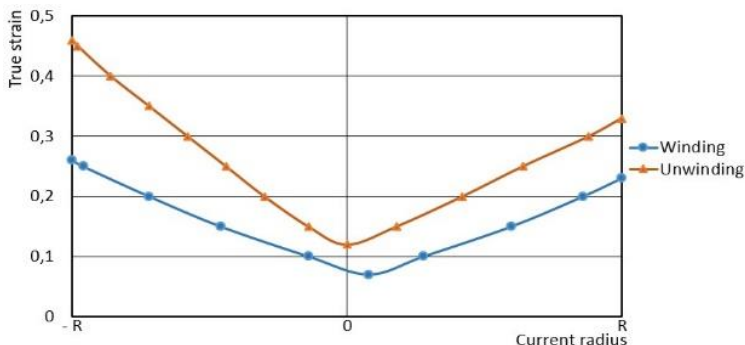


Fig. 1. The distribution of the true strain over the cross section of the workpiece

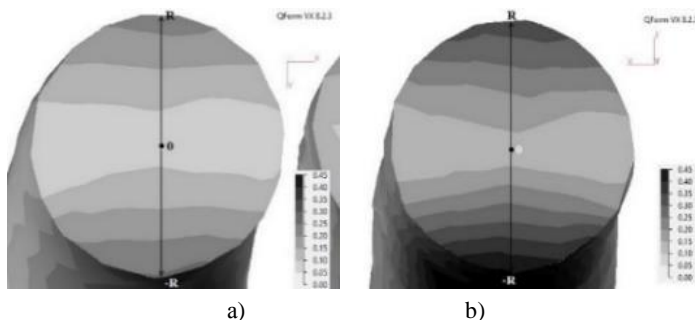


Fig. 2. The distribution of the true strain over the cross section of the wire:
a) winding state; b) unwinding state

Fig. 1-2 show that the plastic deformation is localized at the surface decreasing along the cross section in the direction of the workpiece centreline and can be adjusted using the calculations and statements presented in [2]. The plastic deformation in the central part of the workpiece drops to 0.07 for the state of winding and to 0.12 – in a straightened spiral.

As indicated in [2], in one winding and unwinding cycle, the calculated degree of deformation at $\delta/(2R) = 0.375$ should be 0.48. The profile length along the neutral section was taken to remain unchanged. Therefore, the operations performed on the workpiece should not lead to lengthening. However, the results of a real experiment turned out to prove the opposite. In the real experiment, it was possible to achieve a relative elongation of the workpiece of about 4.5%. We did not take into account the tension

applied to the rear end of the workpiece, which resulted in slight wrinkles formed on the contact surface (it is associated with the distribution graph asymmetry). The rear tension also affected the elongation.

According to the simulation results, the degree of deformation obtained during spiraling and further straightening of a workpiece varies from 0.46 for the inner layers of the workpiece (which is close to the calculated values) to 0.34 for the external ones.

References

1. Zrnik J. Grain refinement and deformation behaviour of medium carbon steel processed by ECAP. *Key Engineering Materials*. 2014. Vol. 592-593. pp. 307-312.
2. Loginov Yu.N., Khamatov D.D. Method of wire hardening by plastic deformation. Patent RF, No. 2709554. Applied: 23.11.18. Published: 18.12.19. Bulletin No. 35. 15 p.
3. Loginov Yu.N., Khamatov D.D. Strain resistance of pure silver (99.99%) under large plastic deformations. *Materials Today: Proceedings*. 2019. Vol. 19. pp. 2160-2162.

CONTROL OF MAGNESIUM ALLOY PROPERTIES USING METHODS OF SEVERE PLASTIC DEFORMATION

Zasytkin S., Brilevsky A.

*Institute of Advanced Technologies, Togliatti State University, Togliatti, Russia
zvs181@mail.ru*

Low-alloy bioresorbable magnesium alloys are a promising material for the production of biomedical products because they have the best biocompatibility, and their insufficient initial strength can be increased by means of severe plastic deformation (SPD). This article presents the results of a study that looked at the influence of various SPD methods on the microstructure and mechanical properties of magnesium alloys Mg-1Zn-0.15Ca and Mg-1Zn-2.8Y.

Alloys produced by SOMZ LLC were used for the purpose of this research. Their chemical composition is shown in Table 1.

Table 1 – Chemical composition and mechanical properties of the alloys

Marking	Chem. composition, weight %			Type of SPD	σ_b , MPa	δ , %
	Zn	Ca	Y			
S9	0.98	-	2.9	ECAP	310	19
S10				Extrusion	310	4
S3-VIK				CIF	250	20
S11-VIK1	1.0	0.18	-	CIF	200	26
S11-VIK1P				CIF + rolling	260	21

The Mg-1Zn-2.8Y alloy was subjected to three types of SPD: 1) ECAP of 4 passes B_c at 425°C and 0.4 mm/s; the specimen was marked as S9; 2) Extrusion at 500°C R6.25 + rotary forging (RF) 20→18 mm, 25°C – specimen S10; 3) Homogenization at 450°C/12h + comprehensive isothermal forging (CIF) in the temperature range (400÷300)°C involving 5 passes with a 25°C decrease in temperature during each pass – specimen S3-CIF.

The Mg-1Zn-0.15Ca alloy was subjected to the following types of SPD: 1) Homogenization at 450°C/12h + VIC in the temperature range (400÷300)°C involving 5 passes with a 25°C decrease in temperature during each pass – S11-VIK1; 2) Homogenization at 450°C/12h + CIF in the temperature range (400÷300)°C involving 5 passes with a 25°C decrease in temperature during each pass + upsetting + isothermal rolling – S11-VIK1P. The microstructure of the specimens was analyzed using Nikon L150 and Axiovert 401 optical microscopes at the IMSP RAS, Ufa. Tensile tests were performed using a compact Kammrath&Weiss machine with a traverse movement speed of 10 mm/sec (deformation rate of 10^{-3} s^{-1}) at room temperature for specimens with a working part size of 2×4×10 mm. In total, three specimens were tested for each individual condition. The study of the microstructure of the Mg-1Zn-0.15Ca alloy in the initial state showed that the alloy has a typical coarse-grained structure for casting with a conditionally uniform distribution of excess phases (Fig. 1a). After comprehensive isothermal forging, the structure became fine-grained (with a grain size of about 4 mm) and uniform at both the micro and macro levels (Fig. 1b). Additional rolling does not produce any significant structural changes after CIF (Fig. 1c)

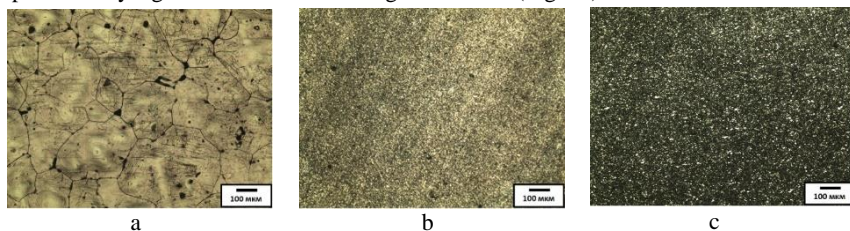


Fig. 1-Microstructure of Mg-1Zn-0.15Ca alloy a) in the initial state; b) after CIF; c) after CIF + rolling

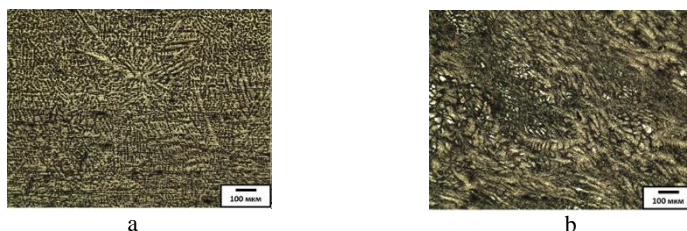


Fig. 2-Microstructure of S3 alloy a) in the initial state; b) after Mg-1Zn-0.15Ca

In its initial state, the Mg-1Zn-2.8Y alloy has the structure of large equiaxed grains with sizes up to several hundred microns and a dendritic parameter of the order of 8-15 microns (Fig. 2a). After homogenization and CIF, the structure became fine-grained with an average grain size of 3-5 microns (Fig.2b). The results of the mechanical tests (Table 1) showed that ECAP would be the best SPD method of the three applicable to the Mg-1Zn-2.9Y alloy delivering a combination of high tensile strength (310 MPa) and large elongation (19%). However, when analyzing the test results for the alloy Mg-1Zn-0.16Ca, one can see that rolling applied after CIF operation can significantly increase the strength of the alloy (from 200 to 260 MPa) leading to a slight decrease in ductility (from 26% to 21%). A sequence of SPD operations applied to the alloy Mg-1Zn-2.9 may help achieve comparable ECAP strength characteristics.

References

1. Vinogradov A. et al. High performance fine-grained biodegradable Mg-Zn-Ca alloys processed by severe plastic deformation. *Metals*. 2019. Vol. 9, No. 2. p. 186.

INTERNAL STRESS EVOLUTION IN THE PRESTRESSING STRAND PRODUCTION

Medvedeva E., Golubchik E., Konstantinov D., Ivekeeva P.
Nosov Magnitogorsk State Technical University, Magnitogorsk, Russia
fekla_med@mail.ru

There is a current global increase in construction operations with a widespread use of reinforced concrete structures, where high-strength prestressing strands are used as a main element. The combination of a complex design and a critical application of the finished product (and, consequently, high requirements for its properties) is complicated by the fact that prestressing strands are a product of a multi-stage technology consisting of multi-pass operations, often incorporating technological effects of various physical nature. In view of this, one of the most successful research methods for such science-intensive technologies is a multiscale modeling method, factoring in both micromechanics of steel deformation and the evolution of internal stresses.

Developed models are presented the finite-element modeling results of stranding, reduction, straightening and mechanical-thermal treatment (MTT) of prestressing strand (PSC strand). Computer models took into account the distribution of residual stresses formed at the preliminary stage of wire drawing. During the simulation, the effect of MTT on the internal stresses of the wires was studied: residual stresses after the drawing process and additional stresses after the stranding. All studied methods demonstrated a positive effect not only from the point of eliminating internal stresses, but also from the point of view of their favorable redistribution. The reduction of PSC strand in a monolith tool with strain degree 1-3% allows to minimize tensile stresses on the surface of the wires and save compressive stresses in the center of the wires. The straightening by a group of 5 rolls made it possible to reduce the tension of outer wires twice. The MTT application, combining the effects of various physical nature, made it possible to control over a wide range the redistribution of residual stresses in the wires after high strain degrees and the additional stresses created during the stranding, which affect the preservation of the geometric parameters of the PSC strand. The study showed that to eliminate longitudinal residual stresses, the magnitude of the tension in the MTT is the most important parameter. Therefore, with a minimum value of tension, the residual stresses are not redistributed either in the central or in the surface layers, regardless of the temperature of the MTT. However, with tension above 70 kN and a temperature of 380-400°C, the residual stresses in the center and on the surface of the wires are balanced or almost completely eliminated.

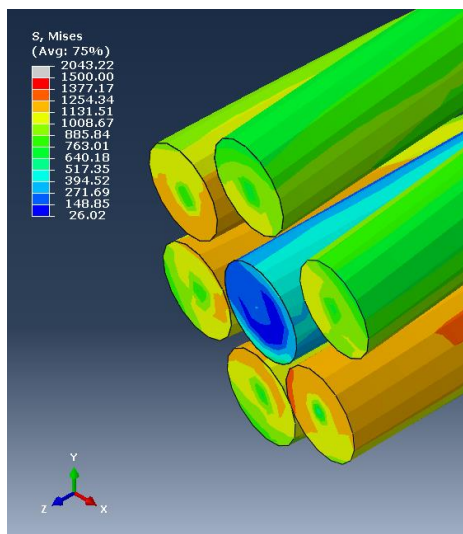


Fig.1. Mises stresses in the cross section of PSC strand

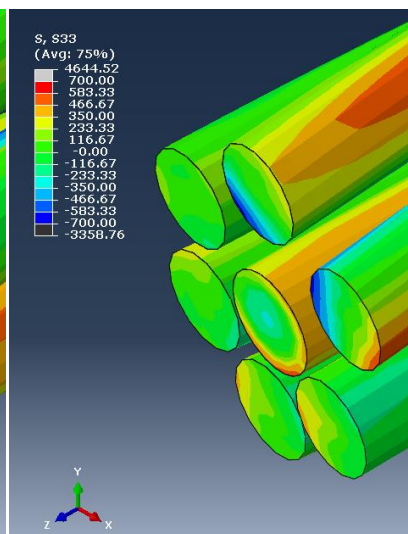


Fig.2. Longitudinal stresses in the cross section of PSC strand

Comparison of the distributions of the Mises stresses (fig.1) and longitudinal stresses (fig.2) showed that the straightening with depth up to 5 mm for a 12.5 mm rope in one group of rolls significantly changes the stress state (mainly its outer wires). The longitudinal stresses of the outer wires are reduced by 1.7–2 times, and in some wires they even reach near zero values. Mises stresses were reduced in all outer wires by 1.5–2 times, which favorably reduces the untwisting of the rope. However, a further increase in the depth can adversely affect the preservation of the strand geometry and lead to an increase in pulling force.

The reported study was funded by RFBR according to the research project №16-38-00619 mol_a.

References

1. D. V. Konstantinov, A. G. Korchunov, M. V. Zaitseva, O. P. Shiryaev, D. G. Emaleeva. Macro- and Micromechanics of Pearlitic-Steel Deformation in Multi-stage Wire Production. *Steel in Translation*. 2018. V. 48. Pp. 458–462.
2. A. G. Korchunov, M. A. Polyakova, D. V. Konstantinov, M. Dabalá. Mechanical properties of prestressing strands and how they tend to change under thermo-mechanical treatment. *CIS Iron and Steel Review*. 2019. Vol. 18. Pp. 14–19.
3. A. Korchunov, E. Medvedeva, P. Ivekeeva, D. Konstantinov. FEM research of internal stresses evolution in the prestressing strand production. *Proceedings 29th International Conference on Metallurgy and Materials*. 2020. pp. 215–221.

RESEARCH OF THE HEATING TEMPERATURE INFLUENCE ON THE TECHNOLOGICAL PLASTICITY OF THE STEEL GRADE 15KH13N2 (AISI 414) APPLICABLE TO THE SCREW ROLLING PROCESS

Zavartsev N.¹, Korsakov A.¹, Mihalkin D.¹, Alyutina E.¹,
Akhmedjanov A.², Samoylov S.², Ulyanov A.³, Niklyayev A.³

¹Russian Research Institute of the Tube & Pipe Industries (ROSNITI),
Chelyabinsk, Russia

²South Ural State University (National Research Institute), Chelyabinsk, Russia

³JSC "Volzhsky Pipe Plant", Volzhskiy, Russia
korsakov@rosniti.ru

The formability of steels and alloys in pipe mills is determined by ductility and deformation resistance, the two of which ensure the technological plasticity of metals. In order to obtain new data on the dependence of technological plasticity on the heating temperature, tests were carried out on specimens taken from forged and continuously cast billets made of 15Kh13N2 steel (AISI 414) and the results were compared with those obtained earlier for steel grades 10GFBU (AISI 1010) and Steel 20 (AISI 1020). The technological plasticity of 15Kh13N2 steel (AISI 414) billets was studied in the temperature range from 1,000 to 1,250 °C. Graphs were built showing a dependence of the torque on the rotation angle and the number of torsions to failure on the heating temperature. To assess the uniformity of properties distribution across the cross section, we compared the test results obtained for specimens from the peripheral and central areas of the workpieces. The study was carried out using the thermomechanical modeling system "Gleeble 3800". The billet heating intervals were determined that are associated with maximum technological plasticity minimizing defect formation on the hollow billet inner surface during flashing. The most rational temperature range for the cross-roll piercing of forged billets made of 15Kh13N2 steel (AISI 414) is from 1,050 to 1,125 °C (in this interval, the relative deviation of the technological plasticity does not exceed 11%). The average number of torsions before failure within the rational temperature range is 17.2 ± 1.4 . The maximum number of torsions before fracture (18.5) was observed when the specimens were heated to 1,100 °C, while the minimum one (11.1) corresponds to the heating temperature of 1,250 °C. Raising the heating temperature above 1,100 °C leads to a gradual decrease in the technological plasticity of steel. Piercing of 15Kh13N2 steel (AISI 414) forged billets outside the range of maximum technological plasticity can cause the formation of internal defects in hollow billet and pipes.

Introduction

An ever rising demand is currently observed for stainless steel pipes, especially in oil and gas industry and in particular for 13Cr steels. This type of steel has a number of unique properties, which justify its use despite the high cost of products made of this material [1, 2].

The formability of steels and alloys in pipe mills is determined by two main properties – ductility and deformation resistance, the two of which ensure the technological plasticity of metals.

Both are interrelated and depend on the nature of the metal, its structural state, temperature and deformation rate, the surface of the workpiece, the environment and other factors.

Screw rolling is one of the most widespread and productive methods of producing seamless pipes. In a rotary piercing process, a favorable stress state makes it possible to deform non plastic cast material, as well as hard-to-deform steels [3].

The stress-strain behavior typical of the rotary piercing process differs drastically from the one typical of any other metal testing method. Therefore, the experimental data on the mechanical properties of steel in hot conditions are not indicative in this case and are hardly applicable. Significantly more reliable results are supplied by the hot torsion test method.

The aim of this research is to obtain new data on the technological plasticity of specimens of forged and continuously cast billets made of steel 15Kh13N2 (AISI 414) and to understand how it changes depending on the heating temperature, as well as to compare such data with the data obtained earlier [4] for Steel 20 (AISI 1020) and 10GFBU (AISI 1010).

Materials and Methods of Research

The “Gleeble 3800” digital closed-circuit thermomechanical modeling system with the “Torsion” mobile hot-torsion module was selected for this research. The equipment is located at South Ural State University in Chelyabinsk.

A template for these test specimens were made from forged billets with a diameter of 340 mm (Fig. 1 and 2).

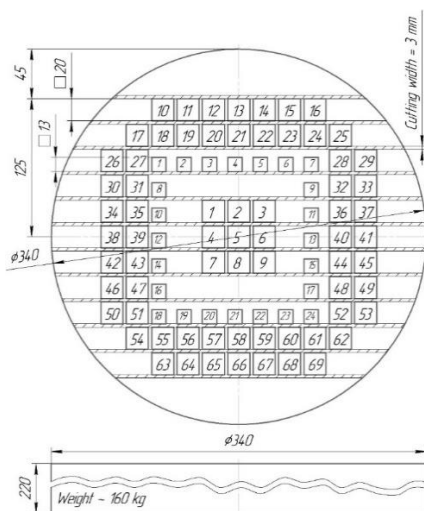


Fig. 1. Layout for torsion test specimen cutting



Fig. 2. Specimens made of steel 15Kh13N2 (AISI 414) for hot torsion tests in the Gleeble 3800 unit

The essence of this method is to determine the twist angle of the specimen required for its destruction (plasticity), as well as the maximum twisting force or torsion moment (deformation resistance).

Although the stress-strain behavior during hot torsion differs from that observed during piercing, the results of such tests make it possible to establish the optimum temperature interval in which piercing is to be carried out, which is consistent with the piercing test results obtained from an experimental screw-rolling mill and pipe production practice [5]. All tests are carried out until the specimen fractures.

The steel grades and the quantities of specimens are presented in Table 1.

Table 1. Steel grades and quantities of specimens

Steel grade	15Kh13N2 (AISI 414) (forged)	15Kh13N2 (AISI 414) (CCB)
1250	3	-
1225	3	-
1200	3	3
1175	3	-
1150	3	-
1125	3	-
1100	3	3
1075	3	-
1050	3	-
1000	3	3

Specimens are heated to the required temperature at a rate of 5 °C/s by direct transmission of electric current with subsequent exposure of 1.5 min in order to achieve a minimum temperature gradient in the working area of the specimen. The temperature of the specimen is measured by two thermocouples fixed to the specimen. The first thermocouple is located in the center of the working area and controls the heating temperature before testing. The second thermocouple is situated close to the working area, on the stationary gripper side and monitors how the temperature is changing during the test.

The strain rate was determined based on the calculations performed as part of the previously developed technique [4, 6, 7].

In the paper [1] describing hot torsion tests performed for Steel 20 (AISI 1020) and 10GFBU (AISI 1010) for VTZ JSC, an average value of the strain rate of 15 s⁻¹ was chosen, which corresponded to the rotation frequency of the mounting clip $f \approx 16.5$ r.p.s.

Thus, in order to ensure the conditions under which the most correct comparative analysis was possible for all steel grades and due to the fact that no modes were adjusted on the TPA 159-426 piercing mill during piercing of the steel grade 15Kh13N2 (AISI 414) [1, 8], the same modes were used (i.e., with the strain rate of 15 s⁻¹). The same strain rate was applied in all tests.

The following parameters were monitored during hot torsion tests in a continuous mode: rotation angle, torque, temperature around the working area of the specimen. The latter was measured by means of a thermocouple, whereas the temperature in the work-

ing area of the specimen was measured by means of a pyrometer. Based on the data obtained, we built graphs showing the dependence of the torque M on the rotation angle θ and determined the rotation angle θ_p and the number of revolutions N_p before the fracture.

Results

The experimental torsion curves in the Angle of Rotation – Torque coordinates obtained at various specimen deformation temperatures are shown in Figure 3 for specimens made from rolled billets, and in Figure 4 for specimens made from CCB of steel grade 15Kh13N2 (AISI 414). Each graph shows the torsion curves for three specimens tested at the same temperature.

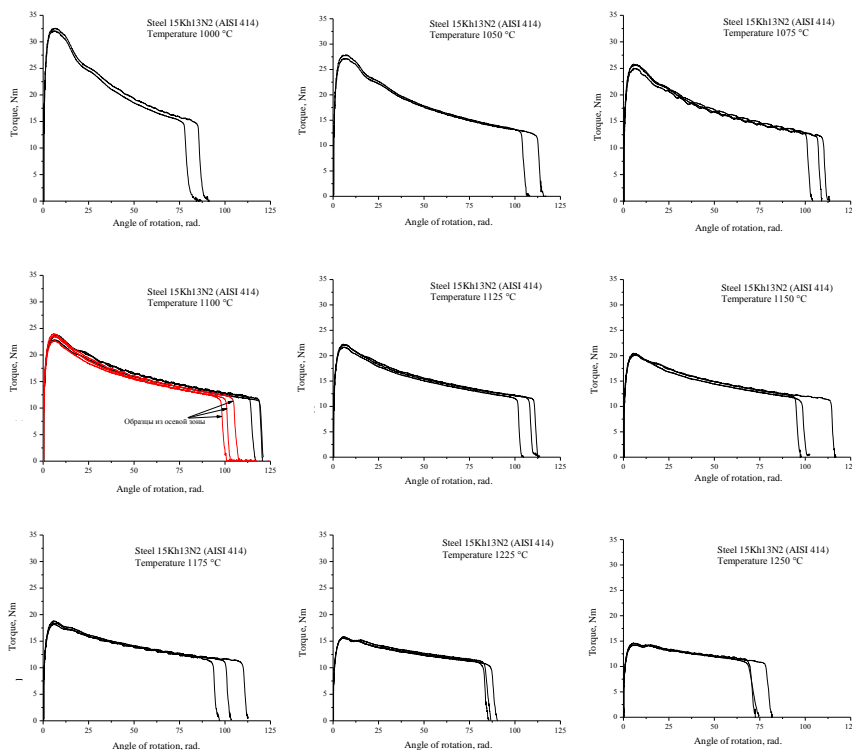


Fig. 3. Experimental curves obtained during the torsion tests conducted on steel grade 15Kh13N2 (AISI 414) specimens in the as-forged state at different test temperatures (1,000 to 1,250°C)

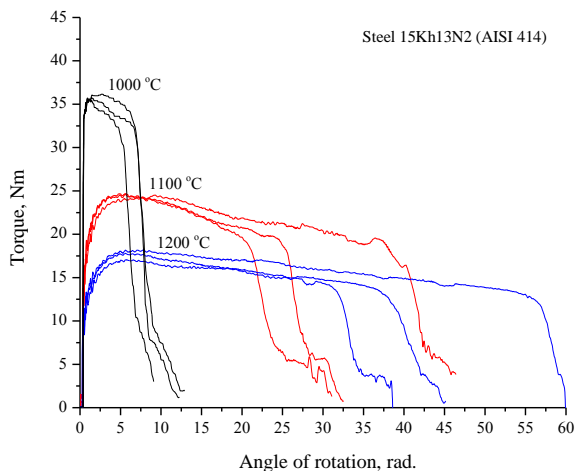


Fig. 4. Experimental curves obtained during the torsion tests conducted on steel 15Kh13N2 (AISI 414) specimens in the as-cast state (CCB) at different test temperatures (deformation curves for nine specimens are shown: three specimens for each temperature regime)

It can be observed from the presented figures that the torque M required for initial deformation increases with an increase in the angle of rotation θ and reaches its peak value. With a subsequent increase in the angle of rotation, a dive in torque is observed, which is probably associated with deformation heating. According to the pyrometer, the heat of 200-400°C is applied in the deformation zone depending on the test temperature (Figure 5). According to the thermocouple in the vicinity of the working area, the temperature during the deformation process changed insignificantly (no more than 5 °C), which may indicate early localization of the deformation and, as a consequence, deformation heating.

The dependence of the torque on the angle of rotation under the same temperature conditions has good reproducibility (the deformation curves for the three specimens tested under the same conditions coincide).

The fracture process is supposed to commence in the point in which the deformation curve separates from the tangent drawn to the descending section. It is associated with strain softening (Figure 6). The obtained data for the studied steels are presented in Figure 7.

For the 15Kh13N2 (AISI 414) steel in the as-forged state, the dependence of technological plasticity on temperature at the beginning of the deformation process is non-monotonic and reaches its maximum at the temperature of about 1,100°C (Fig. 7). The peak value for this dependence is 17.25 ± 1.8 revolutions (the experimental dispersion is $\pm 10\%$).

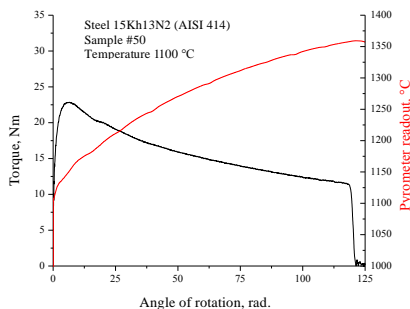


Fig. 5. Change in temperature of the deformation zone as the load is applied

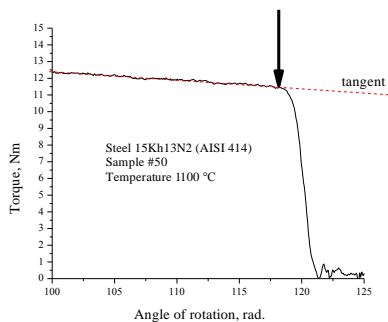


Fig. 6. Determination of the onset of sample fracture

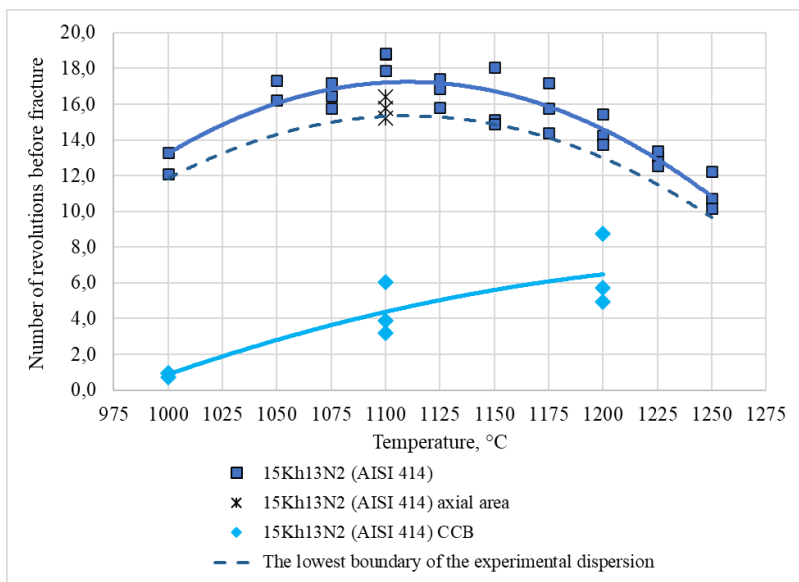


Fig. 7. The technological plasticity of the studied steels at different test temperatures

The specimens cut from the axial area of the forged billet were tested at the temperature of 1,100°C because the maximum technological plasticity of the 15Kh13N2 (AISI 414) steel in the as-forged state was determined at this temperature (the highest number of revolutions before fracture of the specimen). The obtained plasticity data are located at the low boundary of the experimental dispersion ($\pm 10\%$) for the base metal (Fig. 7).

The technological plasticity of the 15Kh13N2 (AISI 414) steel grade for the as-cast state is significantly lower than that for the as-forged state (Fig. 7). This is probably due to the presence of defects in the blank. The temperature dependence of plasticity ob-

tained in this case is different since it increases monotonically.

Thus, it can be concluded that the technological plasticity of the 15Kh13N2 (AISI 414) steel in the as-forged state is significantly higher than in the as-cast one (the number of revolutions before failure is 2-14 times higher). Therefore, the use of the 15Kh13N2 (AISI 414) steel for the production of seamless hot-rolled pipes is only possible on condition that the billet has undergone preliminary deformation processing. The use of CCB is significantly limited or completely impossible.

There is a direct relationship between the choice of the rational heating temperature for piercing and the number of revolutions before failure: the temperature at which the specimen is able to withstand a higher torsion until its destruction will be recommended.

The average values of the number of revolutions to failure $\langle N_p \rangle$ depending on the test temperature of the specimens cut from the peripheral part of the billet made of steel grade 15Kh13N2 (AISI 414) are shown in Fig. 8.

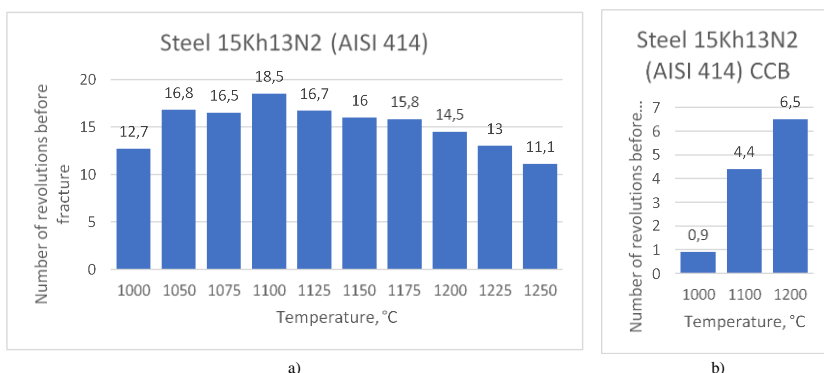


Fig. 8. Histograms showing the average number of revolutions to failure depending on the test temperature of specimens cut from steel 15Kh13N2 (AISI 414): a) as-forged state; b) CCB

The histograms clearly show that various types of billets made of steel grade 15Kh13N2 (AISI 414) (as-forged and CCB) have different temperature ranges that correspond to maximum technological plasticity. If the deviation of $\pm 10\%$ from the optimal value is considered as acceptable, then the temperature range of the maximum technological plasticity for forged billets is 1,050 – 1,125°C (with the average number of revolutions to failure from 16.5 to 18.5). For continuously cast billets (CCB), the temperature range of the maximum technological plasticity starts from 1,200°C and probably goes beyond the boundaries of the studied temperature ranges (3 times lower than the average number of revolutions to failure, which is about 6.5).

In order to carry out a comparative analysis of the hot torsion test results obtained for various steel grades and types of billets, the curves presented in Fig. 7 are shown together with the curves depicting the technological plasticity of Steel 20 (AISI 1020) and 10GFBU (AISI 1010) in the as-cast state, which were obtained earlier under similar test conditions (Fig. 9) [4].

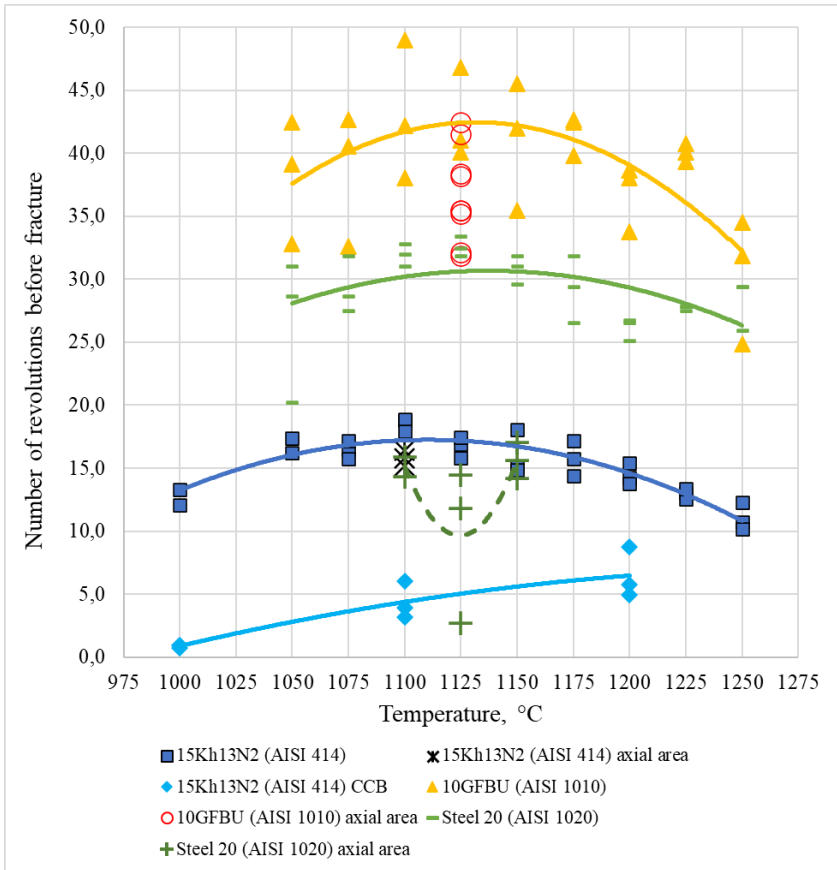


Fig. 9. Technological plasticity of various grades of steel and types of billet depending on various test temperatures

The 15Kh13N2 (AISI 414) steel grade in the as-cast state was found to have the lowest technological plasticity (Fig. 9) (the average number of revolutions before failure varies from 1 to 6.5). Therefore, further consideration of this steel is not advisable, since it is practically unsuitable for rotary piercing.

Steel 20 (AISI 1020) and 10GFBU (AISI 1010) in the as-cast state have significantly greater results (Fig. 9) than the 15Kh13N2 (AISI 414) steel in the as-forged state: the 10GFBU (AISI 1010) steel grade has the largest number of revolutions before failure (an average of 33.7 to 44.5); with the average number of revolutions to failure from 26.2 to 33.1, Steel 20 is in the median position; the 15Kh13N2 (AISI 414) steel in the as-forged state shows an average of 11.1 to 18.5 revolutions before failure.

The situation with the specimens cut from the axial areas of billets looks different to the one with the specimens cut from the peripheral areas and also varies depending on the steel grade (Fig. 9):

- for 10GFBU (AISI 1010), the average number of revolutions before fracture for the specimens cut from the axial area of the billet and tested at the temperature of 1,125°C is 36.7, which is 14% lower than the number of revolutions for the specimens cut from the peripheral areas (42.7) of the billet and tested at the same temperature;
- for Steel 20 (AISI 1020), the average number of revolutions before fracture for the specimens cut from the axial area of the billet and tested at the temperatures from 1,100 to 1,150°C is 13.2, which is 58.5% lower than for the specimens cut from the peripheral areas (31.8) and tested at the same temperatures (i.e. lower than the performance of the as-forged billet made of steel 15Kh13N2 (AISI 414));
- for the 15Kh13N2 (AISI 414) steel grade in the as-forged state, the number of revolutions before fracture for the specimens cut from the axial area of the billet and tested at the temperature of 1,125°C averages 15.8, which is 5.4% lower than for the specimens cut from the peripheral areas of the billet (16.7) and tested at the same temperature.

Thus, the 15Kh13N2 (AISI 414) steel grade in the as-forged state does not experience such a significant variation in technological plasticity across the cross section of the billet from the peripheral regions to the axial zone as do Steel 20 (AISI 1020) and 10GFBU (AISI 1010) in the as-cast state. It means that there is a lower risk of the formation of internal defects associated with metal structure heterogeneity over the cross section.

Conclusions

1. The torsion curves for the steel grade 15Kh13N2 (AISI 414) have a typical form for hot tests: with an increase in the rotation angle, the torque increases to a certain maximum value before it drops down as a result of significant heating of samples which occurs due to the partial conversion of the mechanical energy into heat at a high strain rate. The presence of high-temperature processes of deformation softening is also possible.

2. The obtained data suggest that the temperature range of 1,050-1,125 °C would be most rational, in terms of technological plasticity, for the screw rolling of forged billets made of steel 15Kh13N2 (AISI 414) (the relative deviation of technological plasticity in the above range does not exceed 11%). The average number of revolutions before fracture within the rational temperature range is 17.2 ± 1.4 . The maximum number of revolutions to fracture (18.5) is observed at the heating temperature of 1,100 °C, and the minimum number of revolutions (11.1) – at the heating temperature 1,250 °C. With an increase in the heating temperature of samples above 1,100 °C, a gradual decrease in the technological plasticity of steel is observed.

3. For steel 15Kh13N2 (AISI 414) in the as-cast state, a gradual increase in the technological plasticity is observed with an increase in the deformation temperature. At the same time, the obtained values are significantly lower (by 8–14 revolutions) than those obtained for this steel grade in the as-forged state. Thus, the use of CCB made of steel 15Kh13N2 (AISI 414) for the manufacturing of hot-rolled seamless pipes of proper quality by means of screw rolling followed by rolling without additional measures is associated with the inevitable destruction of the workpiece metal during piercing and formation of a large number of defects.

4. A comparative analysis of the hot torsion test results of various steel grades showed that the technological plasticity of Steel 20 (AISI 1020) and 10GFBU (AISI 1010) in the as-cast state is significantly better compared with steel grade 15Kh13N2

(AISI 414) in the as-forged state (the number of revolutions to failure is 2 or more times higher). At the same time, CCB of Steel 20 (AISI 1020) and 10GFBU (AISI 1010) have a significant heterogeneity of properties across the cross section (thus, their technological plasticity profoundly deteriorates from the peripheral regions to the axial zone). Steel grade 15Kh13N2 (AISI 414) in the as-forged state does not have this drawback. Due to prior deformation processing, uniformity of properties across the cross section of the billet is achieved, therefore this steel grade can be successfully pierced in screw rolling mills and rolled into pipes of proper quality.

5. Piercing of forged billets made of steel grade 15Kh13N2 (AISI 414) outside the range of maximum technological plasticity can cause internal defects in hollow billets and pipes.

References

1. Trutnev N.V., Krasikov A.V., Ulyanov A.G., Lube I.I., Kosmatskii Y.I., Korsakov A.A. Mastering of seamless pipes production from martensitic class stainless steel of 13Cr grade type at the JSC “VTZ” TPA 159–426 pipe mill. *Ferrous Metallurgy. Bulletin of Scientific, Technical and Economic Information*. 2018. (12). pp. 68-71. (In Russ.)

2. Laev K. A. The influence of alloying and heat treatment on the structure and properties of corrosion-resistant high-chromium steels of martensitic and super martensitic classes for the manufacture of oil and gas pipes. PhD dissertation. South Ural State University, Chelyabinsk, 2016.

3. Urbanski S., Kazanecki J. Assessment of the strain distribution in the rotary piercing process by the finite element method. *Journal of Materials Processing Technology*. 1994. Vol. 45, No. 1-4. pp. 335-340.

4. Kuryatnikov A.V. Determination of the temperature range of the metal maximum plasticity by hot torsion in relation to the process of rotary piercing. *Proizvodstvo prokata*. 2014. No.1. pp. 20-27. (in Russ.)

5. Danilov F.A. *Hot Rolled Steel Pipe Production*. Moscow: Metallurgiya, 1954. 615 p.

6. Chekmarev A.P. *Rotary piercing*. Moscow: Metallurgiya, 1967. 240 p.

7. GOST 3565-80. *Metals. Method of torsion test*. Moscow: Izdatelstvo standartov, 1981. 15 p.

8. M. Akhmedyanov, S. V. Rushchits, M. A. Smirnov. Hot deformation of martensitic and supermartensitic stainless steels. *International Conference on Industrial Engineering-2016, Materials Science Forum 870* (Trans Tech Publications, Switzerland, 2016). pp. 259–264.

APPLICATION OF THERMAL ANALYSIS METHOD FOR STRUCTURAL TRANSFORMATION OF HOT-ROLLED CARBON BILLETS FOR HIGHSTRENGTH ROPES

Pivovarova K., Emaleeva D.

*Nosov Magnitogorsk State Technical University, Magnitogorsk, Russia
emaleevadg@mail.ru*

High-strength reinforced stabilized ropes are the base of modern efficient building technologies for fabrication of prefabricated reinforced concrete with preliminary tension of reinforced bars, as well as constructions with consequent post-tensioning.

Equipment and technological routes for manufacture of reinforced ropes used by the leading foreign and domestic hardware enterprises are analyzed. It allowed to establish that the modern development tendencies of science, machinery and technologies are characterized by searching the efficient complex for effect on metal microstructure with combination of processing methods with different physical nature. The aim of this effect is in reaching high-strength state of processing material with adding to it the complex of special properties, meeting the requirements of operating conditions of reinforcing products in iron ore constructions of responsible application. Detailed examination and understanding of the physical mechanisms of forming of structural-phase states of applied materials is being more and more actual for realization of such tasks. These mechanisms substantiate temperature and temporal, force and deformation parameters of multi-stage treatment and provide maximal possible dispersity degree of steel microstructure parameters and its transition in high-strength state. The method of trial quenching is used conventionally for examination of structural-phase transformations (critical points). This method is standardized in many countries, however, it has several deficiencies: labour intensity, low productivity and (sometimes) subjectivity. Thereby instrumental control methods of investigation, such as dilatometry, differential scanning calorimetry (DSC) and differential thermal analysis (DTA), allowing to fix temperature intervals of phase transformations and to receive information about the values of critical points in metals and alloys are widely used at recent time. The obtained experimental values are used for building the thermo-kinetic diagram of continuous heating and the diagram of isothermal transformation. These diagrams are applying for examination of the essence of transformation processes occurring in different temperature zones and regularities of decomposition of overcooled austenite. The regularities of forming of structure and properties of several grades of hot-rolled high-carbon steel billets (e.g. steel 80P via dilatometric method [1]) are examined rather widely at present time. However, such experiments for steel 80 using DTA/DSC method are not described in the literature; nevertheless, they are widely used for investigation of alloyed steels [2–9]. Additionally, DTA/DSC methods are most requested than dilatometric method, owing to their high sensitivity to coursing of phase transformations [10]. Thereby, the aim of this work is formulated as examination of structural-phase transformations of initial hotrolled billets made of high-carbon steel via the method of differential scanning calorimetry.

The obtained experimental data of the DSC method have confirmed necessity of usage of austenitization in the temperature range 930–980 °C in production of high-strength reinforced ropes for responsible applications. This technology provide increase of austenite homogenization degree as well as suppression of free ferrite forming in high-carbon hot-rolled billets. Experimental data of DSC method are informative, their usage in combination with metallographic methods allow to test the heat treatment procedures, providing forming of dispersed ferrite-carbide mixture in steel microstructure.

The reported study was funded by RFBR according to the research project №18-58-45008 IND_a.

References

1. Chukin D. M., Ishimov A. S., Zherebtsov M. S. Usage of GLEEBLE 3500 complex for determination of critical points in microalloyed steel 80P. *Mezhdunarodnyi nauchno-issledovatel'skiy zhurnal*. 2012. No. 5. pp. 131–133.

2. Zilnyk K. D. et al. Martensitic transformation in Eurofer-97 and ODS-Eurofer steels: A comparative study. *Journal of Nuclear Materials*. 2015. Vol. 462. pp. 360–367.
3. Raju S. et al. A study on martensitic phase transformation in 9Cr-1W-0,23V-0,063Ta-0,56Mn-0,09C-0,02N (wt.%) reduced activation steel using differential scanning calorimetry. *Journal of Nuclear Materials*. 2010. Vol. 405. pp. 59–69.
4. Chandravathi K. S. et al. Effect of isothermal heat treatment on microstructure and mechanical properties of reduced activation ferritic martensitic steel. *Journal of Nuclear Materials*. 2013. Vol. 435. pp. 128–136.
5. Vdovin K. N., Lisovskaya M. A., Pivovarova K. G. The use of thermal analysis to study the structure and properties of roll steels. *Metal Science and Heat Treatment*. 2014. Vol. 56. pp. 302–305.
6. Grebenkov S. A., Skudnov V. A., Shatsov A. A., Kleiner L. M. Deformation strengthening of low-alloyed martensite steels of the system Cr-Mn-Ni-Mo-V-Nb. *Proceedings of Nizhny Novgorod State Technical University n. a. R. E. Alekseev*. 2014. No. 3 (105). pp. 228–238.
7. Shiryaev O. P. MMK-Metiz: saving, enlargement, modernization. *Chernye metally*. 2013. No. 10. pp. 24–26.
8. Vedeneev A. V., Ezhov V. V., Kuzmenko A. I. The module of 4-fold twisting for increase of productivity of rope machines. *Chernye metally*. 2013. No. 10. pp. 48–52.
9. Sukhorukov V. V., Vorontsov A. N., Volokhovskiy V. Yu. Control of hoisting rope wear for hot metal cranes of metallurgical enterprises. *Chernye metally*. 2013. No. 10. pp. 56–60.
10. Gadeev D. V. Investigations of phase transformations using the methods of structural and thermal analysis in dual-phase alloys on titanium base : Dissertation ... of Candidate of Engineering Sciences. Ural Federal University. Ekaterinburg. 2012. 24 p.

MODELING OF A NEW CHANNEL ROLLING METHOD IN THE DEFORM SOFTWARE PACKAGE

Ustinova E., Shvarts D., Mikhaylenko A.

*Ural Federal University named after the first President of Russia B.N. Yeltsin,
Yekaterinburg, Russia
ustinoval694@gmail.com*

The most important component of any rolling operation is the calibration of the rolls. The ability to obtain a finished product of high quality at minimal cost is determined by the right calibration. There exists a well-known practical method of rolling channels that relies on the flared flange method. However, it has a number of drawbacks. The biggest drawback is related to the difficult strip entry conditions when a flared flange strip is entering a straight flange check gauge. This leads to the need to use sophisticated entry guides and can result in inaccurate length and geometry of the channel leg [1].

Specialists of the Department of Metal Forming at the Ural Federal University are currently working on creating a new methodology for optimizing the roll calibration operation for channel rolling based on a systematic approach – Two-Stage Optimization Concept [2-6]. The new approach helped obtain a completely new type of channel gauge with inward bent flanges (Fig. 1), which can be used for the flared flange method.

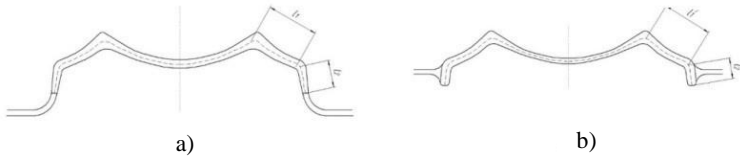


Fig. 1. Channel gauges with inward bent flanges:
 a) intermediate gauge; b) prefinishing check gauge

The flanges are bent on 1/3 of their length. It is proposed to use the resultant gauges as intermediate (Fig.1, a) and prefinishing check (Fig.1, b) gauges in the flared flange method. Straightening of the flanges will be carried out in a straight flange finishing gauge with an increased flange angle.

The roll calibration for channel 16 in Section Mill 650, which is currently in operation at the Azovstal Iron & Steel Works, was selected as a prototype process. We simulated this operation [7]. In our view, the gauge design can be improved. Thus, in particular, flared flange gauges can be used as shown in Fig. 1. The simulation in DEFORM showed significant advantages of the optimized gauge over the prototype one: the strip entry conditions have been considerably improved, which contributes to the symmetry of the finished sections and helps reduce the power consumption, the roll wear and the roll remachining cost (Fig. 2).

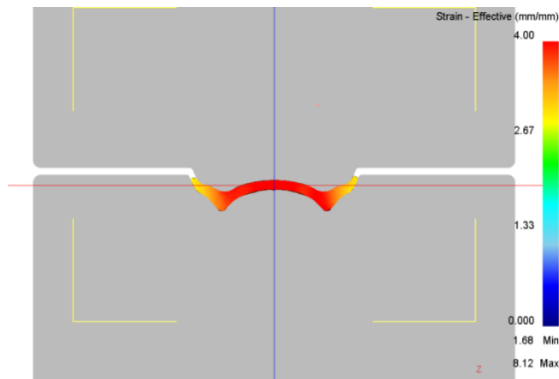


Fig. 2. Rolling in the new shape gauge

The reported study was funded by RFBR, project number 20-38-90246.

References

1. Smirnov V.K., Shilov V.A., Inatovich Yu.V. Roll calibration. Moscow: Teplotekhnika, 2010. 490 p.
2. Shvarts D.L., Michaylenko A.M., Ustinova E.I. Optimization of roll calibration for channel rolling. Chernye Metally. 2019. No. 9. pp. 4-8.
3. Li H., Zhao Z., Zhang J. et al. Analysis of flatness control capability based on the effect function and roll contour optimization for 6-h CVC cold rolling mill. Interna-

tional Journal of Advanced Manufacturing Technology. 2019. Vol. 100, No 9-12. pp. 2387-2399.

4. Wu L., Liu J., Dhanasekar M., Wang H., Wen Z. Optimisation of railhead profiles for curved tracks using improved non-uniform rational B-splines and measured profiles. *Wear*. 2019. Vol. 418-419. pp. 123-132.

5. Wolf C., Stadler A. T., Baumgartner W. Cross-section optimisation for cold-rolled steel beams using a genetic algorithm. *METAL*, Conference Proceedings. Brno, 2016. pp. 507-512.

6. Prinz K., Steinboeck A., Kugi A. Optimization-based feedforward control of the strip thickness profile in hot strip rolling. *Journal of Process Control*. 2018. Vol. 64. pp. 100-111.

7. Ilyukovich B.M., Nekhaev N.E., Merkuriev S.E. et al. Rolling and calibration. *Dnepropetrovsk*. 2002. Vol. V. p. 482.

DEVELOPMENT OF THE ASYMMETRIC ROLLING TECHNOLOGY AS A SEVERE PLASTIC DEFORMATION METHOD FOR NARROW ALUMINUM STRIPS WITH A GRADIENT STRUCTURE SHOWING HIGHER STRENGTH AND DUCTILITY

**Kozhemyakina A.¹, Pesin A.¹, Tandon P.², Pustovoytov D.¹,
Biryukova O.³, Ilina N.¹, Dubey A.K.², Shahare H.Y.²**

¹*Nosov Magnitogorsk State Technical University, Magnitogorsk, Russia*

²*Indian Institute of Information Technology, Design and Manufacturing,
Jabalpur, India*

³*Polytechnic College, Magnitogorsk, Russia
kozhemiyakina.a@yandex.ru*

Development of aluminum nanomaterials is globally seen as one of the key areas of technological progress. Such materials demonstrate high physical, mechanical and performance properties and are a subject of study for researchers in physics, mechanics of materials, and metal forming. One of the innovative nanostructuring technique for metallic materials includes the method of severe plastic deformation (SPD). A key parameter characterizing ultrafine-grained (UFG) materials is the grain size, namely, the structural elements separated by high-angle boundaries. It is this parameter that determines a typical scale of processes that influence the physical, mechanical and performance properties of nanostructured materials. In addition to the grain size, the properties of UFG materials are significantly influenced by such factors as the state and parameters of grain boundaries, phase composition, density and configuration of existing crystallographic defects, texture, precipitations and segregations, etc. There is a range of factors that characterize the grain boundaries in SPD materials: a defective structure of boundaries determining the degree of their non-equilibrium state; a range of grain-boundary angles describing the share of high-angle or special boundaries; the chemical composition of grain boundaries in alloys in which atoms of alloying elements may be redistributed in space as a result of SPD. Moreover, the above nanostructural parameters may vary within a wide range depending on SPD schedules. It is the formation of high-angle boundaries that determines the considerable difference of UFG metals and alloys produced by SPD methods from ordinary materials processed by conventional metal forming methods.

However, the existing SPD methods are characterized with certain technical drawbacks limiting their wider application in industry. Such drawbacks mainly include small sizes of semi-finished products, low manufacturability and, consequently, limited performance and economic feasibility of such technologies. The stated factors considerably curb the commercial production and use of UFG metallic materials.

To find a solution to the above stated scientific and technical problems, the authors propose unconventional SPD methods that are based on asymmetric rolling realized due to mismatching velocities of the work rolls, contact friction conditions, and a combination of various deformation methods. It should be noted that the Laboratory of Mechanics of Gradient Nanomaterials at NMSTU houses a unique industrial and laboratory rolling mill 400 with a separate roll drive, which was built as part of the Megagrant under Resolution P220 of the Government of the Russian Federation and which has no counterparts in Europe.

For the first time, we theoretically determined the difference between asymmetric rolling as an SPD method and a conventional asymmetric rolling process; found regions that combine the required values of accumulated deformation and the shear angle for various aluminum alloys, which produce a UFG structure when these values are met; developed algorithms for determining rational process parameters of asymmetric rolling as an SPD method; developed and described algorithms for determining rational process parameters of asymmetric rolling when it is combined with other SPD processes.

The reported study was funded by RFBR (Project No. 20-31-70001), by the Megagrant (Agreement No. 074-02-2018-329, Subject 2018-08 MG), and by RSF (Agreement No. 20-69-46042, Subject 2020-06 RNF), by a grant of the RFBR (contract No. 18-58-45013\19 IND_a from 14.10.2019).

References

1. Pesin A.M. Simulation and development of asymmetric deformation processes aimed at increasing efficiency of sheet rolling. Simulation and Development of Metal Forming Processes. 2002. No. 1. pp. 107-113.
2. Pesin A.M. Scientific school of asymmetric rolling in Magnitogorsk. Vestnik of Nosov Magnitogorsk State Technical University. 2013. No. 5 (45). pp. 23-28.
3. Pesin A., Salganik V., Trakhtengerts E., Cherniakhovskiy M., Rudakov V. Mathematical modelling of the stress-strain state in asymmetric flattening of metal band. Journal of Materials Processing Technology. 2002. Vol. 125-126. pp. 689-694.
4. Salganik V.M., Pesin A.M., Chikishev D.N., Berezhnaya G.A., Pustovoytov D.O. Asymmetric rolling processes: theory and technological solutions. Magnitogorsk, 2013. 128 p.

SESSION 2 – Fundamental Problems of Metal Forming during Transition to Innovative Technology

THEORETICAL AND EXPERIMENTAL ANALYSIS OF A NECK PROFILE IN CYLINDRICAL SPECIMENS

Erpalov M.

*Ural Federal University named after the first President of Russia B.N.Yeltsin,
Yekaterinburg, Russia
m.v.erpalov@urfu.ru*

Tensile testing of cylindrical specimens plays a key role in determining the mechanical properties of various metals and alloys. It is also the main type of acceptance testing for metal products. Moreover, the scope of its application can be expanded if the stage of localized deformation is subjected to analysis. At the same time, the main difficulty in studying the formation and development of the neck is the inhomogeneous distribution of both axial and radial stresses. There exists a number of mathematical models [1-3] that allow to calculate stresses in the minimum section of a specimen, as well as evaluate the stress triaxiality in the center of this section. However, any such model is based on the assumption that the researcher knows two dimensions – the diameter of the sample in the minimum cross section of the neck d and the neck curvature radius R .

This paper uses the finite element method to analyze the neck profile in various materials. As a result of theoretical analysis, an analytical equation is proposed that describes the neck profile:

$$\rho(z) = \frac{d_1}{2} - \frac{d_1 - d}{2} \left(1 + \frac{z^2}{c} \right)^{-1}, \quad (1)$$

where z and ρ – axial and radial coordinates of points on the specimen surface, respectively, d_1 – diameter of the specimen at the moment the strain is starting to localize in the neck, c – coefficient determined by the material properties, $c > 0$. Eq.1 assumes that the minimum cross-section of the specimen has the coordinate $z_0 = 0$ and is located in the middle of the gauge.

Theoretical studies prove the high efficiency of the proposed equation. The approximation accuracy of the neck profile over the entire gauge length of the specimen was at least 96%. The average accuracy in the specimen's neck is approximately 99.5% (Fig. 1).



Fig. 1. The approximation of the neck profile with the help of Eq.1 based on FEM

The advantage of Eq.1 is that it makes it easy to determine the neck curvature radius:

$$R = \frac{c}{d_1 - d} . \quad (2)$$

For experimental analysis of the localized deformation stage, a program was developed with the help of the Wolfram Mathematica software that can do approximation of the neck profile with the proposed equation based on the video of the test process or on individual photos. The program consists of several modules. With the help of the first module, one can split the video file of the test process into separate frames. The second module helps download and analyze data from the testing machine. The third module uses the Sobel filter, and one can use it to select the boundaries of the specimen with the neck for each frame. The last module approximates the neck using Eq.1 and calculates the stress triaxiality in the center of the specimen, as well as the true stress value at each moment of the test. Fig.2 shows the neck approximation results for a specimen with the diameter of 5 mm and the original gauge length of 25 mm made of steel 09G2S.

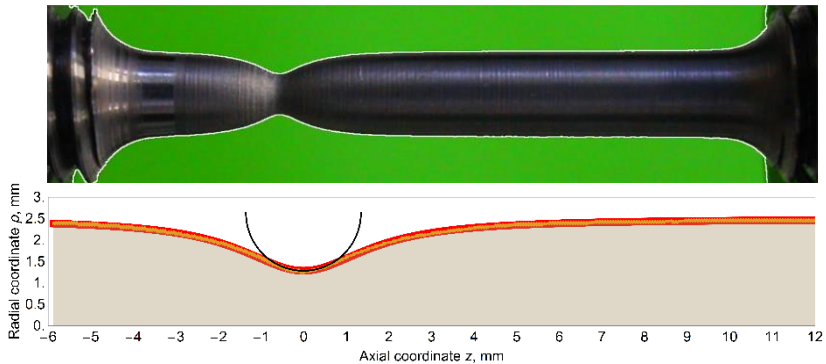


Fig. 2. Experiment-based approximation of the neck profile using Eq.1

References

1. Bridgman P.W. Studies in Large Plastic Flow and Fracture: With Special Emphasis on the Effects of Hydrostatic Pressure. New York-London: Harvard University Press, 1952.
2. Davidenkov N.N., Spiridonova N.N. Analysis of the stress state in the neck of a stretched sample. Factory Laboratory. 1945. Vol. 6. pp. 583-593. (in Russ.)
3. Ostsemin A.A. On the analysis of the stress state in an elliptical neck of a specimen under tension. Factory Laboratory. 2009. Vol. 4. pp. 19-28 (in Russ.)

PECULIARITIES OF CONTACT INTERACTIONS BETWEEN CARBON STEEL WIRE AND DIE IN DRAWING WITH TORSION

Gulin A.¹, Polyakova M.¹, Pivovarova K.¹, Stolyarov A.²,
Narasimhan K.³, Prasad M.J.N.V.³.

¹*Nosov Magnitogorsk State Technical University, Magnitogorsk, Russia*

²*OJSC "MMK-METIZ", Magnitogorsk, Russia*

³*Indian Institute of Technology Bombay, Mumbai, India*
a.gulin@magtu.ru

It is well-known that the effectiveness of deformation processing of metals depends on the contact interaction between the tool and the workpiece. However, at present there exist no science-based approaches to predicting the effectiveness of deformation processing of metal and alloys and how it correlates with further process operations. Deformation processing of steels involves a complex exposure to many factors. The basic metal deformation techniques include tension, compression, bending, and twisting. Application of different deformation schedules can change the structure and properties of the processed metal in a different way. The contact interaction between the processed metal and the tool is of special importance. In conventional metal processing, the surface layer is studied based on the phenomenological approach of continuum mechanics. The paper [1] states that the total thickness of the contact layer with alternating deformations as a result of rough surface interaction is equal to the height of microasperities or twice that height. It is well-known that drawing through conical dies is the basic operation in wire manufacturing. The process is characterized with complicated stress-strain state patterns in the deformation zone of the processed metal. That is why, after drawing, the metal has low ductile properties. And that is the reason why heat treatment operations should be included in the wire manufacturing process. The papers [2, 3] demonstrate that the contact area between the wire and the die has peculiar microstructure and properties.

Through theoretical and experimental research, it was proved that, during drawing, a 20-40 μm layer is formed on the wire/tool contact surface, where the strain intensity in metal is higher as compared with the strain in bulk material [4-7].

One of the ways to increase the effectiveness of wire drawing is to rotate the die. The results of the studies show that as the wire rotation rate rises, the drawing effectiveness increases while the drawing stress drops [8-11]. Currently, there exist techniques that combine drawing with torsion [12-14]. Each of such techniques has its technical peculiarities. But the complicated stress-strain state patterns typical of the combined rod drawing and torsion process results in a specific interaction between the contact surface and the tool, which makes both theoretical and experimental studies more complicated [15, 16].

This paper examines the strain in the surface layers of a high carbon 0.7%C steel wire which come in contact with the die in the combined drawing and torsion process. Modeling of the wire surface behavior under combined deformation processing made it possible to analyze the peculiar distribution of strain along the main axes X, Y, and Z. The maximum strain was observed in the area of about 10 μm from the wire/die contact surface.

The reported study was funded by RFBR according to the research project №18-58-45008 IND_a.

References

1. A.N. Levanov. Contact Frictions in Metal Forming Processes. Moscow: Metallurgiya, 1976. p. 416.
2. K. Hosoda, M. Asakawa, S. Kajino, Y. Maeda. Wire Journal International. 2008. November. p. 68.
3. S. Kajino, M. Asakawa. Journal of Materials Processing Technology. 2006. Vol. 177. p. 704.
4. A.Y. Stolyarov. Steel in Translation. 2012. Vol. 42(1). p. 70.
5. S. Kajino, M. Asakawa. Journal of Materials Processing Technology. 2006. Vol. 177. p. 704.
6. D.-H. Cho, S.-A. Lee, Y.-Z. Lee. Tribology Letters. 2012. Vol. 45. p. 123.
7. C. Cordier-Robert, B. Forfert, B. Bolle, J.-J. Fundenberger, A. Tidu. Journal of Materials Science. 2008. Vol. 43. p. 1241.
8. N. Guo, B. Song, B.-S. Wang, Q. Liu. Acta Metallurgica Sinica (English Letters). 2015. Vol. 28(6). p. 707.
9. A. Blackmore. Wire Journal International. 2006. Vol. 39(4). p. 98.
10. B. Goes, A. Martin-Meizoso, J. Gil-Sevillano, I. Lefever, E. Aernoudt. Engineering Fracture Mechanics. 1998. Vol. 60(3). p. 255.
11. F. Knap. Wire World International. 1987. Vol. 29(4). p. 94.
12. G.I. Raab, A.G. Raab. Patent 2,347,633.
13. V.A. Bakshinov, B.A. Kolomiets, V.N. Lebedev, M.Yu. Usanov, V.A. Khari-tonov, M.V. Chukin. Patent 2,498,870.
14. M.V. Chukin, M.A. Polyakova, E.M. Golubchik, V.P. Rudakov, S.E. Noskov, A.E. Gulin. Patent 2,467,816.
15. S. Alexandrov, Y.-R. Jeng, Y.-M. Hwang. ASME Journal of Manufacturing Science and Engineering. 2015. Vol. 137. paper 051003.
16. G.S. Gun, M.V. Chukin, D.G. Emaleeva, N.V. Koptseva, Yu.Yu. Efimova. Vestnik of Nosov Magnitogorsk State Technical University. 2007. Vol. 3. p. 84.

UNDERSTANDING THE INFLUENCE OF REDUCTION MODES ON THE DEFORMATION UNEVENNESS IN A TUBE WALL

Radkin Yu., Bobarikin Yu.

*Sukhoi State Technical University of Gomel, Gomel, Republic of Belarus
yradkin@gmail.com*

The accuracy of geometrical dimensions and the shape of hot-deformed seamless tubes is the most important quality characteristic of this type of metal products. In this case, particular attention is paid to the dimensional accuracy of the tube wall. A deviation in the wall thickness may lead to the unevenness of mechanical properties over the tube section, as well as to the appearance of defects on the tube surface [1].

Forming a finished tube on a stretch reduction mill is one of the most important stages in the production of hot-deformed seamless tubes. A reduction mill is a mill that runs in a continuous mode and consists of three roll stands arranged in a series. As a result of successive reduction of gauges along the stands, the diameter of the rolled tube decreases; in this case, the wall thickness can increase, decrease or remain unchanged [2].

Determination of the rolling modes is one of the main tasks related to the development of reduction processes.

The aim of this research is to determine the influence of reduction speed modes on the deformation unevenness degree in the production of hot-deformed seamless steel tubes.

The process of reducing a rough tube to produce a 93.17x12.45 mm tube of steel grade TT309 (L80 type1) was examined.

A number of numerical experiments was carried out to simulate the reduction process performed in different speed modes. The characteristics of the modes are shown in Fig. 1.

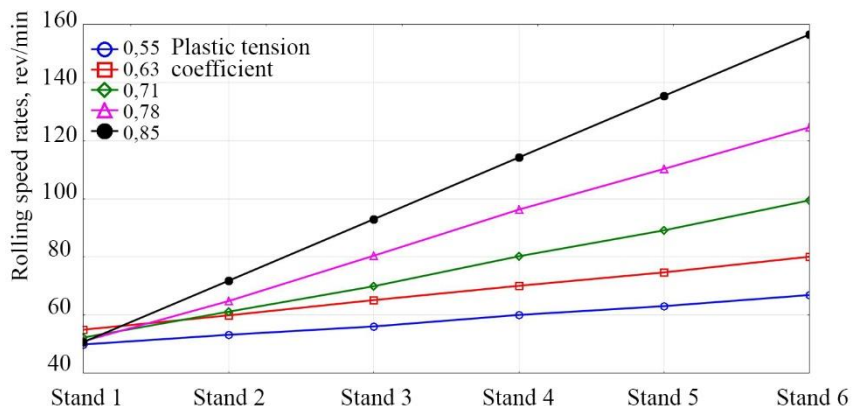


Fig. 1. Reduction Speed Modes

Using numerical simulation, the results of the stress distribution in the deformation zones of the stretch reduction mill stands were obtained (Table 1).

Table 1

Stresses in the deformation zones of the stretch reduction mill stands

Plastic tension coefficient	Effective stresses, MPa					
	Stand number					
	1	2	3	4	5	6
0.55	43.3	45.3	47.1	46.1	46.3	46.9
0.63	42.1	45.1	45.8	46.3	46.6	46.2
0.71	42.9	44.3	44.7	45.4	45.3	45.8
0.78	41.9	44.2	44.9	45.5	45.4	45.7
0.85	43.2	45.9	46.3	45.9	45.9	47.1

Having analyzed the color-coded charts of the stress state and geometric parameters of the longitudinal and cross sections of the billet in the deformation zones of the stretch reduction mill stands, the authors determined that when the plastic tension coefficient is higher than 0.8, a thinning of the tube wall takes place. When the plastic tension coefficient is below 0.6, there is an imbalance of internal stresses across the tube

section, which affects the accuracy of the tube profile and contributes to the formation of nonconformity defects.

Thus, the optimal value of the plastic tension coefficient is in the range of 0.6-0.8. Sticking to the above range will contribute to a uniform stress distribution in the billet during the reduction process and thus improve the profile accuracy and the overall quality of hot-deformed seamless steel tubes.

References

1. Marcin Knapinski, Yuri L. Bobarikin, Yaroslav I. Radkin. The rolling tool development in order to improve the geometry of a tube profile and to reduce the wear of mill rolls. *New Trends in Production Engineering*. 2019. Vol. 2, Issue 2. pp. 321-330.
2. Danchenko V.N., Kolikov A.P., Romantsev B.A., Samusev C.B. Tube production technology. Moscow: Internet inzhiniring, 2002. 638 p. (in Russ.)

STRESS STATE OF DIES FOR HEXAGONAL RODS PRODUCTION

Malakanov S.

*Nosov Magnitogorsk State Technical University, Magnitogorsk, Russia
samalakanov@mail.ru*

Calibrated hexagonal rods are widely used in various industries in the manufacture of fasteners (bolts, nuts, etc.) and pipe fittings (fittings, adapters, etc.) [1-4]. The most common method of manufacturing a calibrated hexahedron is to draw through monolithic polyhedral dies, which are made in the form of a steel casing with a carbide insert pressed into it [5-7]. For the manufacture of dies are used solid alloys of grades HG30, HU30, containing tungsten carbide and cobalt. The following physical and mechanical properties of alloys depend on the content of elements: compressive strength — 4600—4905 MPa; bending strength — 1400—1750 MPa; tensile strength 720—1150 MPa; modulus of elasticity 574,000-608,000 MPa; Poisson's ratio 0.21-0.23.

The design of die is the most important factor related to forming energy and deformation behavior of material. The efficiency of production of hexagonal rods largely depends on the durability of dies. The premature failure of the dies is caused due to their intensive wear and destruction due to the action of substantial radial forces from the deformable workpiece. In the process of drawing circumferential tensile stresses arise in the zones adjacent to the corners of the polyhedral hole of the die, lead to the formation and development of cracks with subsequent destruction (Fig. 1).

Figure 2 shows the distribution of the contact normal pressure N when drawing a hexagonal rod from a hexagonal billet (Fig. 2).

Quantitative and qualitative distribution of radial, circumferential, axial stresses along the length of the working channel was determined on the basis of the developed technique of computer simulation of the stressed state of polyhedral dies using the finite element method.



Fig.1. Destroyed carbide monolithic die by GOST 5426-76

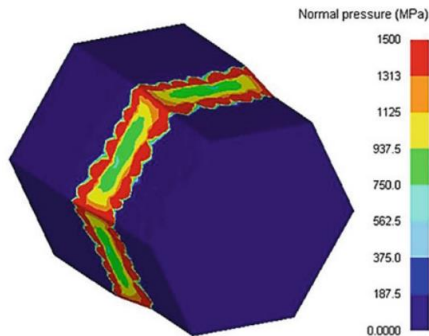


Fig.2. Distribution of contact normal pressure on the surface of the workpiece (drawing a hexagonal rod from a hexagonal billet)

The stressed state of polyhedral sector drawing is determined. It is found that the implementation of the insert in the form of sector elements excludes the concentration of tensile circumferential stresses in the longitudinal section of the die passing through the edges of the hexagon.

The reported study was funded by RFBR according to the research project №16-38-00026 mol_a.

References

1. Zhelezkov, O.S., Malakanov, S.A., Dampilon, V.G. Determination of energy-strength parameters when drawing a hexagonal profile in a monolithic drawing. (2009) *Processes and Equipment of Metallurgical Production, Magnitogorsk*, pp. 154-158.
2. Arseniev V.V. (2002) The current state of production of hardware in Russia. *Steel* 3:96-97
3. Zaytsev M.A., Sorokin V.N., Kleimenova N.V. (1985) Production and application of high-precision profile profiles in the national economy. *Metallurgy* 2:30-32
4. Batalov A.G., Oleinikov N.D., Kireev V.I. (1982) Steel shaped profiles of high accuracy. Kirov Regional Printing House, Kirov
5. Vladimirov Y.V. (1996) Manufacture of metal products and calibrated metal in foreign countries in 1991-1995. *Ferrous Metall* 1:26-31

6. Dukmasov V.G., Vydrin V.N., Tishchenko O.I. (1990) Production of precision rolled products. Metallurgy, Moscow

7. Vydrin V.N., Grosman A.B., Pavlov V.K. (1977) Production of shaped profiles of high accuracy. Metallurgy, Moscow

EFFECT OF COMBINED BENDING & TWISTING DURING STEEL WIRE DRAWING ON THE DEVELOPMENT OF MICROSTRUCTURE & PROPERTIES

Deepak Kumar Singh

*Indian Institute of Technology Bombay, Mumbai, India
depakmnit@gmail.com*

High production rates and lower input costs without compromising the quality are of great relevance today. Some processes involve multiple stages. For example, rope manufacturing involves drawing, bending and twisting. Industries are trying to streamline such multiple step processes to obtain a single continuous process, which will certainly save energy and time and improve efficiency. However, proper research is needed into processing parameters, equipment design and the properties of the final product resultant from a continuous process. This paper looks at the combined bending and twisting process involved in the cold drawing of pearlitic wires and how it influences the microstructural development and mechanical properties of the wire.

Among all the steel products, cold drawn pearlitic steel has the highest strength. It ranges from 5 to 6 GPa. Such steel is suitable for various applications, e.g. for suspension bridges, steel cord, concrete reinforcement, wind mill blades for cleaner & greener energy production etc. 0.7% C steel was chosen for the experiments, during which it was subjected to different kinds of deformation processing such as tensile deformation, alternating bending, twisting and their combination. Experimental research was carried out in order to understand the influence of different kinds of plastic deformation on the microstructure of carbon steel wire with a near eutectoid composition. Through scanning electron microscopy, the pearlite behavior after deformation processing at different total deformation degrees was studied. TEM analysis was also carried out. Mechanical properties such as tensile strength and hardness were tested. And a comparative analysis of all the properties was conducted.

References

1. T. Gladman, I.D. McIvor, F.B. Pickering. Some aspects of the structure-property relationships in high-carbon ferrite-pearlite steels. Journal of the Iron and Steel Institute. Vol. 210. 1972. pp. 916–930.

2. Ning Guo, Baifeng Luan, Qing Liu. Influence of pre-torsion deformation on microstructures and properties of cold drawing pearlitic steel wires. Materials and Design. 50 (2013). pp. 285–292.

3. Xiaodan Zhanga, Andrew Godfrey, Niels Hansenb, Xiaoxu Huang, Wei Liua, Qing Liu. Evolution of cementite morphology in pearlitic steel wire during wet wire drawing. Materials Characterization. 61 (2010). pp. 65 – 72.

4. Xiaodan Zhang, Andy Godfrey, Xiaoxu Huang, Niels Hansen, Qing Liu. Microstructure and strengthening mechanisms in cold-drawn pearlitic steel wire. Acta Materialia. 59 (2011). pp. 3422–3430.

DEVELOPMENT OF CONTROL PROGRAM FOR HOT TORSION TEST UNIT

Erpalov M.

*Ural Federal University named after the first President of Russia B.N.Yeltsin,
Yekaterinburg, Russia
m.v.erpalov@urfu.ru*

This paper looks at torsion testing of cylindrical specimens with the aim to study the rheological properties of materials, primarily in the hot state. One of the main problems of hot tests is the effect of strain rate on flow stresses [1]. When it comes to testing cylindrical specimens, this problem is successfully solved by imposing certain conditions on the speed mode testing, and namely, the strain rate should be proportional to the strain of the specimen [2]. The paper [3] describes an algorithm to control the test unit. The algorithm involves changing the angular velocity of the active grip of the test unit according to the exponential dependence:

$$\omega = \sqrt{3} \frac{l}{r} c k e^{kt}, \quad (1)$$

where l and r are the length and radius of the specimen gauge, respectively, c – constant determining the total duration of the test, $k = \dot{\xi}/\varepsilon$ – constant defining the region in which the rheological properties of the material are analyzed, where ξ is a strain rate and ε is strain.

The test unit for torsion testing of specimens at temperatures of up to 1,250°C has been developed and manufactured at the Ural Federal University. The test unit is equipped with a SDS20-34100 stepper motor connected to the active grip via gearbox. A personal computer controls the rotation of the output shaft of the stepper motor according to the adjusted program written in Servo Motor Language. However, the capabilities of this language are very limited and there is no possibility of setting an exponential function in the control program. To solve this problem, one should calculate discrete control actions and write them to EEPROM of the embedded controller. Nevertheless, there are strict restrictions that apply to discrete control – i.e. the angular velocity ω_i , rpm, acceleration a_i and revolutions per s^2 must be given by integers. This leads to overcontrol by the position of the motor shaft at the initial stage of the test and the inability to obtain reliable data on the rheological properties of the material being tested.

The paper proposes a new approach to the calculation of discrete control actions taking into account the existing restrictions on the part of the embedded software, which is implemented as a program for their automatic calculation. The essence of the proposed approach is that, with the selected time step, the target values of the angular acceleration and the angular velocity are calculated in a way that eliminates overload by the position of the motor output shaft. For this, at each time step, the following condition has to be satisfied (Fig.1):

$$\left\| \int_{t_i}^{t_i^*} a_i dt + \int_{t_i^*}^{t_{i+1}} \omega_i dt - \int_{t_i}^{t_{i+1}} \sqrt{3} \frac{l}{r} c k e^{kt} dt \right\| \rightarrow \min . \quad (2)$$

Fig.2 shows an example of implemented test unit control program, which satisfies the condition that $\dot{\xi}/\varepsilon = \text{const}$.

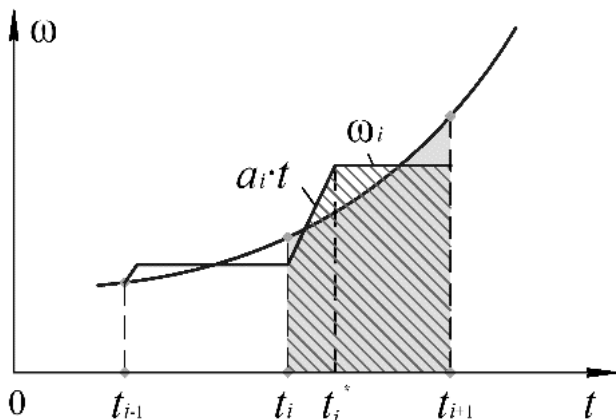


Fig. 1. Determining the target values of angular velocity and acceleration

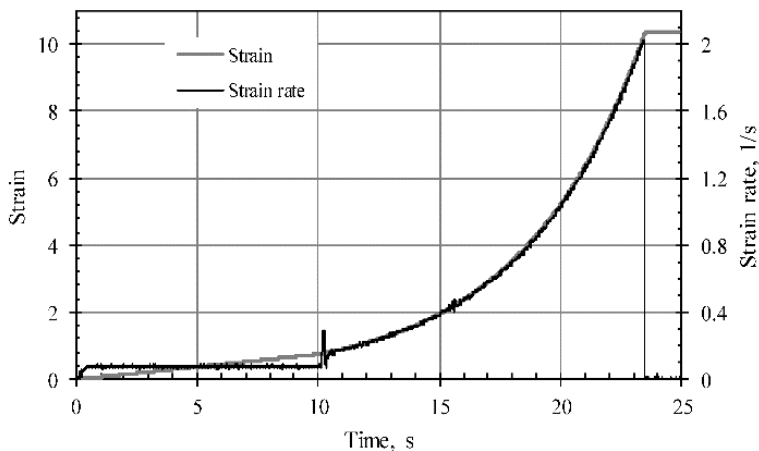


Fig. 2. Example of implemented test unit control program

References

1. Erpalov M.V., Kungurov E.A. Examination of hardening curves definition methods in torsion test. *Materials Physics and Mechanics*. 2018. Vol. 38, No. 1. pp. 82-89.
2. Erpalov M.V., Pavlov D.A., Kungurov E.A. Method of determining shear deformation resistance of materials. Patent RF, No. 2713809.
3. Erpalov M.V., Pavlov D.A. Control and experimental data processing in torsion testing with variable acceleration. *CIS Iron and Steel Review*. 2018. Vol. 16. pp. 71-75.

APPROACHES TO CLASSIFICATION OF COMBINED AND INTEGRATED PROCESSES IN METAL FORMING

Lopatina E., Polyakova M.

*Nosov Magnitogorsk State Technical University, Magnitogorsk, Russia
lopatina.yekaterina2016@yandex.ru*

According to the review [1], the priority task in the development of metallurgical industry is to create combined and integrated processes based on different kinds of plastic deformation, heat treatment, and casting operations. Combined metal forming processes play a significant role in the creation of new technologies. They also increase the efficiency of manufacturing new materials for various purposes. A great variety of combined and integrated processes have been developed in recent years. The most popular processes include casting-and-rolling, rolling-and-forging, rolling-and-pressing+thermal hardening, etc. Due to high degrees and rates of deformation applied during combined and integrated processes, an ultrafine-grained structure can be obtained in the processed metals. It is a well-known fact that the ultrafine-grained structure may affect the mechanical properties of the processed metals [2].

All the existing metal forming processes can be classified into two groups: direct (simple) methods and combined ones [3]. It should be mentioned that the views on defining technological features and assigning a method to one group or the other differ greatly. For example, the method of rolling-and-drawing can be characterized in different ways. At the same time, this process can be referred to as “drawing-and-rolling”. Besides, there exists no unified classification of combined process [3]. One of the reasons is that all methods have different features and aims and use different equipment. Some of them require the use of evaluation criteria. Such terms as practical utility, expediency and efficiency are to be applied in all cases. Every engineer can come up with specific evaluation criteria. Such features as type of deformation, deformation degree, stress-strain state, deformation zone, process temperature, grain size of the processed metal, friction coefficient, etc. can be used as evaluation criteria for any combined or integrated method.

Results of scientific research carried out by Russian and foreign scientists lay the scientific basis for creating new combined or integrated processes. Moreover, one has to have some basic knowledge in the related disciplines, such as material science, solid state science, tribology, etc. This topic is of relevance because there is a lack of consensus about how to approach the classification of combined and integrated methods.

The reported study was funded by RFBR according to the research project №18-58-45008 IND_a.

Reference

1. Sidelnikov S.B. Classification and application of combined processing of non-ferrous metals and alloys. Proceedings of Universities. Non-Ferrous Metallurgy. 2005. No. 3. pp. 45-49.
2. Sidelnikov S.B., Samchuk A.P., Sidelnikov A.S., Voroshilov D.S., Bespalov V.M., Trifonenkov A.L. Research of the rheological properties of electrical wire rod from aluminum alloys with transition and rare-earth metals obtained by methods of

continuous casting and forming. Bulletin of the South Ural State University. 2015. Vol. 15, No. 2. pp. 89-95.

3. Oginskiy I.K., Taratuta K.V., Vostotskiy S.N. Combined processes in metal pressure processing. Material Processing by Pressure. 2018. No. 1. (46). pp. 167-174.

FEATURES OF ROLLING HARD-TO-DEFORM STEELS AND ALLOYS IN A SHELL MADE OF SOFT MATERIAL

Salikhyanov D.¹, Kamantsev I.²

¹Ural Federal University named after the first President of Russia B.N. Yeltsin,
Yekaterinburg, Russia

²Ural Branch of The Russian Academy of Sciences, Yekaterinburg, Russia
d.r.salikhianov@urfu.ru

An effective way of rolling high-strength and hard-to-deform steels and alloys is a method of rolling these materials in a shell made of soft material [1, 2]. This allows to significantly reduce the rolling force and prevent cracking due to softer stress-state scheme [1–3].

The main problem related to obtaining high-quality metallic materials is the plastic instability phenomenon expressed in local thinning and thickening of the core material, either over the entire thickness (“waviness”) [4] or at the end sections (“dog-boning”) [3]. In the manufacture of special-duty products (such as foils made of U-10Mo alloy), plastic instability is extremely undesirable [3], because it leads to different thicknesses and properties along the length of the product. The effect is illustrated in Fig. 1 showing an example of sandwich sheet rolling of model materials. Fig. 2 shows the thickness variation of hard material along the length of the product after sandwich sheet rolling.

The authors [4, 5] showed that the main cause of plastic instability is the difference in flow stresses between the core and shell materials. The authors [4, 5] propose some local thinning criteria, which impose restrictions on the choice of materials for the shell. Thus, the aim of this work was to analyze the mechanics and causes of plastic deformation instability during sandwich sheet rolling of clad materials, as well as the environment in which it occurs and ways to prevent it.

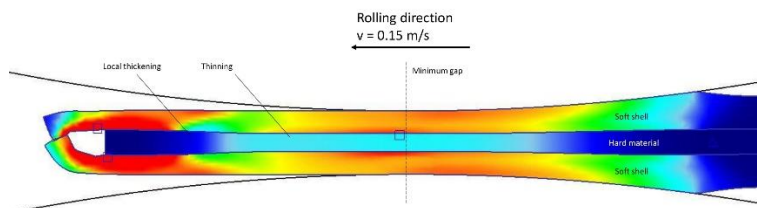


Fig. 1. The plastic instability phenomenon in sandwich sheet rolling

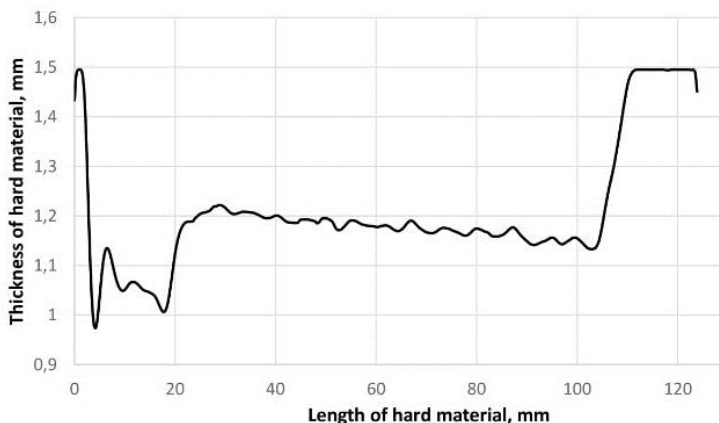


Fig. 2. Along-the-length thickness variation in high-strength material after sandwich sheet rolling

This research study was carried out as part of the governmental assignment No. 0836-2020-0020 and was supported by Act 211 of the Government of the Russian Federation (Agreement No. 02.A03.21.0006), as well as by the scientific research assignment No. AAAA-A18-118020790142-9 by the Institute of Engineering Science of the Ural Branch of the Russian Academy of Sciences.

References

1. Afonya A.A., Sansome D.H. A theoretical analysis of the sandwich rolling process. *International Journal of Mechanical Sciences*. 1973. Vol. 15, pp. 1-14.
2. Huang M.N., Tzou G.Y., Syu S.W. Investigation on comparisons between two analytical models of sandwich sheet rolling bonded before rolling. *Journal of Materials Processing Technology*. 2003. Vol. 140. pp. 598-603.
3. Soulami A., Burkes D.E., Joshi V.V., Lavender C.A., Paxton D. Finite-element model to predict roll-separation force and defects during rolling of U-10Mo alloys. *Journal of Nuclear Materials*. 2017. Vol. 494. pp. 182-191.
4. Imai T., Utsunomiya H., Matsumoto R. Finite Element Analysis of Plastic Instability Phenomenon in Cold Rolling of Clad Sheets. *Procedia Engineering*. 2017. Vol. 184. pp. 306-312.
5. Hwang Y.-M., Hsu H.-Hs., Lee H.-J. Analysis of plastic instability during sandwich sheet rolling. *International Journal of Machine Tools and Manufacture*. 1996. Vol. 36, No. 1. pp. 47-62.

SIMULATION OF CONTACT BETWEEN ROLLS OF A ROLLING MILL IN THE CONDITIONS OF EQUAL ACCELERATION WITH SLIPPAGE AND LUBRICATION

Kharchenko M., Konev S., Zhelezkov O., Zambrgiteckaya E., Salganik V.
Nosov Magnitogorsk State Technical University, Magnitogorsk, Russia
kharchenko.mv@bk.ru

Over time, a lubricant, which is one of the most important components, can become less efficient. Researchers are getting more and more questions related to the development of methods for controlling friction and wear. Because of the great relevance of such methods, a more detailed study is needed that would also include a series of laboratory tests.

Objective. Using an original laboratory equipment, to perform physical modeling of a heavily loaded friction pair ‘work roll/backup roll’ and to look at the rolling friction that occurs between two uniformly accelerating and slowing down cylinders with a lubricated elastic contact.

Equipment Used. A unique set of equipment was built to study the lubrication regimes of elastic frictional contact during a sliding uniform acceleration motion. It consists of a basic electro-mechanical unit, which is a standard friction machine — a SMC-2 tribometer [1,2], and an original automated control system, which encompasses original computer software, an original set of hardware and connection circuits (Fig. 1).

Implementation. For this research study, an experiment planning matrix was developed that includes four input (variable) parameters (external load P , N; lubricant consumption Q , ml/min; relative slip of samples ΔV , % (from 0 to 100%); acceleration/deceleration a , m/s^2) and two output parameters (friction torque, M_{tr} , Nm and wear Δm , gr). The characteristics of the studied samples are presented in [3,4]. As a result, we obtained curves showing a relationship between the friction torque and the acceleration rate (Fig. 2), which suggest that as the rolling speed in the contact area increases, the friction torque, just like the friction coefficient, decreases. This is in good agreement with the already known research results obtained by prominent scientists from Russia and abroad [5,6]. However, if we conduct an analytical study for the obtained curves using differential calculus methods to search for the extremum of function and its change rate, we can absolutely say that different experiment modes are associated with different periods of operation in which the friction coefficient would be at its lowest. The friction coefficient variation range does not depend on the amount of lubricant or the acceleration or deceleration rates.

Conclusion. As a result of the preliminary studies, it was suggested that the obtained minimum friction torque values on the Gerssi-Stribek curve, which reflects the most effective lubrication regime for contacting bodies, can vary over a fairly wide range. This can be derived not only from the obtained curves showing a relationship between the total rolling speed in the contact area and the friction torque, but also from the flow rate of the supplied lubricant and the mutual slip of the contacting bodies.

To better understand their interaction, as well as to explore a possible friction control mechanism based on actively changing input parameters, research in this area of tribology will be continued and a new methodology will be developed that will help evaluate the tribological conjugation efficiency based on wear and define the lubrication modes for specific cases of frictional contact.

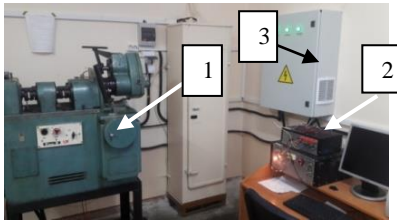


Fig. 1 General view of a laboratory complex with a retrofitted control system:

1. SMC-2 friction machine;
2. The unit for processing and converting information;
3. Switching unit

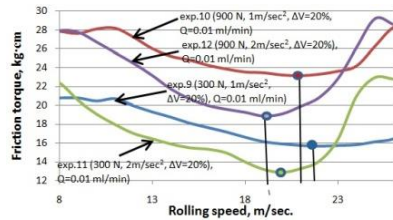


Fig. 2 The graph showing how the friction torque changes depending on the rolling speed in the contact area with different sliding conditions

This research work was carried out as part of the governmental assignment No. FZRU-2020-0011 by the Ministry of Science and Higher Education of the Russian Federation.

References

1. Kharchenko M.V., Dema R.R., Nefediev S.P., Osipova O.A. Universal testing complex for determining the tribotechnical characteristics of lubricants based on the serial friction machine SMC-2. Proceedings of Russian Universities. Engineering. 2017. No. 10 (691). pp. 60-68.
2. Platov S.I., Dema R.R., Kharchenko M.V., Amirov R.N. Experience of application of liquid lubricating materials during wide strip hot rolling. 3rd International Scientific and Technical Conference on Scientific and Technical Progress in Ferrous Metallurgy - SATPIFM 2017.
3. Levantsevich M.A., Kharchenko M.V., Dema R.R. Study of the Conditions for the Formation of an Adsorption Lubrication Mode of Heavily Loaded Friction Couples with Modeling in a Laboratory Setup. Journal of Friction and Wear. 2019. 40, 4. pp. 277-283. DOI: 10.3103/S106836661904007X
4. Kharchenko M.V., Zambrgitskaya E.S., Suvorova E.V. Modelling of the Process of the Friction Couple Contacting and Examining the Conditions of Forming an Adsorbating Monolayer on the Friction Surface Regarding the Use of a Lubricant Material. Materials Today: Proceedings. 2019. Vol.11. pp.155-162. DOI: 10.1016/j.matpr.2018.12.124
5. Chichinadze A.V., Berliner E.M., Brown E.D. et al. Friction, wear and lubrication (tribology and tribotechnology). Moscow: Engineering, 2003. 576 p.
6. Kragelsky I.V. Friction, Wear and Lubrication. Reference. In 2 books. Ed. by I.V. Kragelsky, V.V. Alice. Moscow: Engineering, 1978. Book 1. 1978.

INFLUENCE OF PROCESS PARAMETERS ON THE PROPERTIES OF CONTINUOUSLY EXTRUDED COPPER BUSES

Koshmin A.¹, Zinoviev A.¹, Chasnikov A.², Grachev G.²

¹National University of Science and Technology MISiS, Moscow, Russia

²Svelen Ltd., Saint Petersburg, Russia

koshmin.an@misis.ru

Due to such copper properties as high electrical conductivity, ductility and machinability, copper alloys are currently the most popular material for conductors. There are a lot of techniques for processing and production of copper conductors. The CONFORM™ process [1], which has recently become more widespread, has a special place among them. In spite of significant advantages delivered by the process, it has quite a few problems which are associated with the stability of the working tool, dynamic recrystallization during extrusion and the lack of understanding of the structural evolution that takes place in material under extrusion. This work was carried out to further the results of the previous research [2, 3]. To understand the possibility of controlling the physical and mechanical processes that arise during the extrusion of commercially pure copper, the influence of temperature-rate parameters on the properties and microstructure was investigated. Rods cast at various drawing speeds with the help of the UP-CAST® technology were extruded on an MFCCE 350 conform equipment at the rates of 4.5 and 6 m/min. The microstructure of the cast rods and extruded buses (Fig. 1) was studied using an optical microscope; hardness and electrical conductivity were also measured.

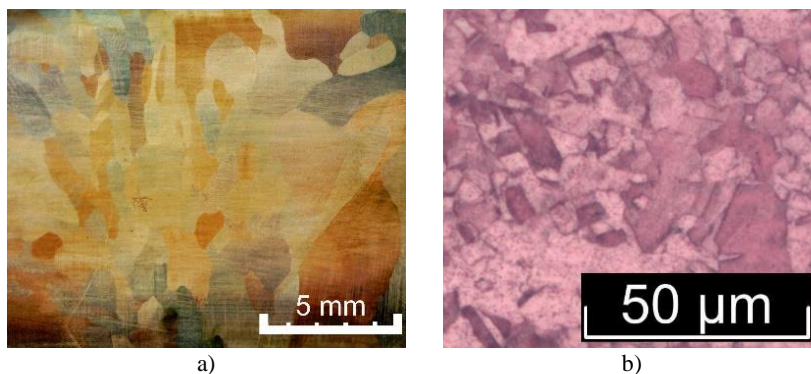


Fig. 1. Optical photos of the specimens' structure:

a) as-cast at the rate of 300 mm/min; b) as-extruded at the rate of 4 m/min

Using finite element modeling (FEM), the patterns of strain, stress and temperature distribution in the deformation zone were studied. The experimental results showed that in spite of the increase in the extrusion speed and, consequently, the temperature in the deformation zone, extruded buses do not experience any significant change in their properties. For all specimens, the average grain size was $10 \div 20 \mu\text{m}$, hardness - $65 \div 68 \text{ HRV}$.

References

1. Green D. Continuous extrusion-forming of wire section. Journal of the Institute of Metals. 1972. Vol. 100. pp. 295–300.
2. Zinoviev A.V., Koshmin A.N., Chasnikov A.Ya. Understanding how the M1 alloy microstructure is formed in the deformation zone during continuous extrusion of bus bars. Tsvetnye Metally. 2018. No. 10. pp. 81-85.
3. Zinoviev A.V., Koshmin A.N., Chasnikov A.Ya. Effect of continuous extrusion parameters on alloy M1 round section bar microstructure and mechanical property formation. Metallurgist. 2019. Vol. 63. pp. 422-428.

UNDERSTANDING THE FORMING MECHANISM OF MECHANICAL PROPERTIES IN NEW COLD-RESISTANT HIGH-STRENGTH STEEL

Kuznetsova A., Nikitenko O., Alekseev D., Poletskov P., Emaleeva D.
Nosov Magnitogorsk State Technical University, Magnitogorsk, Russia
allakuznetsova.mgtu@mail.ru

In today's Russia, to manufacture lifting and handling equipment and mining machinery, it is feasible to use high-strength weldable structural steels with a guaranteed yield strength of over 600 MPa. The technical and economic efficiency of using high-strength steels is associated with reduced weight and increased lifting capacity of structures, as well as a longer service life due to increased strength and cold resistance [1, 2].

The global production of high-strength weldable steel plates with a yield strength of over 600 MPa and a low-temperature impact strength (down to -60 °C) heavily relies on the technology of quenching and high-temperature tempering.

This study is aimed at searching for the best heat treatment schedule for plates made of new, sparingly alloyed cold-resistant steel with a guaranteed yield strength of over 600 MPa.

In this research, we used a steel grade 20G2SMRA developed by *Termodeform-MGTU* Research Center, which has the following chemical composition (wt. %): 0.20 C, 0.55 Si, 1.6 Mn, 0.3 Mo, 0.004 B [3]. Test samples of plates were melted, rolled and heat treated at the above mentioned centre.

The quenching and tempering temperature schedules applied varied within the below ranges:

– the quenching temperature was gradually raised from $A_{c3}+30$ °C to $T_{\max}=1,000$ °C with a step of 50 °C, water cooling;

– the tempering temperature was raised from 200 °C to 600 °C with a step of 100 °C.

Samples were prepared for dilatometric, metallographic and mechanical tests.

The best heat treatment schedule should ensure maximum values of impact strength and acceptable strength after quenching and further tempering.

Regarding the new steel grade 20G2SMRA, we applied a differential scanning calorimetry method and determined the critical points: $A_{c1}=725$ °C and $A_{c3}=814$ °C.

The relationship between the steel microstructure and the quenching temperature and their correlation with mechanical properties are shown in Fig. 1, a.

Optimum tempering temperature was determined considering its effect on structural changes and, consequently, on hardness HV1 and impact strength KCV^{-60} (Figure 1, b).

The conducted studies showed that the best hardening heat treatment schedule for plates made of steel grade 20G2SMRA was as follows:

- quenching from the temperature of 850 ± 20 °C – it ensures maximum impact strength $KCV^{-60} = 40$ J/cm² at acceptable hardness $HV1 = 452$;
- further high-temperature tempering at 600 °C – it helps obtain the required combination of hardness $HV1 = 291$ and impact strength $KCV^{-60} = 61$ J/cm².

Due to such an advantageous combination of hardness and impact strength at the test temperature of -60 °C, the steel grade 20G2SMRA can be applied for structures used in Far North.

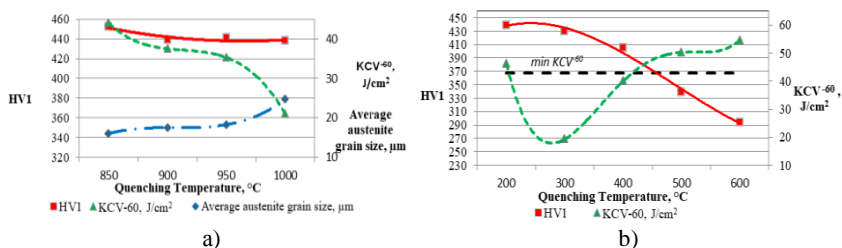


Fig. 1. Austenite grain size, impact strength KCV^{-60} , and hardness $HV1$ as a function of the quenching temperature (a);

Effect of the tempering temperature on the distribution of hardness $HV1$ and impact strength KCV^{-60} in steel grade 20G2SMRA (b)

This research study was funded by the Ministry of Education and Science of the Russian Federation – under the grant by the President of the Russian Federation (Agreement No. 075-15-2020-205 dated 17.03.2020).

References

1. Chukin M.V., Poletskov P.P., Nabatchikov D.G. et al. Analysis of technical requirements for steel plates resistant to ultra-low temperatures. Bulletin of South Ural State University. Series: Metallurgy. 2017. Vol. 17, No. 2. pp. 52–60.
2. Khlusova E.I., Sych O.V. Creation of cold-resistant structural materials for the Arctic. Background, experience and the present-day situation. Innovations. No. 11 (241). 2018. pp. 85-92.
3. Poletskov P.P., Nikitenko O.A., Kuznetsova A.S., Salganik V.M. The study of transformation kinetics for overcooled austenite of the new high-strength steel with increased cold resistance. CIS Iron and Steel Review. 2020. Vol. 19. pp. 56–59.

HYBRID PROCESSING AS AN EFFECTIVE WAY TO IMPROVE PHYSICAL AND MECHANICAL PROPERTIES OF MAGNESIUM ALLOYS

Linderov M.¹, Brilevesky A.¹, Merson D.¹, Vinogradov A.²

¹Togliatti State University, Togliatti, Russia

²Norwegian University of Science and Technology – NTNU, Trondheim, Norway
dardtvi@gmail.com

Bioresorbable magnesium alloys gain an increasing attention every year, as is evidenced by numerous review articles, like those (e.g. [1]) that summarize experimental data accumulated to date on numerous alloy systems. The obtained physical and me-

mechanical properties are discussed in relation to the microstructure and processing techniques applied, including contemporary methods of severe plastic deformation. However, the classical problem of obtaining the desired combination of high strength and ductility is still open. This is largely due to the fact that magnesium alloys have low plasticity due to the small number of allowed slip systems at room temperature. Besides, the alloys designed for medical applications have to be non-toxic, which imposes significant limitations on design strategies and the range of alloying systems to be used. Among the most promising alloys in terms of practical application there are the binary systems Mg-Zn and Mg-Ca, as well as the ternary systems Mg-Zn-Ca and Mg-Zn-Y. This paper compares the physical and mechanical properties of the low-alloy Mg-Zn-Ca system obtained through hybrid processing (i.e. a combination of different deformation methods) with the results found in the literature for similar alloys. Conclusions are made about the prospective application of hybrid processing.

Experimental details

Mg-1Zn-0.16Ca alloy ingots were homogenized at 450°C for 12 hours and then subjected to warm multistep isothermal forging (MIF) followed by cold isothermal rolling (MIF+IR) as described in [2]. 10×4×3 mm² specimens for mechanical testing were cut by spark erosion from the central part of the processed billet. The uniaxial tensile test was carried out on a Kammrath&Weiss machine at a constant nominal strain rate of 1×10⁻⁴s⁻¹.

Results and discussion

Figure 1 schematically shows the physical and mechanical characteristics obtained for the Mg-1Zn-0.16Ca alloy after hybrid treatment in comparison with the results obtained by other authors for magnesium alloys of a similar system, but with a different nominal content of alloying elements, in the as-cast state and after extrusion. The latter is the most common deformation technique applied for such materials, as described in the literature.

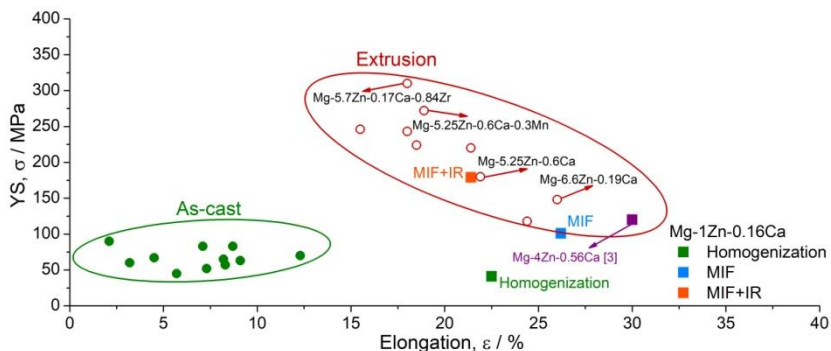


Fig. 1. Yield stress and elongation of Mg-Zn-Ca magnesium alloys (the data from [1] and [3] are compiled in the graph with the present results)

Based on the commonly observed trends and the worldwide research results, the physical and mechanical properties obtained for the Mg-1Zn-0.16Ca alloy are in good agreement with the data reported in [3] for a similar alloy that was subjected to equal-channel

angular pressing. Separately, it should be noted that the use of multistep isothermal forging together with isothermal rolling made it possible to increase the yield stress of the initially low-alloy magnesium alloy by more than 4 times compared with the state after casting and subsequent homogenization, due to which the properties of such alloy are close to those of high-alloy alloys. This is of fundamental importance for bioresorbable medical materials where a minimum content of alloying elements is desired so that the amount of alloying elements entering the body did not exceed the permissible concentrations.

References

1. Jiang P., Blawert C., Zheludkevich M.L. The Corrosion Performance and Mechanical Properties of Mg-Zn Based Alloys – A Review. *Corrosion and Materials Degradation*. 2020. 1, pp. 92-158.
2. Method for hybrid treatment of magnesium alloys. Patent RF, No. 2716612.
3. Vinogradov A.Yu., Vasilev E.V., Linderov M.L., Merson D.L., Rzhetskaya E.O. The influence of equal channel angular pressing on the structure and mechanical properties of magnesium Mg-Zn-Ca alloys. *Science Vector of TSU*. 2015. No. 4 (34). pp. 18-24.

FEM MODELING OF THE TUBE WORKPIECE HOT GUILLOTINING PROCESS

Orlov G., Malanov A.

*Ural Federal University named after the first President of Russia B.N.Yeltsin,
Yekaterinburg, Russia
artmalanov@mail.ru*

The aim of this research is to find a solution for the problem of distorted end faces in cylindrical continuously cast billets during hot guillotining process before they are fed in a piercing mill. To solve this problem, a new knife calibration procedure was developed, and a finite element model of the hot guillotining process was built using the DEFORM-3D computer simulation software package (Fig 1). This problem is referred to in the papers [1, 2], namely, the relationship between distorted end faces in workpieces and the formation of end defects in the sleeve. The paper [3] also looks at the impact of knife edge wear on the cut quality when cutting sheets and long products.

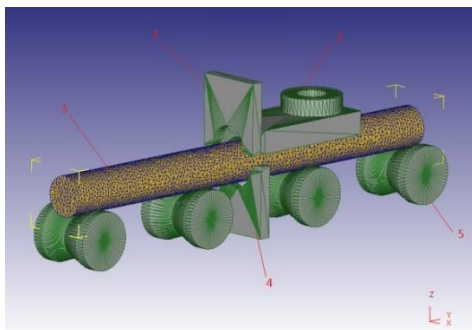


Fig.1. A model of hot guillotine knives

The new knife calibration procedure is performed using several radii to ensure gradual deformation. In order to prevent the free flow of metal in the direction of the gauge exit, the gauge height is also increased. The hot guillotining process was simulated using the proposed calibration procedure. It was found that the geometry of the knife gauges determines the geometry of the end part. Based on the simulation results, it was concluded that the proposed calibration procedure helps reduce the ovality of the end face of the workpiece by 47% compared with the current calibration procedure.

Conclusions: The use of the new knife calibration procedure will reduce the ovality of the workpiece by 47%; one of the ways to minimize the ovality of the end face of the workpiece after cutting can be reducing the width of the upper knife gauge while increasing the height of the lower knife gauge; the computer model of hot guillotine cutters can be used for further research of the hot guillotining process.

References

1. Ovchinnikov D.V., Bogatov A.A., Erpalov M.V. A new method of cutting continuously cast billets. Procurement in Engineering. 2012. No. 8. pp. 35-37.
2. Ovchinnikov D.V. Development, research and implementation of a technology for the production of high-quality tubing from a continuously cast billet. Dissertation. Yekaterinburg: UrFU, 2011. 247p.
3. Ulyanitskiy V.N., Petrov P.A., Orlov A.A. Influence of the cutting tool condition on the power parameters and the cut quality. Mechanical Engineering and Machine Science. 2019. No. 17 (60). pp. 105-112.

METHOD FOR CALCULATING THE TEMPERATURE OF THE DEFORMATION CONE CROSS-SECTIONS IN A COLD PILGER ROLLING MILL

Pilipenko S., Fruzki V.

*Polotsk State University, Novopolotsk, Republic of Belarus
44-08@mail.ru*

The process of pilger rolling is widely used for manufacturing cold and hot deformed precision pipes of a wide range of alloys and steel grades [1-3]. Such modes as cold and warm rolling, as well as rolling without emulsion are used in the cold pilger rolling process. In spite of a relatively small feed (2-6 mm) and considering the deformation cone length (300-500 mm), the metal is shaped in rather tough conditions (the mill stand can make up to 280 double strokes per minute). The cold rolling process generates a significant amount of heat [2-6]. This research paper describes a method that helps compensate for the thermal effect when rolling pipes using salt as grease and without using emulsion for cooling. Fig. 1 shows a comparison of the existing and proposed methods for calculating the working tool calibration [5-6].

The proposed method allows to calculate more precisely the cold pilger rolling process. The results of the calculations have been checked in practice and have confirmed the efficiency of the method [2-6].

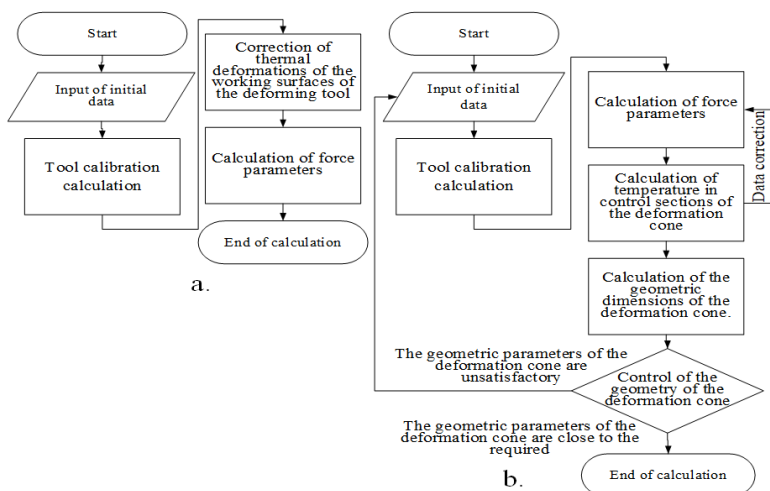


Fig. 1. Existing (a) and proposed (b) calculation methodology

References

1. Strehlau O. Introducing cold pilger mill technology. Available at: <https://www.thefabricator.com/tubepipejournal/article/tubepipeproduction/introducing-cold-pilger-mill-technology>
2. Shevakin Yu.F. Calibration and forces during cold rolling of pipes. Moscow: Metallurgizdat, 1963. 269 p.
3. Teterin P.K. The theory of periodic rolling. Moscow: Metallurgiya, 1978. 256 p.
4. Luo C., Keife H. A thermal model for the foil rolling process. Journal of Materials Processing Technology. 1998. Vol. 74, No. 1–3. pp. 158-173.
5. Pilipenko S.V., Dudan A.V. Development of a method for calculating heat release from plastic deformation during cold pilger rolling of pipes made of titanium alloys. Bulletin of Polotsk State University. Series B. Industry. Applied Science. 2018. No. 3. pp. 13-17.
6. Grigorenko V.U., Pilipenko S.V. On the changing cross-section of the gauge groove in a CPR mill under the influence of thermal expansion. Scientific Bulletin of DDMA. No. 1 (6E). 2010. pp. 37-42.

UNDERSTANDING THE EFFECT OF MULTI-STAGE HEAT TREATMENT SCHEDULES ON THE MICROSTRUCTURE AND PROPERTIES OF CRYOGENIC STEEL

Nikitenko O., Poletskov P., Kuznetsova A.

*Nosov Magnitogorsk State Technical University, Magnitogorsk, Russia
olganikitenko@list.ru*

One of the strategic objectives in the industrial development of today's Russia is to develop the industrial facilities and to increase an export share of liquefied natural gas in the Arctic regions of the Russian Federation (Fig. 1). This predetermines the need to

create and develop processing technologies for new materials with a complex set of properties designed for extremely low operating temperatures. However, optimum properties and structure can only be obtained as a result of properly chosen heat treatment regime [1], which determines the aim of the present study.



Fig. 1 Sakhalin-2: A large capital expenditure project in Russia

For our research, we chose the structural cryogenic steel grade 0N9A (9 % Ni) [2], that is widely used for the production of LNG storage tanks. Billets were melted, rolled and heat treated at the laboratory facilities of the *Termodeform-MGTU* Research Center.

The following heat treatment schedules were applied:

1. Single hardening from 830°C from a single-phase austenite region, including water cooling and downstream high-temperature tempering at 500°C, 550°C, 600°C.

2. Double hardening: the first stage involves hardening from a single-phase austenite region at the temperature of 830°C, while the second one – from the intercritical range (Ac_1 - Ac_3) at the temperature of 670°C – to achieve microstructural refinement and residual austenite stabilization, then high-temperature tempering at 500°C, 550°C, 600°C.

A set of metallographic tests was carried out at the shared use center of the Nanosteels Research Institute. For differential scanning calorimetry analysis, we used STA 449 F3 Jupiter, a simultaneous thermal analysis instrument by NETZSCH. The amount of residual austenite was determined by an X-ray diffraction meter, Shimadzu XRD-7000.

We determined the critical points of the cryogenic steel grade under study, which turned out to be lower as compared to conventional carbon steels. They are: $Ac_1 \approx 624^\circ\text{C}$ and $Ac_3 \approx 720^\circ\text{C}$. It was found that after double hardening austenite was enriched with alloying elements, which led to an additional 20 °C decrease in Ac_1 .

It was revealed that single hardening and downstream tempering within the studied temperature range resulted in the formation of a structure consisting of tempered martensite, residual austenite, α -phase and carbide particles, which mainly precipitate at the grain boundaries (Fig. 2, a) leading to a brittle behavior of steel. Double hardening and downstream tempering within the stated temperature range resulted in the formation of a disperse lamellar duplex structure consisting of α -phase, stripes of “new” martensite, regions with a structure of tempered martensite and residual stable austenite with a volume ratio of approx. 4 % (Fig. 2, b), which ensures ductility and resistance to breaking at cryogenic temperatures.

The application of the above findings will contribute to developing and improving heat treatment schedules for alloys with the specified composition.

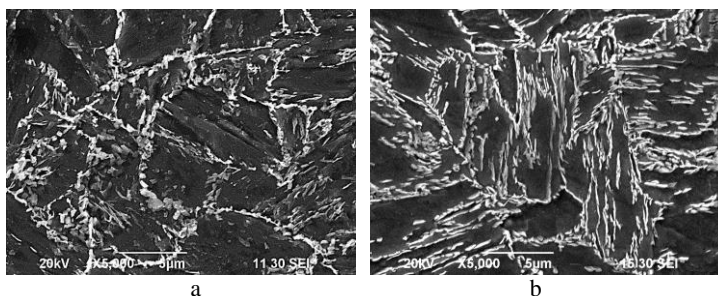


Fig. 2 A typical microstructure of the samples after single hardening from 830 °C and downstream tempering at 600 °C (a); after double hardening from 830 °C and 670 °C and downstream tempering at 600 °C (b)

This study was funded by the Ministry of Education and Science of Russia – the grant of the President of the Russian Federation (Agreement No.075-15-2020-205 dated 17.03.2020).

References

1. Zhang J.M. Ni steel for large LNG storage tanks. *Journal of Materials Engineering and Performance*. 2013. 22 (12). pp. 3867-3871.
2. Poletskov P.P., Nikitenko O.A., Chukin D.M., Gushchina M.S., Fedoseev S.A. On microstructure formation features of 9 % nickel cold-resistant steel and its properties brought about by different heating treatment procedures. *Journal of Chemical Technology and Metallurgy*. 2018. Vol. 53, No. 5. pp. 967-976.
3. Poletskov P., Gushchina M., Polyakova M., Alekseev D., Nikitenko O., Chukin D., Vasilev Y. Development of alloyed pipe steel composition for oil and gas production in the Arctic region. *Resources*. 2019. Vol. 8, No. 2. pp. 67.

ROLLER DIE DRAWING OF SMALL DIAMETER TITANIUM ALLOY WIRE

Sarafanov A., Radionova L., Gromov D., Svistun A.

*South Ural State University (National Research Institute), Chelyabinsk, Russia
sarafanovae@susu.ru*

Traditionally, wire is produced by drawing through solid dies. However, this processing method is not suitable for titanium alloys. Roller drawing places less strict requirements on the surface quality of the billet or lubrication. It also helps reduce the wear and the consumption rate of the drawing tool [1]. In roller drawing, sliding friction is replaced by rolling friction [2]. This reduces tool wear and improves the efficiency of the drawing process bringing down the energy consumption. The use of roller dies is especially important for small wire diameters.

The aim of this work is to develop a roller die design and a technology for manufacturing small diameter wire from titanium alloys.

On the basis of the calculated data [3], a roller die was designed and manufactured that consists of a unit of vertical rollers and a unit of horizontal rollers positioned at 90° to each other and with a 30 mm shift along the drawing axis (Fig.1,a).

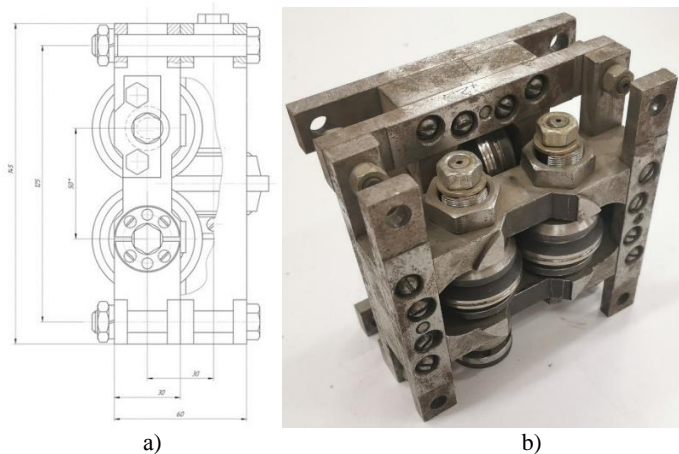


Fig. 1. Roller die: a) design; b) photo

In the course of experimental studies, the geometric parameters of the deformation zone during wire drawing were determined. The forces involved in the roller die drawing process were calculated, namely, the metal pressure on the rollers and the drawing force. Based on the data obtained, requirements were formulated for the design of a roller die for drawing 0.9 to 2.0 mm wires.

Based on the developed drawings, the SUSU Scientific Research Institute of Experimental Mechanical Engineering manufactured a set of roller dies (Fig. 1, b), which can be used to experimentally draw 2.0 to 0.9 mm titanium wire from a workpiece. Theoretical calculations can then be compared with experimental results.

A laboratory drawing mill (Fig.2), which was developed earlier, was used for experimental research. The mill is equipped with a system for measuring the drawing force [4].

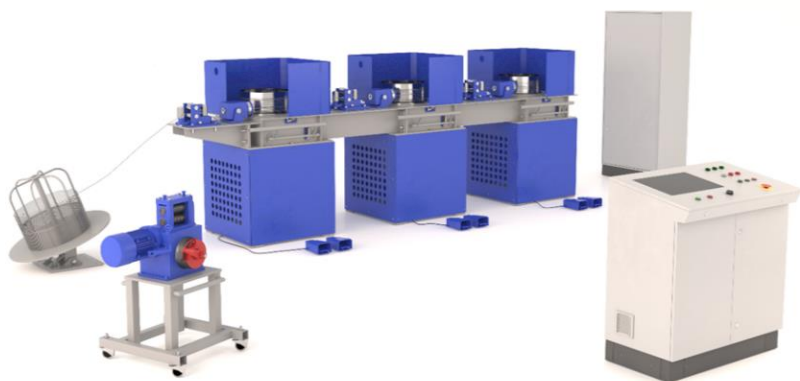


Fig. 2. Automated laboratory drawing mill

Due to the presence of strain gauges on all three blocks of the drawing mill, a complex experiment can be carried out to determine the drawing force required to produce titanium alloy wire, as well as to evaluate the geometry and the surface quality of the wire.

This research was funded by the Ministry of Science and Higher Education of the Russian Federation as part of a governmental assignment related to fundamental scientific research, Contract No. FENU-2020-0020 (2020071GZ).

References

1. Norets A.I., Slavin V.S., Brichko A.G. Drawer stands for obtaining calibrated rolled products: monograph. Magnitogorsk: MAGU, 2012. 180 p.
2. Kharitonov V.A., Manyakin A. Yu., Chukin M. V., Dreminev Yu. A., Tikeev M.A., Usanov M. Yu. Improvement of deformation modes and tools for drawing round wire: monograph. Magnitogorsk: Publishing House of Nosov Magnitogorsk State Technical University, 2011. 174 p.
3. Khramkov E.V., Shter A.A., Yakovleva K.Yu. On the Issue of Designing Roller Dies with Staggered Pairs of Rollers. Bulletin of the South Ural State University. Series: Metallurgy. 2015. Vol. 15, No. 4. pp. 128–134. (in Russ.) DOI: 10.14529/met150417.
4. Radionova L.V., Faizov S.R., Lisovskiy R.A., Lisovskaya T.A. Automated laboratory drawing mill. Russian Internet Journal of Industrial Engineering. 2017. Vol. 5, No. 2. pp. 68-73. DOI: 10.24892/RIJIE/20170211.

SURFACE MODIFICATION BY PLASTIC DEFORMATION AND FUNCTIONAL COATINGS

Belevskii L., Belevskaya I., Belov V., Gubarev E., Efimova Yu.
Nosov Magnitogorsk State Technical University, Magnitogorsk, Russia
belirena@yandex.ru

There are dozens of known methods for modifying and protecting surfaces, and the use of nanotechnologies is creating good opportunities for further progress in this area. However, there are serious problems involved in obtaining a nanocrystalline structure throughout the volume of a part – especially a large part. It is considerably simpler to form such a structure in the part's surface layer. There are conventional methods for surface modification and state-of-the-art methods [1]. It was noted in [2] that a nanocrystalline structure can be formed in a surface layer by employing technologies which have traditionally been used for work-hardening. The use of technologies based on surface plastic deformation (SPD) can significantly increase the strength of steel parts [3, 4]. A nanocrystalline surface structure can be formed by impact SPD (dynamic work-hardening), including with the use of a rotating wire brush (RWB) [5–9]. In this case, SPD is accomplished by impacts administered by the ends of the nap of the RWB. A work-hardening treatment and the application of a coating can be combined into one operation or can be carried out in succession (combination methods and serial methods). Here, we conducted studies of the effect of certain technological factors on the strengthening, reconditioning, and protection of a surface through the application of coatings by friction cladding (FC). The treatment of a surface or the application of coatings with a flexible tool by the methods of friction cladding (FC) and electrofriction cladding (EFC) can be done on lathes or grinders equipped with simple attachments. Such treatment can be administered to helical surfaces and toothed wheels [16] of large

parts. The use of electric current intensifies the process and makes the coating thicker and more ductile. The EFC process merits further investigation. The use of a combination treatment which involves knurling followed by the friction application of a functional coating with a flexible tool makes it possible to increase the diameter of a worn part and obtain an ultrafine structure in the surface layer as a result of plastic deformation. Different types of functional coatings can be formed from pure metals, alloys, and composite materials – including nanocomposites.

The reported study was funded by RFBR according to the research project №17-38-50226 mol_nr.

References

1. A. G. Suslov (ed.), Engineering of the Surface of Parts: Symposium, Mashinostroenie, Moscow (2008).
2. V. S. Mukhin and A. M. Suslov, “Engineering the surface of machine parts,” Vestn. UGATU, No. 4, 106–112 (2009).
3. N. P. Lyakishev and M. I. Alymov, “Structural-grade nanomaterials,” Ross. Tekhnol., 1/2, 71–81 (2006).
4. A. V. Makarov and L. G. Korshunov, “Strength and wear resistance of nanocrystalline structures in the friction surfaces of steels with a martensitic substrate,” Izv. Vyssh. Uchebn. Zaved. Fiz., No. 8, 65–80 (2004).
5. L. S. Belevskii, I. V. Belevskaya, and Yu. Yu. Efimova, “Combination impact-friction treatment with a flexible tool,” Vestnik of Nosov Magnitogorsk State Technical University, No. 4, 53–57 (2014).
6. L. S. Belevskii, I. V. Belevskaya, and Yu. Yu. Efimova, “Nanostructure-forming friction treatment of metal surfaces and the application of functional coatings with a flexible tool,” Poroshk. Metall. Funkts. Pokryt., No. 1, 70–76 (2014).
7. I. V. Kudryavtsev, N. E. Naumchenkov, and N. M. Savina, Fatigue of Large Machine Parts, Mashinostroenie, Moscow (1981).
8. Yu. I. Kurguzov and D. D. Papshev, “Engineering the quality of a surface in its work-hardening with mechanical brushes,” Vestn. Mashinostr., No 4, 54–58 (1986).
9. E. V. Perepichka, Conditioning-Strengthening Treatment of Parts by Brushes, Mashinostroenie, Moscow (1989).

MICROSTRUCTURAL ANISOTROPY ON THE WIRE SURFACE DURING DRAWING

Stolyarov A.¹, Kamalova G.¹, Polyakova M.²

¹*OJSC “MMK-METIZ”, Magnitogorsk, Russia*

²*Nosov Magnitogorsk State Technical University, Magnitogorsk, Russia
174kamalova@mail.ru*

In technological processes of metal processing near the contact area «processed metal workpiece - tool» the thin layer with specific microstructure and properties different from bulk material is formed. Especially this layer is observed when the deformational processing is based on the reactive friction force such as drawing, extrusion etc. Review of such methods is presented in [1, 2]. It is proved both theoretically and experimentally that at drawing on the contact boundary «wire – drawing die» the thin

layer with 20-40 μm is formed in which deformation intensity of the metal is higher than deformation of bulk material [3, 4]. This is of high importance for drawing the wire of small diameters. This wire is widely used for metal cord manufacturing and other kinds of metal products such as thin ropes, meshes for filters, thin wire for electric devices, medical apparatus, watches mechanisms etc. Despite thin wire properties depend to high extent on flow of metal in the surface area this layer as the detached element of deformation zone is not discussed in the classic theory of drawing. Theoretical and experimental investigation results of material flow in thin surface layer are presented in [5, 6]. Authors show that deformation of the material in surface area at friction is nonmonotonic, is followed by formation of layer with specific structure and can be compared with turbulent flow of viscous liquid. But these investigations were performed for tribological system «body - counterbody». Although the materials are subjected to high external force loads in such systems, but they do not undergo volume plastic deformation which is characteristic to metal forming processes. At present time the presence of this layer is determined. But at the same time it is rather difficult to measure the thickness of this layer. For determination of the layer of severe plastic deformation it is proposed in [7] to use the coefficient of rate deformation intensity. For this coefficient assessment it is necessary to get experimental data about the dependence of thickness of layer of severe plastic deformation on drawing regimes. Research of metal microstructure near the friction area for metal forming processes is presented in [7] for upsetting of cylindrical sample and in [8] for extrusion of magnesium alloy AZ31. In both cases for obtaining strongly marked layer on the contact area the tool surface was very rough which ensured the high level of friction force between tools and samples. The aim of this study is to investigate the grain anisotropy of carbon steel wire with different carbon content as the main sign of thin layer formation on the contact area between wire and smooth die surface. Grain anisotropy can be estimated by the coefficient of anisotropy as the ratio of mean quantity of phase particles (grains) which are crossed by secant line perpendicular to deformation axis on the unit of secant line length to the mean quantity of phase particles (grains) which are crossed by secant line parallel to deformation axis on the unit of secant line length. This approach can be used for identification of the deformed layer thickness.

In metal forming processes the layer with highly deformed grains is formed as a result of contact between a workpiece and a tool due to high friction force. The microstructure and properties of this layer are different as compared with material in bulk. Because microstructure of carbon steel depends on carbon content it is necessary to use special method for identification the thickness of this layer. At drawing the wire obtain the specific microstructure when grains elongate along the drawing direction. Their sizes change and it can be estimated by the ratio of grain size along drawing direction and perpendicular to it. This ratio can be denoted as coefficient of anisotropy. Using Thixomet PRO software it was established that coefficient of anisotropy changes from the surface area to the center of the drawn carbon steel wire. On the surface the value of coefficient of anisotropy for low carbon steel wire is less than 0.82 and less than 0.7 for high carbon steel wire. Deeper to the center of the wire the grains and pearlite colonies with value of coefficient of anisotropy more than 0.9 are observed. It means that they become equiaxed at the definite distance from the surface. It is proposed to use the distribution of coefficient of anisotropy in the drawn carbon steel wire from the surface to the center as the method for assessment of thickness of layer with highly deformed

microstructure parameters.

The reported study was funded by RFBR according to the research project № 18-58-45008 IND_a.

References

1. S. Alexandrov, R. Goldshtein, Doklady Physics. 60(1) (2015) 39-44.
2. S. Alexandrov, R. Goldshtein, Physical Mesomechanics. 18(3) (2015) 223-225.
3. K. Hosoda, M. Asakawa, S. Kajino, Y. Maeda, Wire Journal International. 11 (2008) 68-73.
4. A. Stolyarov, V.A. Kharitonov, Steel in Translations. 12 (2012) 45-49.
5. S.Yu. Tarasov, V.E. Rubtsov, Physics of the Solid State. 53(2) (2011) 358-364.
6. S.Yu. Tarasov, A.V. Kolubaev, Physics of the Solid State. 50(5) (2008) 844-851.
7. S. Alexandrov, E. Lyamina, D. Vilotich, L. Shidzhanin, J Appl Mech Tech Physics. 52(3) (2011) 491-495.
8. S. Alexandrov, Y.-R. Jeng, Y.-M. Hwang, J Manuf Sci Eng. 137 (2015) 053003-1 – 053003-7.

SESSION 3 – Cross-disciplinary solutions in advanced materials engineering (iSmart-Metal Forming)

CALCULATION OF STRAINS IN ZIRCONIUM ALLOY ROLLING

Abashev D., Loginov Yu.

*Ural Federal University named after the first President of Russia B.N.Yeltsin,
Yekaterinburg, Russia
9283dima@mail.ru*

The deformed state of a rolled product is determined by the distribution of properties across its cross-section. In its turn, the distribution of these properties will affect the average integral characteristics of the entire product and will determine the behavior of the material during subsequent forming. In many deformation processes, the metal forming calculation is still carried out from the perspective of the isotropy hypothesis. However, the properties of some metallic materials, especially those with a crystalline structure in the form of asymmetrical lattices, can hardly be explained using this hypothesis. Replacing the isotropy hypothesis with the anisotropy hypothesis and applying the latter, for example, to materials with a hexagonal lattice [1] would make the mathematical apparatus of the plasticity theory [2] much more complicated.

On the basis of the isotropy and anisotropy hypotheses, a number of calculations of the stress-strain state in flat rolling has been carried out using the finite element method. Fig. 1 shows the result of solving the problem of rolling a sheet of Zircaloy-4 alloy [3].

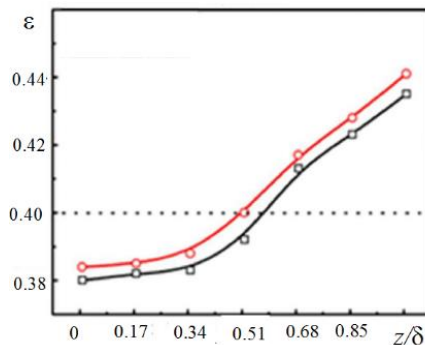


Fig. 1 The calculated distribution of deformation over the relative thickness of the sheet during rolling of the Zircaloy-4 zirconium alloy for isotropic (lower curve) and anisotropic material (upper curve) with a relative reduction of 40%

One can see that the strain ϵ distribution across the thickness of the sheet is not even. Thus, the strain increases towards the periphery, which can be attributed to additional shear strains. In addition, the anisotropy hypothesis based solution of the problem yields a higher deformation degree value.

To assess the situation, one can write down a formula for determining the von Mises strain:

$$\varepsilon = \frac{\sqrt{2}}{3} \sqrt{[(\varepsilon_{xx} - \varepsilon_{yy})^2 + (\varepsilon_{yy} - \varepsilon_{zz})^2 + (\varepsilon_{zz} - \varepsilon_{xx})^2] + 6\varepsilon_{xy}^2 + 6\varepsilon_{yz}^2 + 6\varepsilon_{zx}^2}$$

From this one can see that the ε calculation result can change if either the ratio between the normal deformations ε_{ii} ($i = x, y, z$) or the ratio between the shear deformations ε_{ij} ($i, j = x, y, z$) changes. In this case, the calculations show that the components of the tensor responsible for the shear strain have little effect on the result of the ε calculation. Thus, the ratios between the normal deformations become more relevant.

If, instead of the Mises theory, we use the Hill theory developed for the deformation of anisotropic materials, we shall find that we need to determine the ratios between the values of deformation resistance measured in different directions. In this case one can apply Hill's plasticity theory when setting a problem related to sheet rolling. Such a problem was formulated and solved in relation to the deformation of anisotropic transformer sheet steel [4].

The authors of the paper [3] found a fairly large difference in the Hill equation coefficients for the Zircaloy-4 alloy: $F = 0.294$; $G = 0.478$; $H = 0.52$, which is indicative of a high degree of anisotropy.

References

1. Dyja Henryk, Ozhmegov Kirill V., Kawalek Anna, Galkin Aleksander M. Experimental and computer-assisted modeling of plastic deformation of zircon-based alloys during production of metal products for the needs of the atomic and other branches of industry. *Journal of Siberian Federal University. Engineering & Technologies*. 2015. Vol. 5, No. 8. pp. 609-620.
2. Loginov Y.N., Kotov V.V., Solovei V.D. Transformation of the yielding condition during the deformation of HCP metallic materials. *Russian Metallurgy (Metally)*. 2010. Vol. 2010, No. 3. pp. 235-240.
3. Kumar Gulshan, Lodh Arijit, Singh Jaiveer, Singh Ramesh, Srivastava D., Dey G.K., Samajdar I. Experimental characterization and finite element modeling of through thickness deformation gradient in a cold rolled zirconium sheet. *CIRP Journal of Manufacturing Science and Technology*. 2017. Vol. 19. pp. 176–190.
4. Loginov Y.N., Puzanov M.P. Influence of properties anisotropy on the stress-strain state during rolling of stripes from electrical steel. *Chernye Metally*. 2018. No. 10. pp. 22-26.

INCREASING STEEL WIRE ROPE SERVICE LIFE BY APPLYING A COLOR COATING

Pykhov L.¹, Gallyamov D.¹, Kharitonov V.², Polyakova M.²

¹*JSC BMK, Beloretsk, Russia*

²*Nosov Magnitogorsk State Technical University, Magnitogorsk, Russia*
gallyamov2010@gmail.com

Lifting equipment is widely used in industry and is considered highly hazardous. One of the most critical elements of such equipment is steel wire ropes.

The most promising areas for extending the life of steel wire ropes are to increase the number of wire strands and to apply various color coatings. By increasing the number of wire strands, we can improve the flexibility and strength of wire ropes, and by applying a color coating, we ensure a uniform operation of the wire rope components, make sure there is no contact between the strands and the metallic core and protect them against corrosion.

To produce color coated wire ropes, it is necessary to adjust the rope laying parameters to ensure a high quality coating, fill up the interstrand space with a polymeric material, apply special types of lubrication, select a polymeric material that would ensure the best performance of the wire ropes and apply other special solutions.

Today, JSC BMK produces color coated wire ropes of three different designs: wire ropes with a color coated core, wire ropes with a completely color coated core and wire rope, completely color coated wire ropes. Wire ropes of various design are applied in various operation conditions. For example, when using wire ropes for hoists and cranes, a number of broken wires should be controlled, which would be impossible to do if wire ropes were color coated; thus, in this case, wire ropes with a color coated core are used. In wire ropes with a color coated core, there is no contact between the strands and a uniform load on all the wire rope elements is ensured contributing to their time in service. Regarding the wire ropes for mining shovels, it is critical to control the mechanical wear of the wire rope surface; in this case, the use of steel wire ropes with a completely color coated core and wire rope helps extend their operating life.

Wire ropes are coated with polypropylene and polyethylene composites.

The practice of using color coated wire ropes produced by JSC BMK and the studies conducted on samples of imported wire ropes indicate the need for using lubrication inside the wire ropes. That's why color coated wire ropes are currently produced using special wire rope lubricants [1].

Wire rope life duration depends on compliance with the transportation rules, storage conditions and proper maintenance. Color coating serves to protect wire ropes during transportation and enhances their performance. That's why JSC BMK prepared relevant recommendations.

To test and improve the structures of color coated wire ropes and their production process, we carried out a series of pilot tests using 39-64 mm color coated wire ropes used in crawler mounted mining shovels EKG-5, EKG-8I, EKG-10, EKG-12, EKG-18, EKG-20, P&H 2300 and P&H 2800 operated by Mechel Group sites and other sites. The results showed that the average service life of color coated wire ropes was 41.8% higher than that of similar wire ropes without coating. The longest service life, which exceeds the norm by 1.8-3.6 times, was achieved by 39-57 mm color coated wire ropes installed on mining shovels P&H 2300 and EKG-18 operated by South Kuzbass PJSC, EKG-5 operated by Pugachev Open Pit LLC, and EKG-8I and EKG -10 operated by EVRAZ KGOK JSC. After the tests had been completed, the state of reel and pulley grooves on the EKG-8I and EKG-10 mining shovels was found to have considerably improved.

The conducted pilot tests showed that, due to the use of color coating, the service life of steel wire ropes considerably increased as compared with the conventional ones, the wear rate of mining shovel reels and pulleys decreased, and the equipment downtime was reduced. Thus, the application of color coating on steel wire ropes is a modern and innovative way of increasing their service life.

The reported study was funded by RFBR according to the research project №18-58-45008 IND_a.

References

1. Egorov V.D., Mamykina E.M., Latypov Kh.Yu., Pershin G.D. Steel wire rope production. Moscow: Metallurgiya, 1980. 100 p.

USE OF SPHERICAL BOUNDARIES HYPOTHESES TO VERIFY THE DEFORMATION ZONE DURING DRAWING

Bushueva N., Loginov Yu.

*Ural Federal University named after the first President of Russia B.N. Yeltsin,
Yekaterinburg, Russia
m0rgondagen@yandex.ru*

The plane section hypothesis is often used to derive equations for the purpose of calculating forces in the sheet rolling theory. Many researchers used a spherical coordinate system to derive formulas for describing the stress-strain state of a drawing process in contrast to a flat rolling process [1]. It was assumed that sections which were spherical before deformation retain their spherical shape during deformation. Only one coordinate of the radius vector ρ has a linear dimension in the spherical coordinate system. The two other coordinates have angular dimensions. The stress and strain components along the tangential direction θ are the same during axisymmetric drawing. The angular coordinate φ characterizes the degree of the radius vector deviation from the symmetry axis. The deformation zone is described by a radial structure in the plane (Fig. 1, a). It is bounded by the wire-drawing die borders, which are located at an angle α to the symmetry axis.

The boundary value problem of drawing was set and solved to check this position in RAPID-2D, a software module developed by the Ural Federal University.

The problem was solved for the first drawing pass conditions when an 8 mm copper wire rod was used to obtain a 6.53 mm wire. The elongation ratio was quite high – 1.50. The reduction was 33% and the die angle was 9° . The Siebel friction was 0.1. Real process parameters were used for this research. The hardening curves of the M0 copper grade were applied.

The calculation results are shown as lines of equal level referring to the relative shear strain rate intensity H/H_0 (Fig. 1, b). As can be seen from the figure, the shape of the boundary is close to radial at the exit from the deformation zone. However, at the deformation zone entry the shape is different.

Based on the results, a function graph with a maximum will be obtained while moving along the angular coordinate φ . This deformation zone structure is indirectly indicated by the lines of the frozen lattice. The lines go straight up to the deformation zone entry. But the transverse lines bend slightly at the deformation zone exit. The lines of this type are usually displayed as lines of a parabola with a vertex on the symmetry axis. A different situation can be observed in this case. Here we can talk about two parabolas with vertices located in the two halves of the deformation zone. Two maxima H/H_0 indicate the division of the deformation zone into two halves with the rate intensity localization in the annular zones.

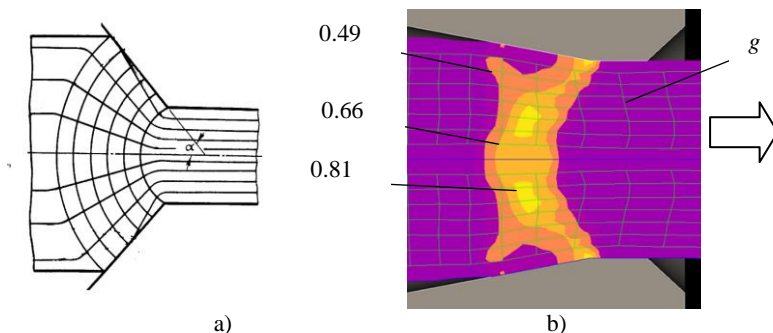


Fig. 1. The deformation zone in the spherical coordinate system (a) and the shear strain rate distribution H/H_0 (b) during the copper wire drawing process: cursor – the drawing direction; g – the frozen lattice

This fact indicates the possibility of additional structural discontinuity in the wire, at least under increased deformation conditions. The relationship between the stress-strain state and defects [2,3] and changes in the metal properties [4,5] and the texturing intensity [6] during drawing was noted in earlier works.

References

1. Perlin I. L., Ermanok M. Z. The Theory of Drawing. Moscow: Metallurgiya, 1971. 448 p.
2. Loginov Y.N., Pervukhin A.E., Babailov N.A. Evolution of surface defects in platinum alloy wire under drawing. AIP Conference Proceedings. 2017. Vol. 1915, No. 040032.
3. Won J., Nam C., Min B. Void initiation and microstructural changes during wire drawing of pearlitic steels. Materials Science and Engineering. 1995. Vol. 203, No. 1–2. pp. 278-285.
4. Loginov Y. N., Vasilevskiy P.A., Radionov L.V. Investigation of the effect of die taper angle on the mechanical properties of drawn semiproduct. Tsvetnye Metally. 2004. Vol. 6. pp. 104-106.
5. Toribio J., Lorenzo M., Vergara D., Kharin V. Influence of the die geometry on the hydrogen embrittlement susceptibility of cold drawn wires. Engineering Failure Analysis. 2014. Vol. 36. pp. 215-225.
6. Pal-Val P.P., Natsik V.D., Pal-Val L.N., Loginov Y., Demakov S.L., Illarionov A.G., Davydenko A.A., Rybalko A.P. Unusual Young's modulus behavior in ultrafine-grained and microcrystalline copper wires caused by texture changes during processing and annealing. Materials Science and Engineering: A. 2014. Vol. 618. pp. 9-15.

NEW PHYSICAL SIMULATION APPROACH FOR ASYMMETRIC ROLLING

Pesin A.¹, Pustovoytov D.¹, Dubey A.²

¹ *Nosov Magnitogorsk State Technical University, Magnitogorsk, Russia*

² *Indian Institute of Information Technology, Design & Manufacturing, Jabalpur, India
pustovoitov_den@mail.ru*

Severe plastic deformation is a very effective way to create ultrafine grain structures in metals and alloys [1], Nowadays many variants of severe plastic deformation techniques are available. Asymmetric rolling process is one of them [2-6], Contrary to other severe plastic deformation methods such as high pressure torsion and equal channel angular pressing, the asymmetric rolling allows to provide the possibility for overcoming the limitation of producing ultrafine grained materials with large dimensions due to its continuous feature [7, 8]. Among the asymmetric rolling processes, the differential speed rolling in which the speeds of the upper and lower rolls are different, is considered to be the most effective for achieving ultrafine grain structure of materials [9, 10]. It is well known that the mechanism of severe plastic deformation during asymmetric rolling comes from its large equivalent strain, which is composed of compressive strain and additional shear strain [11]. Physical simulation of shear strain, which is similar to that occurring in asymmetric rolling processes, is very important for design of technology because it allows to consider a variety of technological variants and to find the best solution in relatively short time and with low costs. Shear testing is complicated by the fact that a state of large shear is not easily achievable in most specimen geometries. Problem of selection of shear testing and specimen geometry has been discussed in numerous publications. A shear-tensile specimen was developed by Hundy and Green [12]. Another example of such a specimen is the so-called "hat specimen" which was developed by Meyer and Manwaring [13], and used thereafter by many other researchers. Another variant is the double shear specimen used by Klepaczko [14]. Very simple specimen geometry (thin foil) has been used by Clifton and Klopp [15] in their pressure-shear plate impact experiments. Peirs, et al. [16] introduced the eccentric notch shear specimen, which was designed for shear testing of sheet metals over a wide range of strain rates. Isakov et al. [17] used modified specimen geometry, based on ASTM B831 [18], which presents specimen geometry intended to determine the ultimate shear strength of wrought or cast aluminum alloys. The specimen geometry' consists of a planar specimen with a gauge section created by two opposing 45° slots through the specimen thickness. This sample geometry' was modified for use in a tension Kolsky' bar. It was shown that the specimen without the thickness reduction exhibits severe distortion outside of the intended gauge section. Failure also occurs outside the gauge section. The specimen with the thickness reduction had a well defined gauge section and deformation was limited within the gauge section. A shear-compression specimen for large strain testing of materials was developed by Rittel et al. [19]. The specimen consists of a cylinder having an inclined gauge section created by two diametrically opposed rectangular slots which are machined at 45° with respect to the longitudinal axis. The specimen was used in numerous investigations, including constitutive testing, texture evolution, and adiabatic shear banding. A miniature version of the shear-compression specimen was used for the characterization of nanomaterials. The modified shear-compression specimen was presented in [20], In the modified specimen, the two diametrically machined gauges were semi-circular (instead of rectangular). This

modification induces large strains on the mid-section of the gauge without the sharp edges and stress concentrations of the former rectangular gauges. The goal of this research is a development of a novel laboratory' testing method which can be used for design of technology of asymmetric rolling as severe plastic deformation method for producing of ultrafine grained metallic materials. Simulation was performed by using an AG IC Shimadzu universal testing machine equipped with a 300 kN load cell. Aluminium alloy Al-6.2Mg-0.7Mn and low-carbon steel AISI 1010 were used as materials for specimens. The specimens consisted of a parallelepiped having an inclined gauge section created by two diametrically opposed semi-circular slots which were machined at 45°. Height of the specimens was 24 mm, section dimensions were 12×12 mm², gauge thickness was 1.5 mm and gauge width was 3.0 mm. The specimens provided dominant shear strain in an inclined gauge-section. The specimens were compressed between two flat dies during shear-compression testing in accordance to the special scheme. The level of equivalent strain was controlled through adjustment of the height reduction of the specimen and number of cycles of shear-compression. Each cycle of the shear-compression testing consisted of two steps. The first step included 10% of height reduction of specimen, after that specimen was rotated by 90°. The second step included width reduction of the specimen for getting the quasi original shape of a parallelepiped. One cycle of shear-compression testing provided equivalent strain $\epsilon \approx 1.0$ in an inclined gauge-section. Multi-cycle shear-compression testing was performed at room temperature with equivalent strain up to $\epsilon \approx 4 \dots 5$. Numerical simulation and analysis of the stress-strain state during shear-compression testing and asymmetric rolling was performed with the commercial FE software DEFORM 3D. The microstructures of the specimens after multi-cycle shear-compression testing were examined by scanning electron microscopes. Ultra fine grained structure was obtained when $\epsilon \approx 4 \dots 5$.

The reported study was funded by RFBR according to the research project № 18-58-45013 IND_a.

References

1. Y. Estrin, A. Vinogradov, Extreme grain refinement by severe plastic deformation: A wealth of challenging science, *Acta Materialia*, 61 (2013) 782–817.
2. Y.H. Ji, J.J. Park, Development of severe plastic deformation by various asymmetric rolling processes, *Materials Science and Engineering: A*, 499 (2009) 14–17.
3. A. Pesin, D. Pustovoytov, Influence of process parameters on distribution of shear strain through sheet thickness in asymmetric rolling, *Key Engineering Materials*, 622–623 (2014) 929–935.
4. A. Pesin, A. Korchunov, D. Pustovoytov, Numerical study of grain evolution and dislocation density during asymmetric rolling of aluminum alloy 7075, *Key Engineering Materials*, 685 (2016) 162–166.
5. J.J. Park, Finite-element analysis of severe plastic deformation in differential-speed rolling, *Computational Materials Science*, 100 (2015) 61–66.
6. F. Zuo, J. Jiang, A. Shan, Shear deformation and grain refinement in pure Al by asymmetric rolling, *Transactions of Nonferrous Metals Society of China*, 18 (2008) 774–777.
7. Y.H. Ji, J.J. Park, W.J. Kim, Finite element analysis of severe deformation in Mg-3Al-1Zn sheets through differential-speed rolling with a high speed ratio, *Materials Science and Engineering: A*, 454–455 (2007) 570–574.

8. W.J. Kim, B.G. Hwang, M.J. Lee, Y.B. Park, Effect of speed-ratio on microstructure, and mechanical properties of Mg-3Al-1Zn alloy, in differential speed rolling, *Journal of Alloys and Compounds*, 509 (2011) 8510–8517.
9. K. Bobor, Z. Hegedus, J. Gubicza, I. Barkai, P. Pekker, G. Krallics, Microstructure and mechanical properties of Al 7075 alloy processed by differential speed rolling, *Periodica Polytechnica Mechanical Engineering*, 56 (2012) 111–115.
10. Loorentz, Y.G. Ko, Effect of differential speed rolling strain on microstructure and mechanical properties of nanostructured 5052 Al alloy, *Journal of Alloys and Compounds*, 586 (2014) S205–S209.
11. Q. Cui, K. Ohori, Grain refinement of high purity aluminum by asymmetric rolling, *Materials Science and Technology*, 16 (2000) 1095–1101.
12. B.B. Hundy, A.P. Green, A determination of plastic stress-strain relations, *Journal of the Mechanics and Physics of Solids*, 3 (1954) 16–21.
13. L.W. Meyer, S. Manwaring, *Metallurgical applications of shock-wave and high-strain-rate phenomena*, Marcel Dekker, New York, 1986.
14. J.R. Klepaczko, An experimental technique for shear testing at high and very high strain rates, *International Journal of Impact Engineering*, 46 (1994) 25–39.
15. R.J. Clifton, R.W. Klopp, Pressure shear plate impact testing, In: *Metals Handbook*, 9th edition, Mechanical Testing, ASM, Metals Park, Ohio, 8 (1985) 230–239.
16. J. Peirs, P. Verleysen, J. Degrieck, Novel technique for static and dynamic shear testing of Ti6Al4V sheet, *Experimental Mechanics*, 52 (2011) 729–741.
17. M. Isakov, J. Seidt, K. Ostman, A. Gilat, V.T. Kuokkala, Characterization of a ferritic stainless sheet steel in simple shear and uniaxial tension at different strain rates, *Proceedings of the ASME 2011 International Mechanical Engineering Congress and Exposition*, (2011).
18. ASTM. B831: Standard test method for shear testing of thin aluminum alloy products, ASTM International, (2005).
19. D. Rittel, S. Lee, G. Ravichandran, A shear-compression specimen for large strain testing, *Experimental Mechanics*, 42 (2002) 58–64.
20. A. Dorogoy, D. Rittel, A. Godinger, Modification of the shear-compression specimen for large strain testing, *Experimental Mechanics*, 55 (2015) 1627–1639.

INFLUENCE OF PUNCH DESIGN ON THE QUALITY OF UPSET PIPE ENDS

Erpalov M.

*Ural Federal University named after the first President of Russia B.N.Yeltsin,
Yekaterinburg, Russia
m.v.erpalov@urfu.ru*

Upsetting is one of the stages in the production of drill pipes and tubing. This process helps improve the performance of products [1-3]. The main technological difficulty during upsetting is to ensure the quality of the inner surface of pipe ends. One of the most common types of inner surface defects is underfilling, which occurs in the area adjacent to the face of the pipe (Fig. 1).

Using the method of computer simulation and having conducted a series of industrial experiments, the authors of the papers [2, 3] looked at possible causes of internal defects and proposed ways to improve the product quality. It is shown that the risk of defects increases if the workpiece is not heated evenly or if the wall thickness exceeds

the nominal value. To improve the quality of products, heating modes for pipe ends and stricter workpiece size requirements are proposed. However, in practice, these requirements are not always properly implemented; therefore, more reliable ways to improve the product quality are needed.

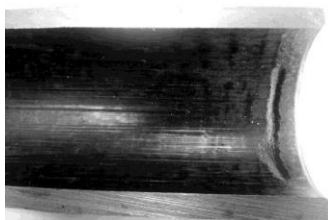


Fig. 1. Underfilling defect on the pipe end inner surface

This paper looks at the influence of punch design on the metal flow during pipe end upsetting. The main attention is paid to the section of the tool that comes in contact with the pipe face. Typically, this section is perpendicular to the pipe axis. However, changing its slope angle can change the metal flow direction. This paper considers seven different options for changing the punch face slope from -15° to $+15^\circ$ at 5° increments.

The study was conducted using finite element simulation in the Deform-2D software. 73.02x5.51 mm pipes per API spec.5CT were taken for workpieces. When setting computer simulation problems, the most unfavorable case in terms of product quality was considered. Thus, the actual value of the pipe wall thickness was set equal to 6.2 mm, and the temperature of the pipe end near the face region was reduced by about 100°C as compared with the rest of the heated section of the pipe.

The simulation results (Fig. 2) show that a changing stem face section slope can significantly affect the metal flow during pipe end upsetting. A bigger slope helps improve the filling of the pipe inner surface and thus ensures the required product quality. No internal defects were observed when the slope reached $+10^\circ \dots +15^\circ$.

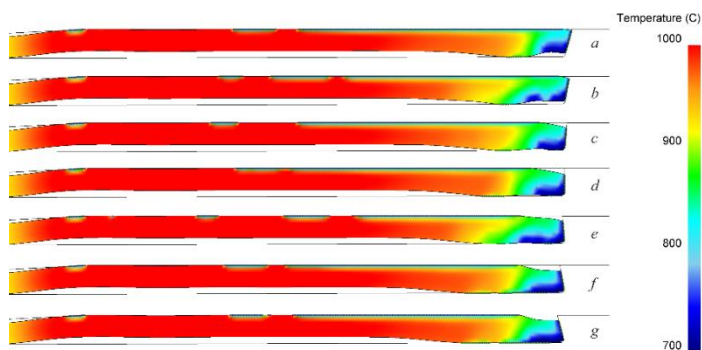


Fig. 2. Pipe wall profile at the beginning of the main deformation stage: *a*) the punch face slope is equal to -15° ; *b*) -10° ; *c*) -5° ; *d*) the face section is perpendicular to the pipe axis; *e*) $+5^\circ$; *f*) $+10^\circ$; *g*) $+15^\circ$

References

1. Vydrin A.V., Barichko B.V., Zinchenko A.V. Determining the upsetting parameters for the ends of drilling pipe. *Steel in Translation*. 2014. Vol. 44, No. 3. pp. 228-231.
2. Erpalov M.V. Increase of efficiency of pipe ends upsetting technology by research on metal forming. *Journal of Chemical Technology and Metallurgy*. 2016. Vol. 51, No. 4. pp. 405-410.
3. Erpalov M.V., Bogatov A.A. Causes of Formation and Ways of Elimination of Defects on the Internal Surface of Upset Tube Ends. *Metal Science and Heat Treatment*. 2016. Vol. 58, No. 1-2. pp. 33-36.

SIMULATION OF COMPONENTS WITH UFG PROPERTIES FOR NUCLEAR INDUSTRY

Naizabekov A.¹, Arbuz A.², Tolkushkin A.¹, Panin E.³, Zhumagaliyev D.¹

¹*Rudny Industrial Institute, Rudny, Kazakhstan*

²*Nazarbayev University, Nur-Sultan, Kazakhstan*

³*Karaganda State Industrial University, Temirtau, Kazakhstan*

zhumagaliyev1997@mail.ru

One of the main problems related to the development of nuclear power and controlled thermonuclear fusion is how to increase the radiation resistance and mechanical properties of the materials used in reactor structures. One of the ways to increase radiation resistance is to use ultrafine-grained (UFG) and nanostructured (NS) materials. Due to the possibility of obtaining larger isotropic products without internal discontinuities, severe plastic deformation delivers the most innovative method to produce ultrafine-grained materials.

When choosing components for simulation, the most appropriate solution would be to use components made of AISI-321 steel bars with an ultrafine-grained structure obtained after radial-shear rolling. Taking into account the cylindrical shape of the bars, as well as the relatively large possible length of the workpieces, it was decided to examine the following components: a fuel assembly frame and a fuel element.

To create a model of AISI-321 stainless steel in the ultrafine-grained state, it is necessary to input the mechanical parameters corresponding to this state in the material database. The key parameter for this is the yield strength of the material. To determine the yield strength values for different grain sizes, we recommend using the Hall-Petch ratio [1-2], which is the following relationship:

$$\sigma_Y = \sigma_0 + kd^{-1/2}, \quad (1)$$

where: σ_Y – required yield strength value, MPa;
 σ_0 – stress that prevents the movement of dislocations, MPa;
 k – constant determined by the material properties;
 d – grain size, μm .

The paper [3] describes the results of an extensive research that was carried out on the Hall-Petch effect in relation to the two most used brands of austenitic stainless steel: AISI-316 and AISI-321. As a result, the following values were obtained for the constants: $\sigma_0 = 150$ MPa; $k = 420$. Consequently, we get the following yield strength val-

ues: $\sigma_Y = 652$ MPa (for the grain size of 700 nm); $\sigma_Y = 1,089$ MPa (for the grain size of 200 nm).

The paper [3] also describes the YS / TS values for AISI-321 steel, as well as data on relative elongation, based on which the following corresponding tensile strength values were obtained: $\sigma_{TS} = 986$ MPa (for the grain size of 700 nm); $\sigma_{TS} = 1,194$ MPa (for the grain size of 200 nm); $\delta = 38$ % (for the grain size of 700 nm); $\delta = 22$ % (for the grain size of 200 nm).

Based on the technical data [4], a value of 340 MPa was set as the maximum pressure in the core when determining the static load value.

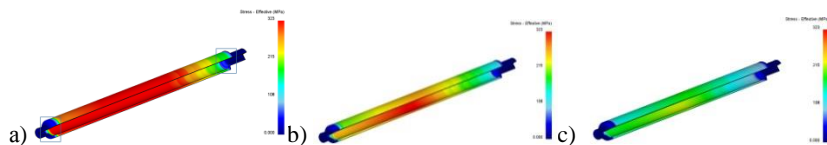


Fig. 1 - Calculation of the static load of the fuel element for the following grain sizes: a – 1,500 nm; b – 700 nm; c – 200 nm

The maximum stress values registered in the fuel assembly model are as follows: in the model with the grain size of 1,500 nm – 274 MPa; in the model with the grain size of 700 nm – 238 MPa; in the model with the grain size of 200 nm – 186 MPa. Based on these values, the following safety factors were obtained for the most loaded areas for all three materials under specified operating conditions: in the model with the grain size of 1,500 nm $\rightarrow 340$ MPa / 274 MPa = 1.24; in the model with the grain size of 700 nm $\rightarrow 340$ MPa / 238 MPa = 1.43; in the model with the grain size of 200 nm $\rightarrow 340$ MPa / 186 MPa = 1.83.

The maximum stress values registered in the fuel element model (Fig. 1) are as follows: in the model with the grain size of 1,500 nm – 313 MPa; in the model with the grain size of 700 nm – 269 MPa; in the model with the grain size of 200 nm – 224 MPa. Based on these values, the following safety factors were obtained for the most loaded areas for all three materials under specified operating conditions: in the model with the grain size of 1,500 nm $\rightarrow 340$ MPa / 313 MPa = 1.08; in the model with the grain size of 700 nm $\rightarrow 340$ MPa / 269 MPa = 1.26; in the model with the grain size of 200 nm $\rightarrow 340$ MPa / 224 MPa = 1.51.

The results of the simulation showed that, for the both components, the use of material in the UFG state would be a more appropriate solution, since in this case the safety factor in the most loaded areas increases by about 15÷40% depending on the obtained grain size.

This research was carried out as part of the state funded project No. AP05131382 under the following program: Grant financing of scientific research in 2018-2020 (Customer – Ministry of Education and Science of the Republic of Kazakhstan).

References

1. N.J. Petch. The cleavage strength of polycrystals. Journal of the Iron and Steel Institute. 174 (1953). pp. 25–28.
2. E.O. Hall. The deformation and ageing of mild steel: III discussion of results. Proceedings of the Physical Society of London. Section B. 64 (1951). pp. 747–753.

3. S.V. Astafurov, G.G. Maier, E.V. Melnikov, V.A. Moskvina, M.Yu. Panchenko, E.G. Astafurova. The strain-rate dependence of the Hall-Petch effect in two austenitic stainless steels with different stacking fault energies. *Materials Science and Engineering: A*. Volume 756, 2019, pp. 365-372.
4. Afrov A.M., Andrushechko S.A., Ukraintsev V.F. et al. *VVER-1000: The physical basis of operation, nuclear fuel, safety*. Moscow: Universitetskaya kniga, Logos, 2006. 488 p.

RESEARCH OF MECHANICAL PROPERTIES OF PRESTRESSING STRANDS UNDER THERMO-MECHANICAL TREATMENT

Korchunov A., Polyakova M., Medvedeva E., Emaleeva D.
Nosov Magnitogorsk State Technical University, Magnitogorsk, Russia
emaleevadg@mail.ru

Prestressing strands are a high-technology product of the metalware industry that is used in heavy-duty pre- and post-stressed concrete structures, as well as in the construction of bridges, nuclear power plants, airports, tunnels, transport infrastructure, residential buildings, heating, power and water supply and water disposal systems. Of great interest is the sector of stabilized prestressing steel strands, which are produced per extremely similar standards in many developed countries and which find application almost worldwide. For the most part, such prestressing strands are used in the production of prestressed reinforced concrete structures. The use of prestressing strands in concrete helps to significantly reduce the amount of steel reinforcement used and thus reduce the cost of reinforced concrete components while enhancing their quality [1]. The most common type of product, both in terms of production output and application scope, includes spiral stabilized prestressing 7-wire strands, in which six wires are spun around a core wire in one layer. For a combination of inherent properties and related production and application factors, strands of this design have been recognized as the most efficient type of high-strength prestressed steel strands. In the world today, one can find quite a number of practically identical standards specifying the dimensions and mechanical properties of prestressing strands. A high degree of convergence between the standards can be attributed to both the use of efficient construction processes and a great similarity of equipment supplied by different manufacturers. In the Russian Federation, the production of stabilized prestressing strands is regulated by GOST R 53772-2010, whereas abroad the European standard pr EN 10138-3:2006 applies. Specific aspects of production and application of prestressing strands for prestressed structures are the subject of numerous theoretical and experimental research papers [2–3]. There are ongoing studies that are looking at new production methods to enhance the mechanical properties of prestressing strands designed for application in extreme conditions. For example, researchers obtained a prestressing strand with the strength exceeding 2,100 MPa, which makes it applicable in prestressed reinforced concrete structures designed for seismic loads.

A series of experimental studies has been conducted to understand the effect produced by different TMT regimes on the mechanical properties of high-strength (1,770 MPa) 12.5 mm 7-wire prestressing strands. For the purpose of the experiments, the following parameters of the stabilization line were used: induction heat temperature — from 360 to 400 °C, process speed – from 50 to 65 m/min, tension force — 64 kN. The

following conclusions can be drawn upon analysis of the results: 1. In the studied range of speeds and heating temperatures applied on the stabilization line, thermo-mechanical treatment does not lead to any significant changes in the steel microstructure produced by patenting and cold drawing. Deformed cementite plates of the ferritecarbide mixture with the thickness of up to $0.047 \mu\text{m}$, a vortex-like structure of the FCM colonies and partially destroyed cementite plates can be observed in the microstructure of steel. When the temperature reaches $400 \text{ }^\circ\text{C}$, early stages of coagulation of the FCM cementite plate fragments can be observed. 2. In reference to the initial state of a laid strand, all the studied TMT regimes were associated with increased values of the tensile strength σ_B , yield strength $\sigma_{0.1}$, full elongation at maximum tension force δ_{max} and modulus of elasticity E . A quantitative increase of the mechanical properties of prestressing strands was identified as a result of thermo-mechanical treatment. The most noticeable increase was observed with the yield strength $\sigma_{0.1}$ – from 28 to 36%, and the full elongation at maximum tension force δ_{max} – a higher than double rise, which is true for all the TMT regimes. 3. The changing process temperature was found to produce a more noticeable effect on the mechanical behaviour of prestressing strands. The effect of the process speed becomes more pronounced as the temperature reaches $400 \text{ }^\circ\text{C}$. 4. The best combination of mechanical properties in prestressing strands can be obtained at the induction heat temperature of $380 \text{ }^\circ\text{C}$ and the stabilization line speed of 50 m/min . It was observed that these parameters were associated with the most even distribution of microhardness in the cross-section of the spun wires.

The reported study was funded by RFBR according to the research project №18-58-45008 IND_a.

References

1. Madatyan S. A. The current level of requirements to prestressing strands. *Beton i zhelezobeton*. 2005. No. 1. pp. 8–10.
2. Egorov V. D., Voronina V. S. Production of prestressing strands in a stress-relieved state. *Stal*. 1983. No. 3. pp. 65–66.
3. Costello G. A. *Theory of wire rope*. Second edition. New York: Springer, 1997. 123 p.

PROCESSING OF THE TITANIUM ALLOY Ti6Al7Nb AS A MEDICAL APPLICATION MATERIAL

Toyusheva D., Loginov Yu.

*Ural Federal University named after the first President of Russia B.N. Yeltsin,
Yekaterinburg, Russia
granatyuk.dashenka@mail.ru*

Pure titanium is commonly used as an implant material in surgical practice. However, where higher strength is required, the Ti6Al4V alloy is used [1-3]. At the same time, a question was raised about the toxic properties of vanadium as an element of the alloy [4]. That's why preference is now given to alloys in which vanadium is replaced by niobium.

According to the international material characterization system [5], the Ti6Al7Nb alloy belongs to the category of two-phase alloys (Alpha / Beta Titanium Alloy) with a polymorphic transformation temperature in the range of $995\text{--}1,025 \text{ }^\circ\text{C}$. The alloy itself

is probably exclusively intended for medical use, i.e. as a material for implants [6]. It should be noted that the alloy has an excellent biocompatibility due to the formation of a surface film of oxides that passivates the metal [7], as well as a good osseointegration ability, i.e. the ability of the implant to integrate with bone tissue [8].

Under certain processing conditions, the Ti6Al7Nb alloy can demonstrate superplasticity [9]. Thus, the authors observed a relative elongation of up to 400% under tension and of up to 790% at the temperature of 850 °C. Such a high level of ductility creates the prerequisites for the manufacture of products and rolled or pressed semi-finished products precisely by metal forming methods.

A large number of implants are available in the form of fasteners, such as screws, helices and nuts. They are normally manufactured from long products with small cross sections, e.g. wires. Typically, the manufacture of high-quality rolled titanium wires is extremely difficult due to increased sticking to the tool. However, there are methods for producing fine products. For example, the Chinese patent CN107214474 [10] describes a production method that includes manufacturing a preform of the Ti6Al7Nb alloy with a known structure and heating the preform in a muffle furnace to the temperature below the polymorphic transformation temperature. After that the workpiece is rolled to tight tolerances. The second stage is descaling. At the third stage, the workpiece gets cold rolled in multifaceted gauges to obtain caked metal. This process is compared to the hot drawing method, which was used before the development of the new technology. It is shown that the resultant material has a better structure and mechanical properties.

The authors of the patent US10323311 [11] proposed to process the alloy at temperatures below the phase transition temperature in the range of 400 to 600°C. It is recommended to use severe deformation methods, for example, angular pressing. At the end of the process, a nanostructured state with the grain size of 1 μm is ensured.

The reported study was funded by RFBR 19-38-90222 Improvement of the principles of alloying and parameters of external influence to increase the thermal stability and the level of physical and mechanical properties of aviation materials based on titanium and nickel.

References

1. Matej Balazic, Januz Kopac, Mark J. Jackson, Waqar Ahmed. Review: titanium and titanium alloy applications in medicine. International Journal of Nano and Biomaterials (IJNBM). 2007. Vol. 1, No. 1, pp. 3-34.
2. Stepanov S.I., Loginov Y.N., Popov A.A., Kuznetsov V.P. Effect of annealing on the structure and properties of titanium alloy with cellular architecture for medical applications. Metal Science and Heat Treatment. 2018. Vol. 60, Iss. 5-6. pp. 315-321.
3. Loginov Yu.N., Stepanov S.I., Golodnov A.I., Mukanov G.Z. Analysis of bending test technique for osteosynthesis titanium plate. The Ural School-Seminar of Metal Scientists-Young Researchers. 2019. pp. 106-112.
4. Froes F. H. Titanium for medical and dental applications—An introduction. Titanium in Medical and Dental Applications. 2018. pp. 3-21.
5. Material property data. Available at: matweb.com.
6. Disegi JA. Titanium-6% Aluminium--7% Niobium Implant Material. AO AS-IF. 1993. pp. 1-20. First Edition.
7. C. Sittig, G. Hahner, A. Marti, M. Textor, N. D. Spencer. The Implant Material,

Ti6Al7Nb: surface microstructure, composition and properties. *Journal of Materials Science: Materials in Medicine*. 1999. V. 10. pp. 191-198.

8. Shapira L., Klinger A., Tadir A., Wilensky A., Halabi A. Effect of a niobium-containing titanium alloy on osteoblast behavior in culture. *Clinical Oral Implants Research*. 2009. 20. pp. 578-582.

9. Watanabe K., Ashida M., Hanawa T., Masuda T., Horita Z., Kral P., Sklenicka V., Takizawa Y., Yumoto M., Otogiri Y. Production of superplastic Ti6Al7Nb alloy using high-pressure sliding process. *Materials Transactions*. 2019. Vol. 60, No. 9. pp. 1785-1791.

10. Zhu Yanli, Li Yinghao, Yang Hui, Hou Fengqi, Zhang Peng, He Yonggang, Lai Yunjin, Luo Wenzhong, Lei Jinwen. Preparation method for high-strength Ti6Al7Nb titanium alloy wire material. Patent CN107214474. Applied: 2017.05.22.

11. Colombo Gian, Anumalasetty Venkata. Nanostructured titanium alloy and method for thermomechanically processing the same. Patent US10323311. Applied: 2013.03.15.

FRICION NANOSTRUCTURING TREATMENT OF METALLIC SURFACES BY FLEXIBLE TOOL

Belevskii L., Belevskaya I., Efimova Yu.

*Nosov Magnitogorsk State Technical University, Magnitogorsk, Russia
belirena@yandex.ru*

In recent years, much attention has been paid to surface nanostructuring and its influence on the service properties of wares, including mechanical. The authors of [1] substantiate a concept according to which the surface layer is an independent subsystem strongly affecting the localization of the plastic flow and destruction of the material. Various methods of intense plastic deformation, including friction ones, can be used for surface nanostructuring [2, 3]. One method of formation of functional nanocrystalline layers on steel surfaces is treatment by sliding indenters [4]. It can be performed in sliding friction conditions, which exclude the heating of friction surfaces or, on the contrary, with heating of the surface from indenter friction and from the effect of the electric current (electromechanical treatment (EMT)) [5]. The deposition of coatings by means of friction of a brass or copper rod upon the detail surface is also referred to as friction treatment [6]. It is proposed to perform surface modification using a flexible tool—rotating wire brushes (RWBs), which have been used for surfacehardening treatment for a long time in various branches of technology [7–9], including the deposition of coatings [10]. The theoretical and experimental investigations into the plastic deformation process of the surface layer and deposition of coatings by a flexible tool were started at Magnitogorsk State Technical University in 1986 [11, 12]. Despite numerous studies fulfilled in subsequent years [13–16], the process that we call friction cladding (FC) is known poorly, which retards its more extended and effective use in various branches of technology.

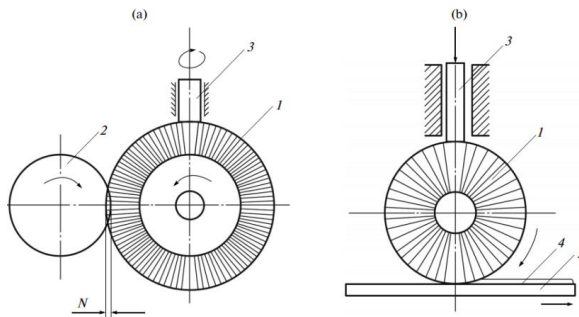


Fig. 1. Schematic diagram of deposition on (a) cylindrical and (b) planar ware surfaces by friction cladding. (1) Flexible tool (RWB), (2) treated ware, (3) billet from the coating material, and (4) coating layer; N is tension

When treating all materials under study using a flexible tool, surfacelayer hardening and texture formation are observed; the most acute texture is formed in surface layers. It is established experimentally that a thin layer of the amorphized material is formed on the surface during the RWB treatment, and this phenomenon most clearly manifests itself for materials with a high melting point, especially for tungsten. Coating particles at the boundary with a matrix are so fine that their shape is not resolved even at large magnifications. The crystallite sizes of the aluminum and brass coatings do not exceed 100 nm. The above gives us grounds to assume that nanostructured or even amorphized layers can be acquired on the surface under definite treatment modes using a flexible tool and functional coatings can be deposited. Turning or grinding lathes equipped with simple attachments can be used for the friction treatment of the surface by the FC method using a flexible tool. The treatment of screw surfaces and gear wheels and largescale articles is also possible. Surface treatment and coating deposition using a flexible tool is a simple, manufacturable, lowcost, and environmentally pure method which should find wider application in machine building and metallurgy.

The reported study was funded by RFBR according to the research project №17-38-50226 mol_nr.

References

1. Panin, V.E. and Panin, A.V., *Fiz. Mezomekh.*, 2005, vol. 8, no. 5, p. 7.
2. Chukin, M.V., Korshunov, A.G., Golubchik, E.M., et al., *Vestnik of Nosov Magnitogorsk State Technical University.*, 2012, no. 4, p. 61.
3. Makarov, A.V. and Korshunov, L.G., *Izv. Vyssh. Uchebn. Zaved., Fiz.*, vol. 24, no. 3, p. 301.
4. Makarov, A.V., Pozdeeva, N.A., and Malygina, I.Yu., *Deform. Razrush. Mater.*, 2010, no. 5, p. 32.
5. Askinazi, B.M., *Uprochnenie i vosstanovlenie detalei elektromekhanicheskoi obrabotkoi (Hardening and Reduction of Articles by Electrochemical Treatment)*, Leningrad: Mashinostroenie, 1977.
6. Garkunov, D.N. and Lozovskii, V.I., *USSR Inventor's Certificate No. 115744*, 1958.
7. Peregichka, E.V., *Ochistnouprochnyayushchaya obrabotka izdelii shchetkami*

(Cleaning/Hardening Treatment of Wares by Brushes), Moscow: Mashinostroenie, 1989.

8. Kurguzov, Yu.I. and Papshev, D.D., Vestn. Mashinotr., 1986, no. 4, p. 54.

9. Proskuryakov, Yu.G. and Ershov, B.C., in *Issledovanie tekhnologicheskikh protsessov uprochnyayushchekali bruyushchei i formobrazuyushchei obrabotki metallov: Mezhvuzovskii sbornik* (Investigation into Production Processes of Hardening/Calibrated and Forming Treatment of Metals), Rostov-on-Don: Inst. Agricult. Mech. Eng., 1970, p. 144.

10. Abinder, A.A., USSR Inventor's Certificate No. 57162, 1940.

11. Kadoshnikov, V.I. and Mironov, Yu.V., USSR Inventor's Certificate No. 1206068, 1986.

12. Belevskii, L.S., Izv. Vyssh. Uchebn. Zaved., Chern. Metall., 1987, no. 7, p. 104.

13. Belevskii, L.S., *Plasticheskoe deformirovanie poverkhnostnogo sloya i formirovanie pokrytiya pri nanesenii gibkim instrumentom* (Plastic Deforming the Surface Layer and Coating Formation under the Deposition by Flexible Tool), Magnitogorsk: Lyceum Russ. Acad. Sci., 1996.

14. Antsupov, V.P., *Teoriya i praktika plakirovaniya gibkim instrumentom* (Theory and Practice of Cladding by Flexible Tool), Magnitogorsk: Magnitogorsk State Tech. Univ., 1999.

15. Zavalishchin, A.N., Smirnov, O.M., and Tulupov, S.A., *Modifikatsiya poverkhnosti metallicheskih izdelii s ispol'zovaniem pokrytii* (Surface Modification of Metallic Wares Using Coatings), Moscow: OrbitaM, 2012.

16. Platov, S.I., Dema, R.R., and Zotov, A.V., Vestn. Magnitogorsk Gos. Tekh. Univ., 2013, no. 1, p. 69

EFFECT OF THE Ti6Al4V ALLOY TRACK ARRANGEMENT ON MECHANICAL PROPERTIES IN DIRECT METAL DEPOSITION

Glebov L., Pashkeev K., Radionova L.

*South Ural State University (National Research Institute), Chelyabinsk, Russia
79193293392@yandex.ru*

Titanium and its alloys are widely used in high-tech industries, such as aerospace industry, shipbuilding, nuclear power, chemical industry and medicine.

Titanium and its alloys are processable by all known metal forming methods: forging, cold and hot rolling, stamping, drawing. Basically, they are processed similarly to stainless steel, but the processing modes applied depend on the amount and the nature of impurities [1].

Laser Metal Deposition (or, LMD) is a process of direct material deposition based on the use of a constant laser source with the laser device moving along the product contours. For this method, it is possible to use several types of materials: metal powder or wire. The LMD process is used to produce infinitely large products of complex geometry with small tolerances and high properties [2]. The process of direct laser deposition is also used to produce new components of complex geometry parts [3], which would require many more production hours or which cannot be produced from separate components when using conventional processing methods [4].

This paper examines the influence of the Ti6Al4V alloy powder path on the microstructure and mechanical properties during Laser Metal Deposition.

The studies on the samples grown using the DMD (direct material deposition) technique were carried out at the laboratories of the South Ural State University in Chelyabinsk, Russia.

The studies were carried out on a FL-Clad-R-4 laser complex equipped with a 4 kW LS-4 laser, a six-axis industrial robot, a KUKA R-120 manipulator with a KUKA DKP-400 two-axis positioner, a TWIN-10-CR-2 powder feeder, as well as auxiliary equipment for creating an argon atmosphere.

30 to 100 micron titanium powder Ti-6Al-4V was chosen for this research. The powder was melted in the previously obtained mode [5]: power $P = 1,800$ [W]; powder feed $K = 27$ [g / min]; laser movement speed $U = 25$ [mm / s]; track displacement in the layer plane $\Delta l = 2.5$ [mm]; track displacement in the vertical plane $\Delta h = 0.3$ [mm]; number of layers $n = 150$.

The samples for mechanical tests were prepared using electrical discharge cutting (Fig. 1). This was necessary because of the high hardness of the obtained samples, which makes their mechanical processing harder. Electric discharge machining avoids heating of the metal in the cut zone and enables to obtain samples with a high surface quality, which is very important when testing brittle materials.

Four groups of samples were obtained with different growth track directions (Fig. 2).



Fig. 1. A electric discharge sawing template for mechanical testing

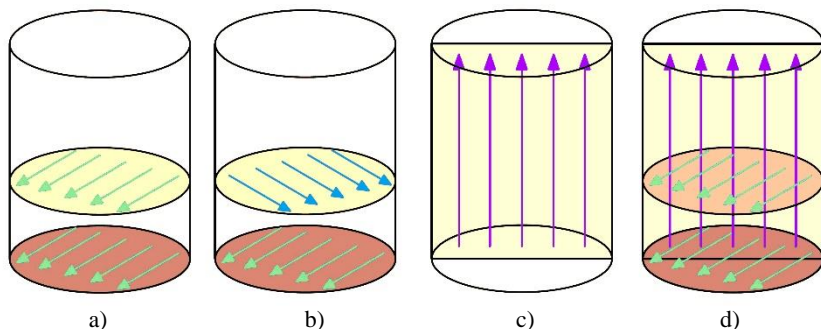


Fig. 2. Layouts of tracks in compression test samples: a) “parallel”; b) “perpendicular”; c) “vertical”; d) “mixed”

The results of the compression tests are presented in Table. 1. The maximum 1,910 MPa was shown by samples with a “vertical” track arrangement, while the minimum strength of 1,794 MPa – by samples with a “parallel” track arrangement. The alloy can resist higher stresses when load is applied perpendicular to the track arrangement than

when load is applied parallel to the tracks. At the same time, the deformation under compression for a sample with a “vertical” track arrangement is higher than for a sample with a “parallel” one. The “vertical” track arrangement provides a combination of high strength and high plasticity in the material. At the same time, the highest plasticity (namely, 33%) was shown by samples with a “mixed” track arrangement.

Table 1. Average values of mechanical properties depending on the track arrangement

Track arrangement in the sample	Compressive strength Rs, MPa	Young's modulus, MPa	Compression strain, %
“parallel”	1794	17642	21.3
“perpendicular”	1847	17678	21.8
“vertical”	1910	16998	26.8
“mixed”	1817	15697	33.0

This paper describes the first study that looks at the influence of the Ti6Al4V alloy powder material deposition track on the mechanical properties during direct laser melting. The conducted studies show that it is necessary to take into account the layout of the tracks during direct laser melting of the powder material when designing complex shape parts or billets that require final machining. Using the Ti-6Al-4V alloy as an example, the authors show that the “parallel” and “perpendicular” track arrangement is reflected in the mechanical properties of the material. The direction of the load application during the mechanical testing also has a noticeable effect. It is possible to increase the ultimate strength of the Ti-6Al-4V alloy from 1,794 to 1,910 MPa by only taking into account the location of the tracks relative to the applied compression load. At the same time, the ductility of the Ti-6Al-4V alloy obtained by direct laser melting can change from 21.3 to 33.0% depending on the track direction and the direction of the compression test. Taking these factors into account when designing critical parts from titanium alloys will make it possible to correctly perform calculations and prevent mistakes. It would be of relevance to investigate the effect of the Ti6Al4V alloy powder material deposition track when testing samples for static tension in the future.

This research work was funded by the Ministry of Science and Higher Education of the Russian Federation as part of a governmental assignment related to fundamental scientific research, Contract No. FENU-2020-0020 (2020071GZ).

References

1. Belov A. F., Williams J. C. Titanium and Titanium Alloys. Scientific and Technological Aspects. Volumes 1 - 3. New York: Plenum 1982.
2. Skvortsova S.V. The structural and texture analysis of titanium alloy Ti-6Al-4V samples obtained by direct metal deposition. IOP Conference Series: Materials Science and Engineering. Vol. 709, Issue 2.
3. Bykovskiy D. P., Petrovskiy V. N., Sergeev K. L., Osintsev A. V., Dzhumaev P.S., Polskiy V. I. Direct metal laser deposition of titanium powder Ti-6Al-4V. IOP Conference Series: Journal of Physics: Conference Series. 941 (2017).
4. Popovich A. A., Sufiiarov V.Sh., Borisov E.V., Polozov I.A. Microstructure and mechanical properties of Inconel 718 produced by SLM and subsequent heat treatment.

Key Engineering Materials. 2015. Vol. 651-653. pp. 665–670.

5. Samodurova M., Logachev I., Shaburova N., Samoiloova O., Radionova L., Zakirov R., Pashkeev K., Myasoedov V., Trofimov E. A Study of the Structural Characteristics of Titanium Alloy Products Manufactured Using Additive Technologies by Combining the Selective Laser Melting and Direct Metal Deposition Methods. *Materials*. 2019. 12. 3269.

WAYS TO EXPAND THE USE OF MAGNESIUM

Zamaraeva Y.^{1,2}, Loginov Yu.^{1,2}

¹*Ural Federal University named after the first President of Russia B.N. Yeltsin, Yekaterinburg, Russia*

²*M.N. Mikheev Institute of Metal Physics of the Ural Branch of the Russian Academy of Sciences, Yekaterinburg, Russia
zamaraevajulia@yandex.ru*

In today's metal production industry, there is an established trend of developing new technologies for making products out of magnesium and its alloys [1]. Some applications of such magnesium products seem to be quite unusual.

A recent trend in building design includes the use of composite panels composed of various metals. The shape and color of copper composite panels distinguish them from the others. In addition to copper cladding, composite panels use cheaper components, including those made of magnesium alloys, as fillers [1].

Being a biocompatible and biodegradable material, magnesium is also finding a wider application in medicine. In comparison with other metals used in medicine, magnesium is essential for proper functioning of the human body, which explains the mass production of dissolve-after-healing implants [2]. In oil production, magnesium balls play a similar role since they are used as valves that temporarily lock wells and self-dissolve under the influence of drilling fluids [3]. Fig. 1 shows the authors' estimation of the working conditions of a magnesium ball in a well saddle.

In the industry of light alloys, magnesium is a competitor to aluminum since it is one and a half times lighter. However, magnesium is a material that is more difficult to deform and is much more oxidizable. Hence, it is desirable to isolate magnesium from the impact of the atmosphere by protecting it with other materials. It led to an idea of creating technologies for the production of layered panels.

The main requirements for composite panel fillers are strength, rigidity, and low specific gravity. The lightest of the structural metals, magnesium and its alloys meet these requirements well. Commercially pure magnesium demonstrates a good mechanical strength. At the same time, addition of small amounts of alloying elements (such as aluminum, zinc, manganese, etc.) helps to significantly improve its mechanical properties with almost no density increase. For example, MA2-1 alloy, which demonstrates the strength and plasticity at the level of cold-formed copper, has a density of 1.8 g / cm³. Therefore, a composite material consisting of M1 copper (density 8.9 g / cm³) and MA2-1 magnesium alloy can potentially be used for the manufacture of indoor finish panels [4].

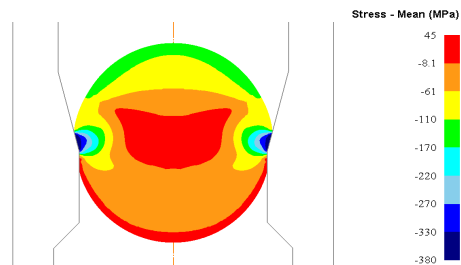


Fig. 1. The configuration of the deformation zone in a magnesium ball under hydrostatic pressure shown as equal-level areas of average normal stresses

Usually, special types of Mg alloys are developed in order to increase plasticity in a hot state. However, during hot deformation, there is a problem of high oxidation and gas saturation. Thus, the development of new low-temperature deformation methods applicable to magnesium is of interest [5,6]. Unfortunately, Russia is lagging behind other countries in the production and mainly in the processing of magnesium. For instance, Russia's output is ten times lower than China's. The great attention paid to magnesium in China can be appreciated based on the fact that the only scientific journal in the field of magnesium processing, the *Journal of Magnesium and Alloys*, is published by KeAi Publishing Communications Ltd in China.

This research was funded by the Russian Foundation for Basic Research (RFBR project No. 20-38-90051) and was carried out as part of a governmental assignment ("Pressure" No. AAAA-A18-118020190104-3).

References

1. Qizhen Li. Dynamic compressive mechanical behavior of magnesium-based materials: magnesium single crystal, polycrystalline magnesium, and magnesium alloy. *Handbook of Mechanics of Materials*. 2019. pp. 846-872.
2. Shmorgun V. G., Slautin O. V., Arisova V. N., Pronichev D. V., Kulevich V. P. Structure and phase composition of diffusion zone in copper M1 + alloy MA2-1 composite. *Metallurgist*. 2020. Vol. 63, Iss. 9-10. pp. 1124-1131.
3. Zhang C., Wu L., Huang G. et al. Effects of Fe concentration on microstructure and corrosion of Mg-6Al-1Zn-xFe alloys for fracturing balls applications. *Journal of Materials Science and Technology*. 2019. Vol. 35(9). pp. 2086-2098.
4. Peng Wan, Lili Tan, Ke Yang. Surface modification on biodegradable magnesium alloys as orthopedic implant materials to improve the bio-adaptability: a review. *Journal of Materials Science & Technology*. 2016. Vol. 32. pp. 827-834.
5. Loginov Y.N., Volkov A.Y., Kamenetskiy B.I. Analysis of the scheme of non-equal channel angular pressing as applied to the formation of sheet magnesium in a cold state. *Russian Journal of Non-Ferrous Metals*. 2019. Vol. 60, Iss. 2. pp. 146-151.
6. Kamenetskiy B.I., Loginov Y.N., Kruglikov N.A. Possibilities of a new cold upsetting method for increasing magnesium plastification. *Russian Journal of Non-Ferrous Metals*. 2017. Vol. 58, Iss. 2. pp. 124-129.

UNDERSTANDING THE EFFECT OF FRICTION CONDITIONS ON THE PARAMETERS OF INNER TIE ROD PRESSING

Vakhitov A., Stolyarov F.

JSC SPA BelMag, Magnitogorsk, Russia

stolyarov.f.a@yandex.ru

When designing the inner tie rod assembly technology, one should analyze all the process stages in order to achieve the required quality. Pressing an inner tie rod body is one of the most important assembly operations for this type of products. The selected process parameters determine the performance of the fixed joint of a ball stud, an insert and a body. Such parameters include punch load, punch travel and die geometry [1].

This study is aimed at assessing the dependence between the punch load and the coefficient of external friction between the external surface of the blank and the internal surface of the die, and determining the dependence between the friction coefficient and the travel speed of body material particles in relation to the ones of the die [2].

To achieve the set objective, we carried out a series of experiments in the DEFORM-2D software environment. The elastic-plastic behaviour of the materials is described by a bilinear stress-strain diagram [1]. To make the calculations easier and faster, an axially symmetric model was built, because the object of interest was solid of revolution.

The simulation showed a dependence between the kinetic coefficient of sliding friction and the relative travel speed of the part and die metal particles. A curve was built to show the relationship between the punch load required to make an inner tie rod body and the time-dependent friction coefficient (Fig. 1). The obtained dependencies will be used to develop a pressing technique for future projects to be implemented by JSC SPA BelMag.

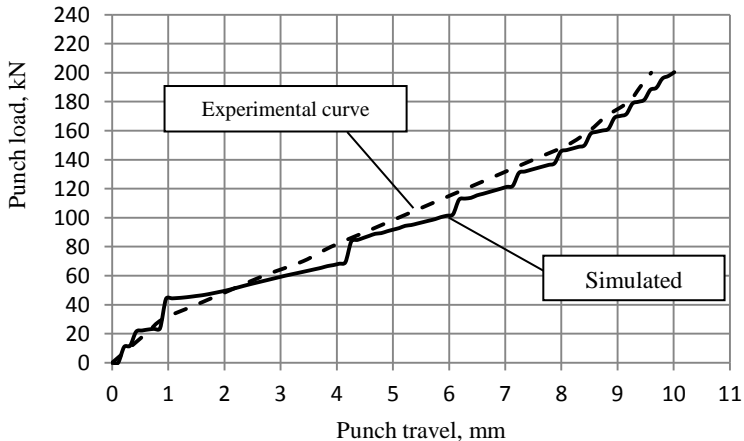


Fig. 1. Punch load versus punch travel: A comparison between experimental and simulation curves

References

1. Gun E.I., Vakhitov A.R. et al. Simulation of an axial joint pressing process. Vestnik of Novos Magnitogorsk State Technical University. 2019. Vol. 17, No. 1. pp. 46-52.
2. MSC/DYTRAN User's Manual. The MacNeal-Schwendler Corporation, 1997.

ROLLING OF ALUMINIUM ALLOY 5083 SHEETS

Snegiryov I.^{1,2}, Loginov Yu.¹

¹*Ural Federal University named after the first President of Russia B.N. Yeltsin, Yekaterinburg, Russia*

²*Kamensk Uralsky Metallurgical Works, Kamensk Uralsky, Russia
igor_snegirev@mail.ru*

Aluminum alloy 5083 contains 4.0-4.9% magnesium. According to Russian standards, it can correspond to alloy AMg4.5 per GOST 4784-97. Additionally, this alloy contains 0.40-1.0% Mn, 0.05-0.25% Cr. According to the matweb.com system, the alloy has high corrosion resistance and moderate strength and finds application in transport machines, pressure vessels, cryogenic plants, towers and drilling rigs, gas and oil pipelines. In order to meet the specification, the H116 metal is processed in any manner necessary to reduce the degree of intergrate and delamination corrosion. Layer corrosion results in peeling or exfoliation of metal layers parallel to the pressing or rolling surface. It is closely related to the fibrous structure of plates, sheets, as well as the linear arrangement of primary intermetallics in them. Delamination, which usually occurs under certain atmospheric conditions and under periodic exposure to seawater, mainly affects plates and heated sheets in a certain structural state. To reach the H321 supply state, the metal undergoes deformation hardening followed by stabilization to a strength equal to about a quarter of that obtained between the annealing states (O) and the solid state (H38). The treatment process should also produce a metal with a certain degree of resistance to intergranular (MCC) and delamination corrosion.

As is shown in articles [1,2], alloys of the aluminum-magnesium system are already prone to delamination during hot rolling. This led to the need to perform experimental rolling of sheets made of these alloys while evaluating their corrosion resistance.

To obtain sheet metal with a thickness of 7.8 mm, ground blanks made of alloy 5083 were subjected to hot rolling in a roughing and then in a finishing stand of a hot rolling mill. Homogenization annealing of the blanks was combined with hot rolling of the ingots. The temperature of the metal prior to hot rolling was 480 °C. The further treatment process consisted of a series of steps.

Stage 1. Condition after hot rolling.

Stage 2. Condition after the first cold rolling pass.

Stage 3. Condition after intermediate annealing.

Stage 4. Condition after the second cold rolling pass.

The tensile strength and yield strength values for the treatment stages are shown as graphs in Fig. 1.

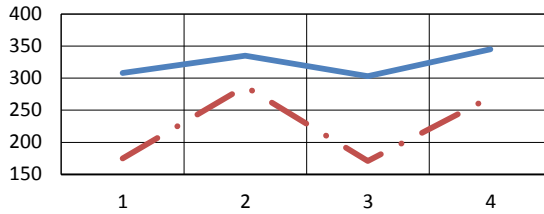


Fig. 1. Graphs showing how the properties of the rolled stock change by processing stage (MPa, top-down): σ_b (MPa), $\sigma_{0.2}$

One can see that the above graphs look fairly similar. However, the yield stress appears to be more sensitive to the processing method, as is shown by the large gradients of values.

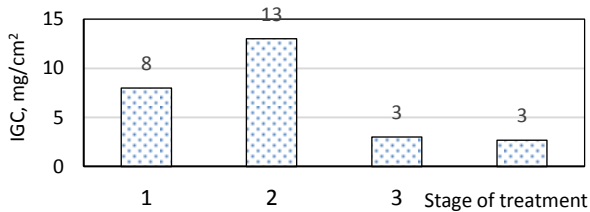


Fig. 2. Changing IGC by processing stage

The IGC measurement showed that the index can vary in the range from 3 to 13, and under the standard requirements it cannot exceed 15 mg/cm². The state of the metal after the first cold rolling pass approaches this indicator. It is assumed that the corrosion resistance of the surface layers of the rolled stock is closely related to the deformed state. So the next step may be to use numerical modeling of a rolling process to simulate the rolling of alloy 5083, as it is done, for example, in the study [3].

References

1. Rusakov G.M., Illarionov A.G., Loginov Y.N., Lobanov M.L., Redikultsev A.A. Interrelation of crystallographic orientations of grains in aluminum alloy AMg6 under hot deformation and recrystallization. *Metal Science and Heat Treatment*. 2015. Vol. 56, Iss. 11-12. pp. 650-655.
2. Sezek S., Aksakal B. Deformation and temperature behaviour during cold, warm and hot flat rolling of AA5454-O alloy. *Materials and Design*. 30 (2009). pp. 3450-3459.
3. Ahmed H., Wells M.A., Maijer D.M., Howes B.J., van der Winden M.R. Modelling of microstructure evolution during hot rolling of AA5083 using an internal state variable approach integrated into an FE model. *Materials Science and Engineering A*. 2005. Vol. 390. pp. 278-290.

ROUGHNESS FORMATION IN HOT-ROLLED TEMPER-ROLLED BAND PRODUCTION

Golubchik E., Medvedeva E., Gulin A., Polyakova M.

*Nosov Magnitogorsk State Technical University, Magnitogorsk, Russia
fekla_med@mail.ru*

The hot-rolled strip, inclusive pickled, annealed and temper-rolled is one of the mainstream metal product. This type of metal products is used for the production of welded building structures, pipes, car parts (in particular, wheel disks, rear suspension link connectors). This is due to the reduction in the number of technological process stage, in particular due to operation exception of cold rolling, and also the transformation of some mechanical properties and performance parameters of cold-rolled products to pickled hot-rolled products [1]. Studies on the development of a new production technology of the pickled hot-rolled strip with increased quality are conducted by scientists of the Nosov Magnitogorsk State Technical University and specialists of PJSC Iron & Steel Works [2,3].

Figure 1 presents a comparative analysis of the experimental strip (a) with the serial tape (b). The results of processing the rolled stock into the finished product are shown in figure 2.



Fig. 1. Tempered strip surface of pilot run (a) and non-tempered strip surface of batch (b)

Based on the visual estimate, the tempered strip has a higher uniformity of roughness without the line of fracture, which is favorable for the process of paint coating applying.



Fig. 2. Stamped wheel from pilot run of pickled temper-rolled strip of 07GBYu steel for the LADA automobile of JSC AvtoVAZ

Thus, the carried out researches have established the formation features of the finished hotrolled strip and also ways of its management, for example by gage interference reducing, on-line management of the reduction process, more detailed processing of the strip ends with cutting out of off-grade pieces.

The reported study was funded by RFBR according to the research project №18-58-45008 IND_a.

References

1. Golubchik E M, Medvedeva E M and Martynova T Yu 2017 Processing of solid and laminate materials 1(46) 59–4
2. Golubchik E M, Medvedeva E M, Telegin V E and Vasil'ev I S 2015 Proceedings of the 12th all-russian scientific and practical conference “Modern problems of the mining and metallurgical complex. science and production” 1 208–12
3. Golubchik E M, Medvedeva E M and Telegin V E 2016 Proceedings of the International scientific and practical conference “New solutions in the field of strengthening technologies: the view of young professionals” 1 254–58.

FINITE ELEMENT MODELING OF THE SLEEPER SCREW HEAD HOT STAMPING PROCESS ACCOUNTING FOR DYNAMIC RECRYSTALLIZATION

Ishimov A.

*¹PJSC NLMK, Lipetsk, Russia
ishimov_as@nlmk.com*

This paper describes the results of finite element modeling of the sleeper screw head hot stamping process, which was carried out in the Simulia Abaqus software package. Grade 20 steel was selected as the material from which sleeper screws were hot stamped. A series of experimental studies was carried out to describe the rheological properties of this steel. Experimental flow curves were obtained under the following deformation conditions: the deformation temperatures were 1,200, 1,150, 1,100, 1,000 and 900 °C; the selected strain rates were 0.01, 0.1, 0.5, 1 and 5 s⁻¹; the true logarithmic strain for all cases was 0.8. Analysis of all experimental strain-stress dependences showed the presence of all dynamic recrystallization process stages (such as work hardening), as well as the presence of the peak stress accompanied by a gradual decrease in the stress level until reaching a plateau. The moment the graph reaches a plateau corresponds to the steady-state process of dynamic recrystallization, when an equal amount of deformed and recrystallized structure is present over the entire volume of the test sample. The only deformation mode in which the dynamic recrystallization process failed to begin corresponded to the deformation temperature of 900 °C and the strain rate of 5 s⁻¹.

To obtain a continuous function describing the rheological properties of the grade 20 steel in the studied range of temperatures, strains and strain rates, an approach was used based on the Arrhenius equation describing thermally activated deformation processes and the Johnson-Mel-Avrami-Kolmogorov equation [1-3]. In general, the system of equations used to describe the experimental data can be written down as

$$\sigma(\varepsilon) = \left\{ \begin{array}{l} \left[\sigma_{sat}^2 + (\sigma_0^2 - \sigma_{sat}^2) e^{-\Omega \varepsilon} \right]^{0.5}, \varepsilon < \varepsilon_c \\ \sigma_p - (\sigma_p - \sigma_{ss}) \cdot \left(1 - e^{-K \left(\frac{\varepsilon - \varepsilon_c}{\varepsilon_p} \right)^N} \right), \varepsilon > \varepsilon_c \end{array} \right\} \quad (1)$$

where σ_{sat} - the steady-state stress as a result of the dynamic recovery process; σ_0 - yield strength; Ω - parameter characterizing the process of work hardening; σ_p - peak strain; σ_{ss} - steady-state flow stress; ε_c - critical strain; ε_p - the strain corresponding to the peak value of the deformation resistance; K and N - parameters characterizing the recrystallization process kinetics.

For the main components included in this mathematical model, a relationship was established using the Zener-Hollomon parameter. The relationship shows the influence of temperature and strain rate and can be written down as $Z = \dot{\varepsilon} \exp(Q/RT)$. A mathematical model was obtained that helps determine the dependence of the flow stress on the deformation parameters for the grade 20 steel in the following ranges of temperatures and strain rates: $T = 900 \dots 1200$ °C, $\dot{\varepsilon} = 0,01 \dots 5$ s⁻¹ as

$$\sigma(\varepsilon) = \left\{ \begin{array}{l} \left[\left(Z^{0,156} \cdot e^{0,8204} \right)^2 + \left(\left(Z^{0,1248} \cdot e^{0,9359} \right)^2 - \left(Z^{0,156} \cdot e^{0,8204} \right)^2 \right) \exp \left(- \left(Z^{-0,0337} \cdot e^{2,8614} \right) \varepsilon \right) \right]^{0,5}, \varepsilon < \varepsilon_c \\ \left(\frac{Z}{e^{-1,66}} \right)^{\frac{1}{5,85}} - \left(\left(\frac{Z}{e^{-1,66}} \right)^{\frac{1}{5,85}} - \left(Z^{0,1911} \cdot e^{-0,2704} \right) \right) \cdot \left(1 - \exp \left[-0,59737 \left(\frac{\varepsilon - \left(Z^{0,1751} \cdot e^{-6,7666} \right)^{1,678}}{\left(Z^{0,1866} \cdot e^{-6,171} \right)} \right) \right] \right), \varepsilon > \varepsilon_c \end{array} \right\} \quad (2)$$

Using the VUHARD subroutine, the resulting mathematical model was integrated into the Simulia Abaqus software package. A finite element simulation was carried out for the sleeper screw head hot stamping process using solid and spring-loaded punch. It was established that, under deformation starting from the temperature of 1,150 °C and taking into account the cooling conditions, the use of a spring-loaded punch will reduce the stamping force by 23%: from 1,900 to 1,460 kN.

References

1. M. Avrami. Kinetics of Phase Change. I. General Theory. Journal of Chemical Physics. 7 (12). pp. 1103–1112 (1939).
2. M. Avrami. Kinetics of Phase Change. II. Transformation-Time Relations for Random Distribution of Nuclei. Journal of Chemical Physics. 8 (2). pp. 212–224 (1940).
3. M. Avrami. Kinetics of Phase Change. III. Granulation, Phase Change, and Microstructure. Journal of Chemical Physics. 9 (2). pp. 177–184 (1941).

INVESTIGATION OF THE STATE OF Cu59ZnPb1 AFTER HOT EXTRUSION

Vorsin A.^{1,2}, Loginov Yu.¹, Shimov G.¹

¹*Ural Federal University named after the first President of Russia B.N. Yeltsin
Yekaterinburg, Russia*

²*JSC Kamensk-Uralsky Non-Ferrous Metal Working Plant, Kamensk-Uralsky, Russia
geosh@bk.ru*

LS59-1 is one of the most common leaded brass brands in the production and application of copper-zinc alloys. According to the ASTM standard, leaded brasses fit in the C31400-C38600 brand range, and the counterpart to LS59-1 brass is the C37000 alloy. Without doubt, when manufacturing semi-finished products from this brass brand, the requirements for mechanical properties should be met. Such properties depend on the state of the metal: if it is in a hot-pressed, annealed or hardened condition. In this case, a distinction is made between the state after hot processing and that after annealing, which can be explained by two reasons: incomplete recrystallization and fixation of various combinations of α and β phases at the final moment of processing [1 -3].

To establish the range of possible fluctuations in the mechanical properties of brass LS59-1, an industrial experiment was conducted using a horizontal hydraulic press with a force of 30 MN from PRESEZZI EXTRUSION S. P. A., during which a bar with a diameter of 26 mm was pressed in a reverse pressing mode.

The variable value was the heating temperature of the ingots for pressing. Figure 1 shows the results of measuring the ultimate tensile strength σ_b and the elongation at break δ . The graph shows the average numbers of 2 to 4 measurements taken at each temperature.

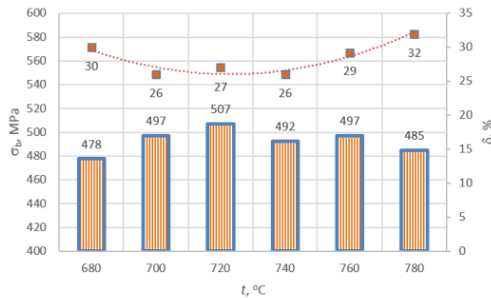


Fig. 1. Dependence of ultimate tensile strength σ_b and elongation at break δ in the temperature function

One can see that the ultimate tensile strength fluctuations are in the range of 478...507 MPa, and the elongation at break fluctuations are from 26 to 32%. It should be noted that for C37000 brass, the range of possible changes in the ultimate tensile strength (website <http://www.matweb.com>) is 372 to 552 MPa. Thus, all the products obtained meet the requirements.

At the same time, if we consider the dependence known for brass of this brand

STANDARDIZATION SYSTEM MANAGEMENT MODEL

Kazantseva T.¹, Pidzhakova E.¹, Tkachuk G.¹, Polyakova M.²

¹*Ural Federal University named after the first President of Russia B.N. Yeltsin,
Yekaterinburg, Russia*

²*Nosov Magnitogorsk State Technical University, Magnitogorsk, Russia
t.v.kazantseva@urfu.ru*

The action of standardization has always been aimed at providing information and accumulating the best practices and the most suitable technical and managerial solutions to specialists thus making the data available for everybody. In current circumstances, when dynamic changes are needed in all fields, it is the standards that can provide a safety cushion and guarantee the reliability of solutions based on the actual experience. And it would be appreciated to believe that exactly the standards will be able to promptly deliver new quality solutions to different problems. In order to make it possible, one should be able to quickly and easily find the object of interest and to create a possibility of making quick alterations to the current standards once new approved and tested solutions emerge. Thus, such alterations should appear in the original document and in all related standards simultaneously [1].

The current classification system is based on a hierarchy. Such rigidity and one-dimensionality of the system ensure high authenticity of information and efficiency in case of insignificant alterations made to the regulatory documents simultaneously. However, when new technologies (including the digital ones) are implemented and a prerequisite of management is a reduced time of response to parameter alteration within the framework of current and future decision-making systems, along with information authenticity assurance, a fast operating system is required.

At the first stage of our research, we have arrived at the conclusion that the best possible system ensuring standard management should be dynamic, flexible and multi-dimensional and should give the possibility to segregate and coordinate information at different levels: fundamental, general, special, and specialized one [2-4]. The database where all information is stored and processed is used as the basis of any information system. In recent years, databases have become more advanced. There are known and widely used such database models as hierarchic, network, relational and semantic [5]. From the point of view of the information system, the semantic model would be of the greatest interest as it can be represented as an oriented graph with peaks corresponding to the objects of interest and arcs specifying the relations between them [6-9]. The objects may be terms, events, properties or processes.

The following terms should be defined for the purpose of building a semantic model: entity, variety of entities, attribute, relation, relation degree. The main advantage of the semantic model is its scalability, due to which one can develop a semantic model that will only be linked to one standard and then make up a system for standard framework servicing. In the modeled situation, the standard corresponds to the concept of entity.

We distinguish the following properties of a standard which can help to quickly identify it: designation, name, classification code in accordance with the All-Russian Classifier for Standards, adoption date, effective date, relevance, alterations, references to other standards, keywords. To create a semantic model, we propose using the following types of relations between the standard and other entities: a part that develops and

makes alterations to the standard, a part that approves the standard, a special information service that maintains the standards and the users. Due to the use of references to other standards, additional relations between them can be segregated, which will ensure quick information updating in case of alterations to separate provisions of the considered standard from all related standards.

The reported study was funded by RFBR according to the research project №18-58-45008 IND_a.

References

1. Belogradin V.Ya., Zazhigalkin A.V., Zvorykina T.N. Technical regulatin on the edge of Industry 4.0. Moscow: Nauchnyi konsultant, 2019. 100 p.
2. Kazantseva N.K., Tkachuk G.A., Nevolina A.L., Shavrin V.S. The Problems of Standards Classification. International Journal of Management. 2020. Vol. 11. pp. 36-42.
3. Kazantseva N.K., Bildanov R.G., Aleksandrov V.A., Loretts O., Kukhar V.S. Preparing a Corporate System of Standards to Digitization. International Journal of Civil Engineering and Technology. 2018. Vol. 9, Iss. 6. pp. 1567–1573.
4. Kazantseva N.K., Kazantseva T.V., Bildanov R.G., Ismuratov D.S., Bedych T.V., Ismuratov S.D., Aleksandrov V.A., Kukhar V.S. What is it necessary to change in the system of standards' mangement. Standards and Quality. 2020. Iss. 6. pp. 23-27.
5. Kazantseva N.K., Kazantseva T.V., Bildanov R.G., Ismuratov D.S., Bedych T.V., Ismuratov S.D., Aleksandrov V.A., Kukhar V.S. Variants of the Digitization for a Specific Technological Process. International Journal of Mechanical Engineering and Technology. 2018. Vol. 9, Iss. 10. pp. 1186–1192.
6. Kudryavtsev V.B., Gasanov E.E., Podkolzin A.S. Intellectual systems. Moscow: Uright, 2017. 219 p.
7. Ustalov D. Expending Hierarchical for Constucting a Semantic Word Network. Computational Linguistics and Intellectual Technologies: Paper from the Annual Conference “Dialogue”. Moscow, 2017. Vol. 1. pp. 369-381.
8. Siray Hunir, Syed Imran Jami, Shaukaf Wasi. Knowledge graph based semantic modeling for profiling in Industry 4.0. International Journal on Information Technologies & Security. 2020. No. 1 (Vol.12). pp. 37-50.
9. Ying Zhao, Chetan Kotak, Chales C. Zhao. Semantical Machine Understanding. 13th International Command and Control Research and Technology Symposia. Seattle, 2008. pp. 17-19.

APPLICATION OF SEVERE PLASTIC DEFORMATION FOR FORGING CYLINDRICAL BILLETS

Andreyashchenko V., Stepanova M.

*Satpaev Ekibastuz Technical and Engineering Institute, Ekibastuz, Kazakhstan
Vi-ta.z@mail.ru*

Methods that implement severe plastic deformation (SPD) have recently been increasingly developed and applied. Interest in SPD is primarily associated with a set of formed properties. The latter are determined by the peculiarities of the crystal structure and the formed ultrafine-grained and/or nanostructure. To solve the problem of deformation of cylindrical billets, we used a forging tool with movable working elements [1]. The movable elements of the tool directly under force form predominantly com-

pressive stresses in the deformation zone and shear deformation. The constant change in the metal flow direction during a single deformation cycle makes it possible to almost completely eliminate tensile stresses and prevent central looseness (Fig. 1).

In this study, we performed the computer simulation of a broaching process in DEFORM-3D, as well as a physical modeling using plastic paraffin as a model material.

The computer simulation showed that the use of a machine with the movable working elements for processing cylindrical workpieces formed a homogeneous stress intensity field. Areas with maximum effective strain values are redistributed in a single reduction cycle along the section of the workpiece, ensuring its uniform processing. The required degree of deformation is determined by the camber angle of the movable elements of the tool and is not adjusted. An increase in the degree of deformation for a single compression contributes to an increase in the values of the stress-strain state parameters. The nature of the stress-strain state is not changed with an increase in the degree of deformation of the workpiece.

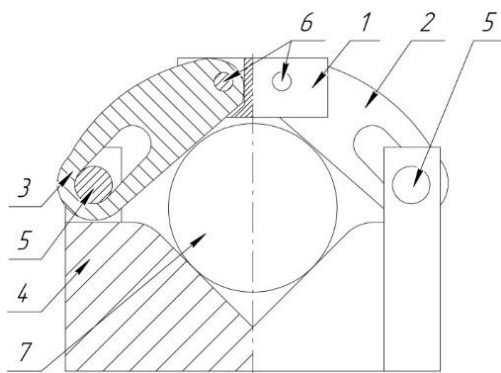


Fig. 1. A forging broaching machine with the movable working elements: 1 is a top die; 2, 3 are movable working elements; 4 is a bottom die; 5 are rotary joints of the bottom die; 6 are rotary joints of the top die; 7 is a workpiece

The physical modeling is in good agreement with the computer simulation. The physical experiment also made it possible to analyze the features of the closure of internal defects during severe plastic deformation. The data obtained made it possible to establish how deformation conditions and technological factors influenced the closure of internal defects in the workpieces. The regression equation was worked out and the degree of influence of each factor was revealed. The factors used were such parameters as the degree of deformation, workpiece tilting around its longitudinal axis, and the filling of defects.

References

1. Andreyashchenko V.A. Forging broaching machine. Patent RK No.33171, B21J 5/00, publ. on 22.10.2018. Bul. No.39.
2. Andreyashchenko V.A., Ivasik V.A., Stepanova M.Sh., Andauov T.Sh., Kravchenko K.K. Analysis of the deformation behavior of billets under severe plastic

deformation. Improving the quality of education, current innovations in science and manufacturing: Proceedings of the International Scientific and Practical Conference. Ekibastuz, Prokopievsk, 2020. pp. 33-37.

3. Andreyashchenko V.A. Finite element simulation (FES) of the fullering in device with movable elements. Metallurgy. 2016. Vol. 55. No. 4. pp. 829-831.

4. Andreyashchenko V.A., Kocich R. Simulation of fullering technology as a plastic deformation method for high quality forgings production. The 25th International Conference on metallurgy and materials METAL. Brno, Czech Republic, 2015. pp. 271-275.

BEHAVIOR OF FINE PEARLITE PLATES IN THE DEFORMATION OF HIGH-CARBON STEEL

Koptseva N.¹, Efimova Yu.¹, Gulin A.¹, Narasimhan K.², Prasad M.J.²

¹*Nosov Magnitogorsk State Technical University, Magnitogorsk, Russia*

²*Indian Institute of Technology Bombay, Mumbai, India*

nara@iitb.ac.in

Thanks to its high strength, high-carbon steel with pearlitic structure is widely used in construction [1-4]. Wire made of patented high-carbon steel is extremely strong, on account of the distinctive deformational properties of the fine-plate pearlite formed in the steel billet and its strain hardening on subsequent cold plastic deformation [4]. The main method of wire production is drawing, which is a relatively simple process and has been extensively theoretically studied. Currently, traditional methods of wire manufacture are so well developed that there is little prospect for considerable change in the strength–plasticity ratio of the material. At many metallurgical and metalware plants, combined deformational treatment of metals has been adopted. By such means, the performance of materials may be improved by deliberate change in their structure and fine structure [5, 6]. By combining simple types of deformation (torsion, extension, compression, and flexure), the efficiency of drawing may be increased, the material consumption may be decreased, and the stress–strain state of the metal may be improved, with consequent increase in the plasticity, while maintaining good mechanical properties. Different combinations of deformation will have different effects on the structure and mechanical properties of the steel. In comparison with traditional drawing, the combination of drawing, flexure, and torsion decreases the interplate distance and strengthens the wire. However, with increase in the strain in drawing, the change in interplate distance and hardness decreases. In terms of modification of the microstructure and increase in hardness, the most effective combination is moderate drawing, flexure in 60-mm rollers, and torsion at 150 rpm. Torsion at lower speeds has little effect. In flexure through rollers with different diameter (90 and 60 mm), torsion has much less influence than in the case of flexure in 60-mm rollers and torsion at 150 rpm.

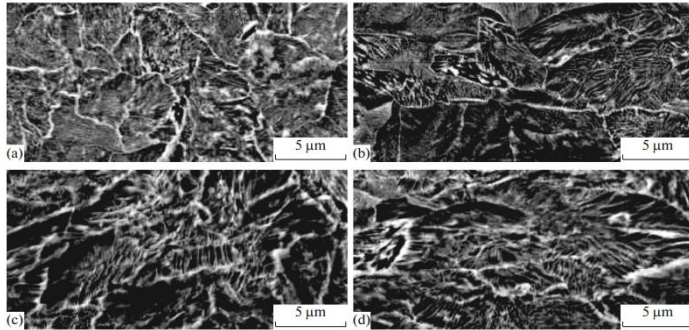


Fig.1. Microstructure of longitudinal section of steel 70 sample after patenting (a) and after drawing protocols 1 (a), 2 (b) and 3 (c)

The reported study was funded by RFBR according to the research project №18-58-45008 IND_a.

References

1. Izotov, V.I., Pozdnyakov, V.A., Luk'yanenko, E.V., Usanova, O.Yu., and Filipov, G.A., Influence of the pearlite fineness on the mechanical properties, deformation behavior, and fracture characteristics of carbon steel, *Phys. Met. Metallogr.*, 2007, vol. 103, no. 5, pp. 519–529.
2. Toribio, J., Role of the microstructure on the mechanical properties of fully pearlitic eutectoid steels, *Fracture Struct. Integr. Relat. Issues*, 2014, vol. 30, pp. 424–430.
3. Hohenwarter, A., Völker, B., Kapp, M.W., et al., Ultrastrong and damage tolerant metallic bulk materials: a lesson from nanostructured pearlitic steel wires, *Sci. Rep.*, 2016, vol. 6. <https://doi.org/10.1038/srep33228>
4. Gridnev, V.N., Gavrilyuk, V.G., and Meshkov, Yu.Ya., *Prochnost' i plastichnost' kholodnodeformirovannoi stali (Strength and Plasticity of Cold-Deformed Steel)*, Kiev: Naukova Dumka, 1974.
5. Kharitonov, V.A. and Gallyamov, D.E., The efficiency improvement of drawing based on the use of complex and integrated processes, *Chern. Metall., Byull. Nauchno-Tekh. Ekon. Inf.*, 2016, no. 8 (1400), pp. 71–77.
6. Sidel'nikov, S.B., Dovzhenko, N.N., and Zagirov, N.N., *Kombinirovannyye i sovmeshchennyye metody obrabotki tsvetnykh metallov i splavov (Integrated and Combined Processing of Nonferrous Metals and Alloys)*, Moscow: MAKSS Press, 2005.

List of Participants

1. Abashev D., Ural Federal University named after the first President of Russia B.N.Yeltsin, Yekaterinburg, Russia,
2. Abdullina D., M.N. Mikheev Institute of Metal Physics of the Ural Branch of the Russian Academy of Sciences, Yekaterinburg, Russia,
3. Abhay Kumar Dubey, PDPM Indian Institute of Information Technology, Design and Manufacturing, Jabalpur,
4. Adishchev P., Nosov Magnitogorsk State Technical University, Magnitogorsk, Russia,
5. Adyev E., Ural Federal University named after the first President of Russia B.N.Yeltsin, Yekaterinburg, Russia,
6. Akhmedjanov A., South Ural State University (National Research Institute), Chelyabinsk, Russia,
7. Akopyan T., National University of Science and Technology MISiS, Moscow, Russia,
8. Alekseev D., Nosov Magnitogorsk State Technical University, Magnitogorsk, Russia,
9. Alyutina E., Russian Research Institute of the Tube & Pipe Industries (ROSNITI), Chelyabinsk, Russia,
10. Andrea Ghiotti, University of Padova, Padova, Italy,
11. Andreyashchenko V., Satpaev Ekibastuz Technical and Engineering Institute, Ekibastuz, Kazakhstan,
12. Antonova O., M.N. Mikheev Institute of Metal Physics of the Ural Branch of the Russian Academy of Sciences, Yekaterinburg, Russia,
13. Arbut A., Nazarbayev University, Nur-Sultan, Kazakhstan,
14. Belevskaya I., Nosov Magnitogorsk State Technical University, Magnitogorsk, Russia,
15. Belevskii L., Nosov Magnitogorsk State Technical University, Magnitogorsk, Russia,
16. Belokonova I., Siberian Federal University, Krasnoyarsk, Russia,
17. Belov N., National University of Science and Technology MISiS, Moscow, Russia,
18. Belov V., Nosov Magnitogorsk State Technical University, Magnitogorsk, Russia,
19. Biryukova O., Polytechnic College, Magnitogorsk, Russia,
20. Bobarikin Yu., Sukhoi State Technical University of Gomel, Gomel, Republic of Belarus,
21. Brilevesky A., Togliatti State University, Togliatti, Russia,
22. Bunits N., National University of Science and Technology MISiS, Moscow, Russia,
23. Burdukovsky V., Ural Federal University named after the first President of Russia B.N.Yeltsin, Yekaterinburg, Russia,
24. Bushueva N., Ural Federal University named after the first President of Russia B.N. Yeltsin, Yekaterinburg, Russia,
25. Bykov V., South Ural State University (National Research Institute), Chelyabinsk, Russia,
26. Charaeva Z., Karaganda State Industrial University, Temirtau, Kazakhstan,
27. Chasnikov A., Svelen Ltd., Saint Petersburg, Russia,
28. Chikishev D., Nosov Magnitogorsk State Technical University, Magnitogorsk, Russia,
29. Deepak Kumar Singh, Indian Institute of Technology Bombay, Mumbai, India,
30. Dubey A., Indian Institute of Information Technology, Design & Manufacturing, Jabalpur,
31. Efimova Yu., Nosov Magnitogorsk State Technical University, Magnitogorsk, Russia,
32. Egorova L., M.N. Mikheev Institute of Metal Physics of the Ural Branch of the Russian Academy of Sciences, Yekaterinburg, Russia,
33. Emaleeva D., Nosov Magnitogorsk State Technical University, Magnitogorsk, Russia,

34. Erpalov M., Ural Federal University named after the first President of Russia B.N.Yeltsin, Yekaterinburg, Russia,
35. Fedchenko O., Karaganda State Industrial University, Temirtau, Kazakhstan,
36. Fomin M., Nosov Magnitogorsk State Technical University, Magnitogorsk, Russia ,
37. Frolova N., M.N. Mikheev Institute of Metal Physics of the Ural Branch of the Russian Academy of Sciences, Yekaterinburg, Russia,
38. Fruzki V., Polotsk State University, Novopolotsk, Republic of Belarus,
39. Gallyamov D., JSC BMK, Beloretsk, Russia,
40. Gamin Y., National University of Science and Technology MISiS, Moscow, Russia,
41. Glebov L., South Ural State University (National Research Institute), Chelyabinsk, Russia,
42. Glukhov A., M.N. Mikheev Institute of Metal Physics of the Ural Branch of the Russian Academy of Sciences, Yekaterinburg, Russia,
43. Golubchik E., Nosov Magnitogorsk State Technical University, Magnitogorsk, Russia,
44. Grachev G., Svelen Ltd., Saint Petersburg, Russia,
45. Grigorenko A., South Ural State University (National Research Institute), Chelyabinsk, Russia,
46. Gromov D., South Ural State University (National Research Institute), Chelyabinsk, Russia,
47. Gubarev E., Nosov Magnitogorsk State Technical University, Magnitogorsk, Russia,
48. Gulin A., Nosov Magnitogorsk State Technical University, Magnitogorsk, Russia,
49. Hailiang Yu, Central South University, Chagsha, Hunan,
50. Harshal Y. Shahare, PDPM Indian Institute of Information Technology, Design and Manufacturing, Jabalpur,
51. Ilina N., Nosov Magnitogorsk State Technical University, Magnitogorsk, Russia,
52. Inatovich J., Ural Federal University named after the first President of Russia B.N.Yeltsin, Yekaterinburg, Russia,
53. Ishimov A., PJSC NLMK, Lipetsk, Russia,
54. Ivasik V., Satpaev Ekibastuz Technical and Engineering Institute, Ekibastuz, Kazakhstan,
55. Ivekeeva P., Nosov Magnitogorsk State Technical University, Magnitogorsk, Russia,
56. Kadach M., National University of Science and Technology MISiS, Moscow, Russia,
57. Kalonov A., M.N. Mikheev Institute of Metal Physics of the Ural Branch of the Russian Academy of Sciences, Yekaterinburg, Russia,
58. Kamalova G., OJSC “MMK-METIZ”, Magnitogorsk, Russia,
59. Kamantsev I., Ural Branch of The Russian Academy of Sciences, Yekaterinburg, Russia,
60. Kazantseva T., Ural Federal University named after the first President of Russia B.N. Yeltsin, Yekaterinburg, Russia,
61. Khalezov A., Ural Federal University named after the first President of Russia B.N.Yeltsin, Yekaterinburg, Russia,
62. Khamatov D., Ural Federal University named after the first President of Russia B.N.Yeltsin, Yekaterinburg, Russia,
63. Kharchenko M., Nosov Magnitogorsk State Technical University, Magnitogorsk, Russia,
64. Kharitonov V., Nosov Magnitogorsk State Technical University, Magnitogorsk, Russia,
65. Kheifets A., M.N. Mikheev Institute of Metal Physics of the Ural Branch of the Russian Academy of Sciences, Yekaterinburg, Russia,
66. Khlebnikova Yu., M.N. Mikheev Institute of Metal Physics of the Ural Branch of the Russian Academy of Sciences, Yekaterinburg, Russia,
67. Khomskaya I., M.N. Mikheev Institute of Metal Physics of the Ural Branch of the Russian Academy of Sciences, Yekaterinburg, Russia,

68. Komkova D., M.N. Mikheev Institute of Metal Physics of the Ural Branch of the Russian Academy of Sciences, Yekaterinburg, Russia,
69. Konev S., Nosov Magnitogorsk State Technical University, Magnitogorsk, Russia,
70. Konstantinov D., Nosov Magnitogorsk State Technical University, Magnitogorsk, Russia,
71. Koptseva N., Nosov Magnitogorsk State Technical University, Magnitogorsk, Russia,
72. Korchunov A., Nosov Magnitogorsk State Technical University, Magnitogorsk, Russia,
73. Korotkova N., National University of Science and Technology MISiS, Moscow, Russia,
74. Korsakov A., Russian Research Institute of the Tube & Pipe Industries (ROSNITI), Chelyabinsk, Russia,
75. Koshmin A., National University of Science and Technology MISiS, Moscow, Russia,
76. Kozhemyakina A., Nosov Magnitogorsk State Technical University, Magnitogorsk, Russia,
77. Kuznetsova A., Nosov Magnitogorsk State Technical University, Magnitogorsk, Russia,
78. Lezhnev S., Rudny Industrial Institute, Rudny, Kazakhstan,
79. Linderov M., Togliatti State University, Togliatti, Russia,
80. Loginov Yu., Ural Federal University named after the first President of Russia B.N.Yeltsin, Yekaterinburg, Russia,
81. Lopatina E., Nosov Magnitogorsk State Technical University, Magnitogorsk, Russia,
82. Luca Pezzato, University of Padova, Padova, Italy,
83. Malakanov S., Nosov Magnitogorsk State Technical University, Magnitogorsk, Russia,
84. Malanov A., Ural Federal University named after the first President of Russia B.N.Yeltsin, Yekaterinburg, Russia,
85. Manuele Dabalà, University of Padova, Padova, Italy,
86. Martyanov Yu., Sukhoi State Technical University of Gomel, Gomel, Republic of Belarus,
87. Medvedev M., Siberian Federal University, Krasnoyarsk, Russia,
88. Medvedeva E., Nosov Magnitogorsk State Technical University, Magnitogorsk, Russia,
89. Merson D., Togliatti State University, Togliatti, Russia,
90. Mihalkin D., Russian Research Institute of the Tube & Pipe Industries (ROSNITI), Chelyabinsk, Russia,
91. Mikhaylenko A., Ural Federal University named after the first President of Russia B.N. Yeltsin, Yekaterinburg, Russia,
92. Naizabekov A., Rudny Industrial Institute, Rudny, Kazakhstan,
93. Narasimhan K., Indian Institute of Technology Bombay, Mumbai, India,
94. Nikitenko O., Nosov Magnitogorsk State Technical University, Magnitogorsk, Russia,
95. Niklyayev A., JSC "Volzhsky Pipe Plant", Volzhskiy, Russia,
96. Nukhov D., Ural Federal University named after the first President of Russia B.N.Yeltsin, Yekaterinburg, Russia,
97. Orlov A., Ural Federal University named after the first President of Russia B.N.Yeltsin, Yekaterinburg, Russia,
98. Orlov G., Ural Federal University named after the first President of Russia B.N.Yeltsin, Yekaterinburg, Russia,
99. Panasenko O., Seversky Pipe Plant Industrial Joint Stock Company, Polevskoy, Russia,
100. Panin E., Karaganda State Industrial University, Temirtau, Kazakhstan,
101. Pashkeev K., South Ural State University (National Research Institute), Chelyabinsk, Russia,
102. Pesin A., Nosov Magnitogorsk State Technical University, Magnitogorsk, Russia,
103. Pidzhakova E., Ural Federal University named after the first President of Russia B.N. Yeltsin, Yekaterinburg, Russia,
104. Piliipenko S., Polotsk State University, Novopolotsk, Republic of Belarus,

- 105.Pivovarova K., Nosov Magnitogorsk State Technical University, Magnitogorsk, Russia,
- 106.Poletskov P., Nosov Magnitogorsk State Technical University, Magnitogorsk, Russia,
- 107.Polyakova M., Nosov Magnitogorsk State Technical University, Magnitogorsk, Russia,
- 108.Potaptev D., Nosov Magnitogorsk State Technical University, Magnitogorsk, Russia,
- 109.Pozhidaeva E., Nosov Magnitogorsk State Technical University, Magnitogorsk, Russia,
- 110.Prasad M.J.N.V., Indian Institute of Technology Bombay, Mumbai, India,
- 111.Pustovoitov D., Nosov Magnitogorsk State Technical University, Magnitogorsk, Russia,
- 112.Pykhov L., JSC BMK, Beloretsk, Russia,
- 113.Rachele Bertolini, University of Padova, Padova, Italy,
- 114.Radionova L., South Ural State University (National Research Institute), Chelyabinsk, Russia,
- 115.Radkin Yu., Sukhoi State Technical University of Gomel, Gomel, Republic of Belarus,
- 116.Salganik V., Nosov Magnitogorsk State Technical University, Magnitogorsk, Russia,
- 117.Salikhyanov D., Ural Federal University named after the first President of Russia B.N. Yeltsin, Yekaterinburg, Russia,
- 118.Samodurova M., South Ural State University (National Research Institute), Chelyabinsk, Russia,
- 119.Samoylov S., South Ural State University (National Research Institute), Chelyabinsk, Russia,
- 120.Sarafanov A., South Ural State University (National Research Institute), Chelyabinsk, Russia,
- 121.Shimov G., Ural Federal University named after the first President of Russia B.N. Yeltsin, Yekaterinburg, Russia,
- 122.Shorokhov E., Russian Federal Nuclear Center-Zababakhin All-Russian Research Institute of Technical Physics, Snezhinsk, Russia,
- 123.Shvarts D., Ural Federal University named after the first President of Russia B.N. Yeltsin, Yekaterinburg, Russia,
- 124.Sidelnikov S., Siberian Federal University, Krasnoyarsk, Russia,
- 125.Snegiryov I., Ural Federal University named after the first President of Russia B.N. Yeltsin, Yekaterinburg, Russia,
- 126.Sosedkova M., South Ural State University (National Research Institute), Chelyabinsk, Russia,
- 127.Startsev A., LLC "RUSAL ETC", Krasnoyarsk, Russia,
- 128.Stefania Bruschi, University of Padova, Padova, Italy,
- 129.Stepanova M., Satpaev Ekibastuz Technical and Engineering Institute, Ekibastuz, Kazakhstan,
- 130.Stolyarov A., OJSC "MMK-METIZ", Magnitogorsk, Russia,
- 131.Stolyarov F., JSC SPA BelMag, Magnitogorsk, Russia,
- 132.Strashkova N., Ural Federal University named after the first President of Russia B.N. Yeltsin, Yekaterinburg, Russia,
- 133.Suaridze T., M.N. Mikheev Institute of Metal Physics of the Ural Branch of the Russian Academy of Sciences, Yekaterinburg, Russia,
- 134.Svistun A., South Ural State University (National Research Institute), Chelyabinsk, Russia,
- 135.Tandon P., Indian Institute of Information Technology, Design and Manufacturing, Jabalpur,
- 136.Timofeev V., Siberian Federal University, Krasnoyarsk, Russia,
- 137.Tkachuk G., Ural Federal University named after the first President of Russia B.N. Yeltsin, Yekaterinburg, Russia,
- 138.Tolkushkin A., Rudny Industrial Institute, Rudny, Kazakhstan,
- 139.Toporov V., Seversky Pipe Plant Industrial Joint Stock Company, Polevskoy, Russia,
- 140.Toyusheva D., Ural Federal University named after the first President of Russia B.N. Yeltsin, Yekaterinburg, Russia,
- 141.Tsyrganovich I., Sukhoi State Technical University of Gomel, Gomel, Republic of Belarus,

142. Tymchenko A., Karaganda State Industrial University, Temirtau, Kazakhstan,
143. Ulyanov A., JSC "Volzhsky Pipe Plant", Volzhskiy, Russia,
144. Usanov M., Nosov Magnitogorsk State Technical University, Beloretsk Branch, Beloretsk,
145. Ustinova E., Ural Federal University named after the first President of Russia B.N. Yeltsin, Yekaterinburg, Russia,
146. Vakhitov A., JSC SPA BelMag, Magnitogorsk, Russia,
147. Vinogradov A., Norwegian University of Science and Technology – NTNU, Trondheim, Norway,
148. Volkov A., M.N. Mikheev Institute of Metal Physics of the Ural Branch of the Russian Academy of Sciences, Yekaterinburg, Russia,
149. Voroshilov D., Siberian Federal University, Krasnoyarsk, Russia,
150. Vorsin A., Ural Federal University named after the first President of Russia B.N. Yeltsin, Yekaterinburg, Russia,
151. Yakivyyuk O., Siberian Federal University, Krasnoyarsk, Russia,
152. Zamaraeva Y., Ural Federal University named after the first President of Russia B.N. Yeltsin, Yekaterinburg, Russia,
153. Zambritckaya E., Nosov Magnitogorsk State Technical University, Magnitogorsk, Russia,
154. Zasyplin S., Institute of Advanced Technologies, Togliatti State University, Togliatti,
155. Zavartsev N., Russian Research Institute of the Tube & Pipe Industries (ROSNITI), Chelyabinsk, Russia,
156. Zeldovich V., M.N. Mikheev Institute of Metal Physics of the Ural Branch of the Russian Academy of Sciences, Yekaterinburg, Russia,
157. Zhelezkov O., Nosov Magnitogorsk State Technical University, Magnitogorsk, Russia,
158. Zhumagaliyev D., Rudny Industrial Institute, Rudny, Kazakhstan,
159. Zinoviev A., National University of Science and Technology MISiS, Moscow, Russia.

Content

SESSION 1 – Innovative Technology and Materials in Metal Forming.....	6
Luca Pezzato, Rachele Bertolini, Stefania Bruschi, Andrea Ghiotti, Manuele Dabalà	
Potential biomedical applications of AZ61 magnesium alloy after large strain extrusion machining (Isem).....	6
Suaridze T., Khlebnikova Yu., Egorova L.	
Hardned tape substrates made on (CU-NI-ME) - alloys for 2 ^d generation high-temperature superconductor wire.....	8
Pustovoitov D., Pesin A., Biryukova O.	
Fem simulation of temperature changes during asymmetric cryorolling of aluminum.....	9
Pashkeev K., Bykov V., Radionova L., Samodurova M.	
Restoration of the steel billet continuous casting machine roller face by direct laser fusion.....	11
Adyev E., Burdukovsky V.	
Technological heredity and the quality of parts made by sheet stamping of titanium alloys.....	13
Konstantinov D., Emaleeva D., Kuznetsova A.	
Application of srrve conception for modeling of ferritic-pearlitic steel wire drawing.....	15
Bunits N., Gamin Y., Kadach M.	
The structure and properties of cunicrsi alloy after radial-shear rolling.....	17
Ivasik V., Andreyashchenko V.	
Treatment of multicomponent al-si-fe alloys.....	18
Kharitonov V., Usanov M., Polyakova M.	
Application of radial-shear strain in the production of long components with ultrafine-grained structure.....	20
Komkova D., Antonova O., Glukhov A., Kalonov A., Volkov A.	
Cold hydrostatic extrusion method for making magnesium rods and fine wires.....	22
Pustovoytov D., Pesin A., Zhilyaev A., Tandon P.	
Fem simulation of strain gradient in low-carbon steel sheets after asymmetric cold rolling.....	24
Martyanov Yu., Bobarikin Yu., Tsyrganovich I.	
Steel wire drawing in double dies: process features.....	26
Belevskii L., Belevskaya I., Efimova Yu.	
New technique of metal surface restoration and reinforcement.....	27
Orlov A., Loginov Yu.	
The metal-saving technology of pipe rolling in a reducing mill.....	29

Pozhidaeva E., Chikishev D. Development and testing of new steel grades by modeling the complex dynamic processes involved in their production and operation	31
Abdullina D., Khomskaya I., Zeldovich V., Frolova N., Kheifets A., Shorokhov E. The effect of high strain-rate deformation and annealing on the evolution of the structure and properties of cu–cr–zr alloys	32
Belokonova I., Sidelnikov S., Voroshilov D., Yakiviyuk O. Structure and properties of rolled sheets made of aluminum-magnesium alloys with different scandium content: a comparative analysis	33
Alekseev D., Poletskov P., Kuznetsova A., Adishchev P., Emaleeva D. Simulated production of semi-finished rolled stock for coiled tubing	35
Voroshilov D., Sidelnikov S., Startsev A., Medvedev M. Assessment of the structure and modification ability of the experimental al-3ti-1b bar ligature obtained by the method of ingotless rolling-extruding	36
Strashkova N., Inatovich J. Understanding the relationship between tension and energy costs in a quarto reversing mill rolling operation	38
Fomin M., Pesin A., Potaptev D. Effect of various process parameters on the bake hardening effect in continuous hot-dip galvanizing line	40
Naizabekov A., Lezhnev S., Tymchenko A., Panin E., Fedchenko O., Charaeva Z. Investigation of asymmetric rolling in relief rolls	41
Konstantinov D., Korchunov A. Micromechanics simulation of cold rod drawing	43
Belov N., Korotkova N., Timofeev V., Akopyan T. Effect of thermomechanical treatment on the structure and physical and mechanical properties of al–7%rem and al–0.6%zr conductor alloys produced by electromagnetic casting	45
Toporov V., Panasenko O., Khalezov A., Nukhov D. Understanding the influence of speed correction modes on the pipe surface quality during continuous rolling	46
Polyakova M., Gulin A., Stolyarov A. Simulation of white layer thickness in combined wire drawing	47
Grigorenko A., Sosedkova M., Radionova L. Mathematical modeling of metal temperature during hot sheet rolling	49
Abhay Kumar Dubey, Harshal Y. Shahare, Pesin A., Pustovoytov D., Hailiang Yu, Puneet Tandon Numerical modeling of combined asymmetric rolling and bending process	51
Khamatov D., Loginov Yu. Simulation of a new method of accumulated deformation	52

Zasyplin S., Brilevsky A. Control of magnesium alloy properties using methods of severe plastic deformation	54
Medvedeva E., Golubchik E., Konstantinov D., Ivekeeva P. Internal stress evolution in the prestressing strand production	56
Zavartsev N., Korsakov A., Mihalkin D., Alyutina E., Akhmedjanov A., Samoylov S., Ulyanov A., Niklyayev A. Research of the heating temperature influence on the technological plasticity of the steel grade 15kh13n2 (aisi 414) applicable to the screw rolling process	58
Pivovarova K., Emaleeva D. Application of thermal analysis method for structural transformation of hot-rolled carbon billets for highstrength ropes	67
Ustinova E., Shvarts D., Mikhaylenko A. Modeling of a new channel rolling method in the deform software package	69
Kozhemyakina A., Pesin A., Pustovoytov D., Biryukova O., Ilina N. Development of the asymmetric rolling technology as a severe plastic deformation method for narrow aluminum strips with a gradient structure showing higher strength and ductility	71
SESSION 2 – Fundamental Problems of Metal Forming during Transition to Innovative Technology	73
Erpalov M. Theoretical and experimental analysis of a neck profile in cylindrical specimens ...	73
Gulin A., Polyakova M., Pivovarova K., Stolyarov A., Narasimhan K., Prasad M.J.N.V. Peculiarities of contact interactions between carbon steel wire and die in drawing with torsion	75
Radkin Yu., Bobarikin Yu. Understanding the influence of reduction modes on the deformation unevenness in a tube wall	76
Malakanov S. Stress state of dies for hexagonal rods production	78
Deepak Kumar Singh Effect of combined bending & twisting during steel wire drawing on the development of microstructure & properties	80
Erpalov M. Development of control program for hot torsion test unit	81
Lopatina E., Polyakova M. Approaches to classification of combined and integrated processes in metal forming	83
Salikhyanov D., Kamantsev I. Features of rolling hard-to-deform steels and alloys in a shell made of soft material	84

Kharchenko M., Konev S., Zhelezkov O., Zambrgitskaya E., Salganik V. Simulation of contact between rolls of a rolling mill in the conditions of equal acceleration with slippage and lubrication	86
Koshmin A., Zinoviev A., Chasnikov A., Grachev G. Influence of process parameters on the properties of continuously extruded copper buses.....	88
Kuznetsova A., Nikitenko O., Alekseev D., Poletskov P., Emaleeva D. Understanding the forming mechanism of mechanical properties in new cold-resistant high-strength steel.....	89
Linderov M., Brilevesky A., Merson D., Vinogradov A. Hybrid processing as an effective way to improve physical and mechanical properties of magnesium alloys.....	90
Orlov G., Malanov A. Fem modeling of the tube workpiece hot guillotining process	92
Pilipenko S., Fruzki V. Method for calculating the temperature of the deformation cone cross-sections in a cold pilger rolling mill.....	93
Nikitenko O., Poletskov P., Kuznetsova A. Understanding the effect of multi-stage heat treatment schedules on the microstructure and properties of cryogenic steel.....	94
Sarafanov A., Radionova L., Gromov D., Svistun A. Roller die drawing of small diameter titanium alloy wire	96
Belevskii L., Belevskaya I., Belov V., Gubarev E., Efimova Yu. Surface modification by plastic deformation and functional coatings.....	98
Stolyarov A., Kamalova G., Polyakova M. Microstructural anisotropy on the wire surface during drawing.....	99
SESSION 3 – Cross-disciplinary solutions in advanced materials engineering (iSmart-Metal Forming)	102
Abashev D., Loginov Yu. Calculation of strains in zirconium alloy rolling	102
Pykhov L., Gallyamov D., Kharitonov V., Polyakova M. Increasing steel wire rope service life by applying a color coating	103
Bushueva N., Loginov Yu. Use of spherical boundaries hypotheses to verify the deformation zone during drawing	105
Pesin A., Pustovoytov D., Dubey A. New physical simulation approach for asymmetric rolling	107
Erpalov M. Influence of punch design on the quality of upset pipe ends.....	109

Naizabekov A., Arbuz A., Tolkushkin A., Panin E., Zhumagaliyev D. Simulation of components with ufg properties for nuclear industry	111
Korchunov A., Polyakova M., Medvedeva E., Emaleeva D. Research of mechanical properties of prestressing strands under thermo-mechanical treatment	113
Toyusheva D., Loginov Yu. Processing of the titanium alloy Ti6Al7Nb as a medical application material	114
Belevskii L., Belevskaya I., Efimova Yu. Friction nanostructuring treatment of metallic surfaces by flexible tool	116
Glebov L., Pashkeev K., Radionova L. Effect of the Ti6AL4V alloy track arrangement on mechanical properties in direct metal deposition	118
Zamaraeva Y., Loginov Yu. Ways to expand the use of magnesium	121
Vakhitov A., Stolyarov F. Understanding the effect of friction conditions on the parameters of inner tie rod pressing	123
Snegiryov I., Loginov Yu. Rolling of aluminium alloy 5083 sheets	124
Golubchik E., Medvedeva E., Gulin A., Polyakova M. Roughness formation in hot-rolled temper-rolled band production	126
Ishimov A. Finite element modeling of the sleeper screw head hot stamping process accounting for dynamic recrystallization	127
Vorsin A., Loginov Yu., Shimov G. Investigation of the state of CU59ZNPB1 after hot extrusion	129
Kazantseva T., Pidzhakova E., Tkachuk G., Polyakova M. Standardization system management model	131
Andreyashchenko V., Stepanova M. Application of severe plastic deformation for forging cylindrical billets	132
Koptseva N., Efimova Yu., Gulin A., Narasimhan K., Prasad M.J. Behavior of fine pearlite plates in the deformation of high-carbon steel	134
List of Participants	136

Научное издание

MAGNITOGORSK ROLLING PRACTICE 2020

Proceedings of the 5th International Youth Scientific
and Technical Conference

Материалы V международной молодежной
научно-технической конференции

Edited by A.G. Korchunov

Под редакцией А.Г. Корчунова

Translated and proofread by O.E. Sukhikh, V.I. Elesina

Перевод и прюфридинг О.Е. Сухих, В.И. Елесина

Подписано в печать 22.12.2020. Рег. № 74-20. Формат 60×84/16. Бумага тип. №1.
Плоская печать. Усл.печ.л. 9,25. Тираж 100 экз. Заказ 374



Издательский центр ФГБОУ ВО «МГТУ им. Г.И. Носова»
455000, Магнитогорск, пр. Ленина, 38

Участок оперативной полиграфии ФГБОУ ВО «МГТУ им. Г.И. Носова»